

Measurement of Precipitated Calcium Citrate in Urine by Murexide-based Indicator  
Displacement Assay and Its Clinical Utility in Calcium Oxalate Urolithiasis



A Dissertation Submitted in Partial Fulfillment of the Requirements  
for the Degree of Doctor of Philosophy in Medical Sciences  
Faculty Of Medicine  
Chulalongkorn University  
Academic Year 2023

วิธีการวัดผลึกแคลเซียมซีเตรตที่ตกตะกอนในปัสสาวะด้วยวิธีการใช้สารมูเร็กซ์ไซด์และประโยชน์  
ทางคลินิกในโรคนิ่วปัสสาวะชนิดแคลเซียมออกซาเลต



วิทยานิพนธ์นี้เป็นส่วนหนึ่งของการศึกษาตามหลักสูตรปริญญาวิทยาศาสตรดุษฎีบัณฑิต  
สาขาวิชาวิทยาศาสตร์การแพทย์  
คณะแพทยศาสตร์ จุฬาลงกรณ์มหาวิทยาลัย  
ปีการศึกษา 2566



ไฮดรอล ดัชนีฤทธิ์ : วิธีการวัดผลึกแคลเซียมซิเตรตที่ตกตะกอนในปัสสาวะด้วยวิธีการใช้สารมูเร็กซ์ไซด์และประโยชน์ทาง  
 คลินิกในโรคนี้่วปัสสาวะชนิดแคลเซียมออกซาเลต. ( Measurement of Precipitated Calcium Citrate in Urine by  
 Murexide-based Indicator Displacement Assay and Its Clinical Utility in Calcium Oxalate Urolithiasis) อ.ที่ปรึกษา  
 หลัก : ผศ. ดร.ชาญชัย บุญหล้า

นี้่วปัสสาวะซึ่งส่วนใหญ่มีแคลเซียมออกซาเลต (CaOx) เป็นองค์ประกอบนั้นเป็นโรคทางเดินปัสสาวะที่พบมาเป็นเวลานาน  
 และมีความชุกและอัตราการเกิดซ้ำสูง พฤติกรรมการบริโภคอาหาร โดยเฉพาะอาหารที่มีสารออกซาเลตสูงและการบริโภคอาหารที่มีสารซิ  
 เดรตต่ำ ทำให้เกิดภาวะสารออกซาเลตในปัสสาวะสูงร่วมกับภาวะสารซิเตรตในปัสสาวะต่ำ ซึ่งเป็นสาเหตุโดยตรงของการเกิดนี้่ว CaOx  
 ดังนั้น การตรวจวัดปริมาณสารออกซาเลตและซิเตรตในปัสสาวะจึงจำเป็นต่อการประเมินความเสี่ยงของการเกิดนี้่ว CaOx ปัจจุบันการวัด  
 ปริมาณซิเตรตในปัสสาวะใช้วิธี High-performance liquid chromatography สามารถวัดโดยตรงได้ แต่มีขั้นตอนการวัดที่ซับซ้อนและ  
 ต้องการผู้วัดที่ผ่านการฝึกใช้งานเครื่องมือเท่านั้น ทางผู้วิจัยจึงตั้งสมมติฐานว่า แทนที่จะวัดปริมาณซิเตรตในปัสสาวะโดยตรง การวัด  
 ปริมาณแคลเซียมซิเตรต (CalCit) ที่ตกตะกอนออกมาจากปัสสาวะโดยการใส่สารแคลเซียมเข้าไปให้มากเกินพอ นั้น น่าจะเป็นอีกวิธีการ  
 ทางเลือกที่สามารถจำแนกกลุ่มผู้ป่วยนี้่ว CaOx ออกจากผู้ที่ไม่เป็นนี้่วได้เช่นกัน ในการศึกษาี้ ผู้วิจัยมีเป้าหมายที่จะพัฒนาการทดสอบ  
 ใหม่ที่วัดปริมาณ CalCit ที่ตกตะกอนออกมาจากปัสสาวะที่มีความอิมมิตัวยิ่งยวด ภาวะความอิมมิตัวยิ่งยวดนี้่วถูกกระตุ้นโดยการเติมสาร  
 แคลเซียมคลอไรด์ที่มากเกินพอเข้าไปในตัวอย่างปัสสาวะ ตกตะกอน CalCit โดยใช้แอมทานอล และละลายตะกอนกลับมาด้วยกรดไฮโดร  
 คลอริก วัดปริมาณซิเตรตในละลาย CalCit ด้วยวิธีการแทนที่อินดิเคเตอร์ (indicator-displacement assay, IDA) โดยใช้สีมูเร็กซ์ไซด์  
 (murexide, Mrx) เป็นอินดิเคเตอร์ จากนั้นทำการตรวจสอบความใช้ได้ของวิธีใหม่นี้ ตรวจสอบความถูกต้องทางคลินิกเพื่อพิสูจน์ว่าวิธีที่  
 พัฒนาขึ้นใหม่นี้มีศักยภาพในการวินิจฉัยโรคนี้่วปัสสาวะชนิด CaOx หรือไม่ ผู้วิจัยพบว่าวิธีการวัดปริมาณ CalCit ที่ตกตะกอนจากปัสสาวะ  
 ด้วยการแทนที่สารมูเร็กซ์ไซด์ซึ่งเป็นอินดิเคเตอร์ (murexide-based indicator displacement assay, Mrx IDA) นี้ผ่านการตรวจสอบความ  
 ใช้ได้ของวิธีทดสอบ ช่วงระยะการวัดที่เชื่อถือได้อยู่ในช่วง 0.4-1.4 mM โดยมี limit of detection (LoD), lower limit of quantitation (LoQ)  
 และ upper LoQ อยู่ที่ 0.08 mM, 0.4 mM และ 1.4 mM ตามลำดับ พร้อมทั้งมี repeatability, reproducibility และ accuracy อยู่ในเกณฑ์  
 ที่ยอมรับได้ สำหรับการตรวจสอบความถูกต้องทางคลินิก ทำการวัดระดับ CalCit ในตัวอย่างปัสสาวะ 24 ชั่วโมง จากผู้ที่เป็นนี้่วปัสสาวะ  
 จำนวน 122 ตัวอย่าง และจากผู้ป่วยนี้่ว CaOx จำนวน 45 ตัวอย่าง ผลการวิเคราะห์ Receiver operating characteristic (ROC) ได้ค่า  
 area under ROC curve อยู่ที่ 0.8227 (95% CI: 0.7522-0.8931) สำหรับการจำแนกผู้ป่วยนี้่ว CaOx ออกจากผู้ที่ไม่ได้เป็นนี้่ว เมื่อ  
 กำหนดค่า cutoff ของระดับ CalCit ที่ 632  $\mu$ M วิธี Mrx IDA นี้ให้ค่า sensitivity, specificity, positive และ negative predictive values  
 (PPV และ NPV), positive และ negative likelihood ratios ( $LH^+$  และ  $LH^-$ ), และ accuracy อยู่ที่ 84.44%, 70.49%, 74.25%, 51.35%,  
 92.47%, 2.41, 0.26, 74.90% ตามลำดับ โดยสรุปผู้วิจัยสามารถพัฒนาการทดสอบเพื่อวัดปริมาณ CalCit ที่ตกตะกอนจากปัสสาวะด้วย  
 Mrx IDA ได้สำเร็จ กระบวนการตรวจสอบความใช้ได้ของวิธีการทดสอบแสดงให้เห็นว่าการทดสอบนี้มีความแม่นยำและเที่ยงตรง การ  
 ตรวจสอบความถูกต้องทางคลินิกให้ค่า sensitivity และ NPV ที่สูง ซึ่งบ่งชี้ว่า หากผลการทดสอบด้วยวิธีนี้เป็นลบ สามารถบอกได้อย่าง  
 ถูกต้องว่าไม่น่าจะเป็นโรคนี้่วปัสสาวะชนิด CaOx ดังนั้น การทดสอบเพื่อวัดปริมาณ CalCit ที่ตกตะกอนออกมาจากปัสสาวะที่พัฒนาขึ้นมา  
 ในงานวิจัยนี้ สามารถใช้เป็นเครื่องมือเพื่อการตรวจคัดกรองโรคนี้่วปัสสาวะชนิด CaOx ได้

สาขาวิชา วิทยาศาสตร์การแพทย์  
 ปีการศึกษา 2566

ลายมือชื่อผู้วิจัย .....  
 ลายมือชื่อ อ.ที่ปรึกษาหลัก .....

## 5974767130 : MAJOR MEDICAL SCIENCES

KEYWORD: Kidney stone, Calcium oxalate, Calcium citrate, Murexide, Indicator displacement assay, Screening test  
 Chaiyadol Tantasith : Measurement of Precipitated Calcium Citrate in Urine by Murexide-based Indicator Displacement Assay and Its Clinical Utility in Calcium Oxalate Urolithiasis. Advisor: Asst. Prof. CHANCHAI BOONLA, Ph.D.

Urinary stone, mainly composed of calcium oxalate (CaOx), is a longstanding urologic condition with high prevalence and recurrence rates. Dietary habits, specifically increased consumption of high oxalate diet and low intake of citrate-containing foods, lead to hyperoxaluria and hypocitraturia that directly contribute to CaOx stone formation. Measurements of urinary oxalate and citrate are essential to estimate the risk of CaOx stone formation. Currently, high-performance liquid chromatography is used for urinary citrate measurement, but it is complicated and requires well-trained technicians. We hypothesized that instead of directly measuring citrate in urine, measurement of calcium citrate (CalCit) precipitated in urine challenging with excessive calcium would be an alternative method to distinguish CaOx stone patients from non-stone subjects. In this study, we developed a new test for measuring precipitated CalCit in supersaturated urine. Supersaturation of urine was induced by adding excessive amount of calcium chloride. CalCit was precipitated by ethanol and redissolved by hydrochloric acid. Citrate content in the redissolved CalCit was determined by an indicator-displacement assay (IDA) using murexide (Mrx) as an indicator dye. Method validation was performed. Clinical validation was subsequently conducted to evaluate whether this method had sufficient performance for diagnosing CaOx urolithiasis. We successfully established the procedure of the murexide-based indicator displacement assay (Mrx IDA) for measuring precipitated CalCit. The measurement interval of the Mrx IDA was between 0.4 and 1.4 mM. Limit of detection (LoD), lower limit of quantitation (LoQ), and upper LoQ were 0.08 mM, 0.4 mM, and 1.4 mM, respectively. Repeatability, reproducibility, and accuracy were well acceptable. For clinical validation, the test was performed in 24-hour urine samples obtained from 122 non-stone subjects and 45 CaOx stone patients. Receiver operating characteristic (ROC) analysis revealed an area under ROC curve of 0.8227 (95% CI: 0.7522-0.8931) for distinguishing CaOx stone patients from non-stone subjects. At the cutoff value of 632  $\mu$ M, the test provided sensitivity, specificity, positive and negative predictive values (PPV and NPV), positive and negative likelihood ratios (LH<sup>+</sup> and LH<sup>-</sup>), and accuracy of 84.44%, 70.49%, 74.25%, 51.35%, 92.47%, 2.41, 0.26, and 74.90%, respectively. Conclusion, we successfully developed the Mrx IDA test for measuring urinary precipitated CalCit. Method validation indicated that this newly established test was precise and accurate. Clinical accuracy testing showed high sensitivity and NPV, suggested that the Mrx IDA test was useful to rule out the CaOx urolithiasis. Therefore, the measurement of urinary precipitated CalCit developed in this study is clinically promising to be used as a screening test for CaOx urolithiasis.

Field of Study: Medical Sciences

Student's Signature .....

Academic Year: 2023

Advisor's Signature .....

## ACKNOWLEDGEMENTS

I wish to express my profound gratitude to my advisor, Asst. Prof. Chanchai Boonla, Ph.D., for his invaluable assistance and guidance during the course of my Ph.D. studies. I am appreciative of his benevolence, enduring support, and consistent care. The successful completion of this study is largely attributable to the mentorship of my professors, who imparted both knowledge, critical thinking skills, and mental support.

Special thanks are due to my thesis committee, consisting of Assoc. Prof. Dr. Wilai Anomasiri, Asst. Prof. Dr. Narisorn Kongruttanachok, Assoc. Prof. Dr. Thasinas Dissayabutra, and Asst. Prof. Dr. Supranee Kongkham, for their valuable advice that greatly contributed to the successful completion of my thesis.

Additionally, I extend my sincere thanks for the support provided during my student exchange experience in Germany. The opportunity for a research exchange scholarship at Charité – Universitätsmedizin, Berlin was enhancing my research, life experiences, and cultural understanding. My gratitude extends my thanks to Professor Hans Bäumlner for providing this enriching opportunity, which contributed significantly to the improvement of my communication skills for laboratory work.

I am grateful for the support provided by "the 100th Anniversary Chulalongkorn University Fund for Doctoral Scholarship". Special acknowledgment goes to the staff of the Faculty of Medical Science for their continuous support of all student requirements. I also appreciate the assistance from Chat GPT, particularly during the critical time of my thesis defense.

A heartfelt thank you goes to the members of Lab 806 for their constant support and encouragement. Finally, I extend my deepest gratitude to my wife and family for their unwavering support, love, and encouragement throughout this academic journey.

Chaiyadol Tantasith

## TABLE OF CONTENTS

	Page
.....	iii
ABSTRACT (THAI).....	iii
.....	iv
ABSTRACT (ENGLISH) .....	iv
ACKNOWLEDGEMENTS.....	v
TABLE OF CONTENTS.....	vi
LIST OF TABLES.....	viii
LIST OF FIGURES .....	xi
Chapter 1 Background and Rationales .....	1
Chapter 2 Review related literature.....	7
2.1 Urinary stone disease epidemiology .....	7
2.2 Types of kidney stones .....	10
2.3 Cause and risks factor of kidney stone disease.....	11
2.4 Citrate and CaOx stone formation .....	12
2.5 Measurement of urinary citrate .....	16
2.6 Measurement of citrate <sup>3-</sup> in the form of CalCit by colorimetric assay. ....	18
2.7 Calcium citrate precipitation .....	20
Chapter 3 Research methodology .....	23
3.1 Study design .....	23
3.2 Urine specimen collection .....	23
3.3 24-h urine sample preparation .....	24

3.4 CalCit precipitation .....	24
3.5 Mrx IDA and $\text{Ca}_3\text{Cit}_2$ standard preparation .....	26
3.6 Method validation.....	28
3.7 Diagnostic accuracy validation .....	32
3.8 Statistical analysis.....	34
3.9 Ethical consideration.....	35
Chapter 4 Results .....	36
4.1 Scanning spectrum of displaced Mrx in $\text{Ca}_3\text{Cit}_2$ concentration-dependent manner .....	36
4.2 Linearity, LoB, LoD, LoQ.....	37
4.3 Precision and accuracy test .....	39
4.4 %yield of $\text{Ca}_3\text{Cit}_2$ precipitation.....	40
4.5 Selectivity of Mrx IDA.....	41
4.6 FTIR analysis of the 2 <sup>nd</sup> pellet sample precipitated urine sample of urolithiasis patients .....	47
4.7 Clinical validation: ROC curve analysis and its parameters .....	49
Chapter 5 Discussion .....	53
Supplement data .....	58
REFERENCES.....	78
REFERENCES.....	87
VITA .....	89



## LIST OF TABLES

	Page
Table 1. Comparison of urine citrate measurement among various methods. ....	17
Table 2. Formula of artificial urine .....	25
Table 3. Potential urine interference, within Mrx IDA reaction.....	31
Table 4. The interpretation of the AUC from ROC analysis .....	33
Table 5. Comparison of absorbance of each $\text{Ca}_2\text{Cit}_3$ standard with the previous concentration.....	37
Table 6. Comparison of $\text{Ca}_2\text{Cit}_3$ level of each $\text{Ca}_2\text{Cit}_3$ standard and their %CV and %recovery values used for calculating LoB, LoD, and LoQ.....	38
Table 7. The formulas and values of LoB, LoD, and LoQ of $\text{Ca}_2\text{Cit}_3$ standard .....	38
Table 8. The observed $\text{Ca}_3\text{Cit}_2$ values of control material .....	39
Table 9. The observed $\text{Ca}_3\text{Cit}_2$ values of control material and %recovery after CalCit precipitation (%yield of CalCit precipitation). ....	40
Table 10. Comparison of precipitated CalCit values between NS group and ST groups. ....	51
Table 11. Cutoff values of urinary precipitated CalCit and diagnostic values for separating NS subjects from ST patients. ....	52
Table 12. (supplement S1). List of chemicals used in this study. ....	58
Table 13. (supplement S2) List of equipment used in this study. ....	60
Table 14. (supplement S3) Artificial urine recipe.....	62
Table 15. (supplement S4) 2 N HCl solution recipe. ....	63
Table 16. (supplement S5) 0.04 N HCl solution recipe. ....	63
Table 17. (supplement S6) 10 mM, HEPES buffer recipe. ....	63

Table 18. (supplement S7) 10 mM, Mrx solution recipe, fresh preparation before measuring.....	63
Table 19. (supplement S8) 10 mM, 10 mM, Cu <sup>2+</sup> solution recipe, fresh preparation before measuring. ....	64
Table 20. (supplement S9) 4.44 mM, Mrx solution, fresh preparation before measuring. ....	64
Table 21. (supplement S10) 4.44 mM, Cu <sup>2+</sup> solution, fresh preparation before measuring.....	64
Table 22. (supplement S11) 2.22 mM Mrx-Cu <sup>2+</sup> solution recipe ( for measuring at 2 mM, about 100 reactions), fresh preparation before measuring.....	64
Table 23. (supplement S12) 200 mM, Ca <sub>3</sub> Cit <sub>2</sub> solution recipe. ....	65
Table 24 . (supplement S13) 20 mM, Ca <sub>3</sub> Cit <sub>2</sub> solution recipe. ....	65
Table 25. (supplement S14) 20 mM, Ca <sub>3</sub> Cit <sub>2</sub> solution recipe, fresh preparation before measuring.....	65
Table 26. (supplement S15) CaCl <sub>2</sub> , 1 M solution.....	66
Table 27. (supplement S16) NaOH, 1 N solution. ....	66
Table 28 (supplement S17) KOH, 50 mM solution. ....	66
Table 29. (supplement S18.) Working solution recipe of potential interferences of Mrx IDA.....	67
Table 30 (supplement S19) Data of urine samples. ....	70
Table 31 (supplement S20) Number of cases and percentage of non-stone and stone group. ....	76
Table 32 (supplement S21) Number of cases and percentage, representing their urinary precipitated CalCit level, corresponding to LoD and LoQ of Mrx IDA. ....	76

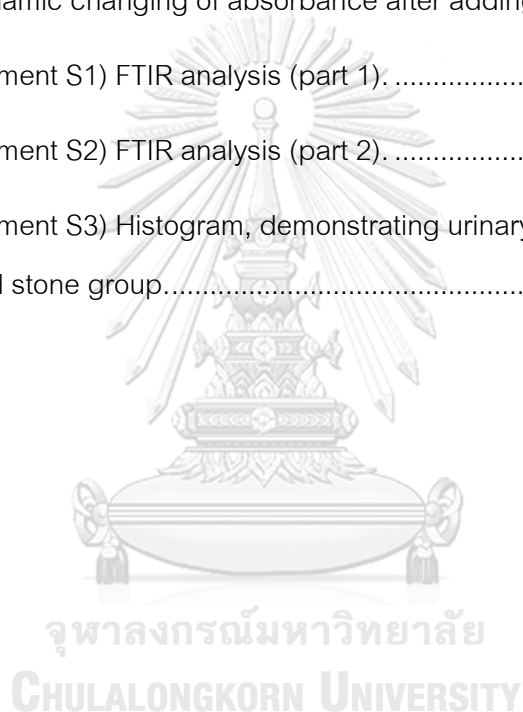
Table 33 (supplement S22) Frequency distribution of urinary precipitated CaCit level  
from non-stone and stone group..... 77



## LIST OF FIGURES

	Page
Figure 1. Conceptual framework of the present study. ....	5
Figure 2 Schematic workflow of the present study. ....	6
Figure 3 Stone belt (red) extends all the way around the world.....	8
Figure 4 Comparison of world map projection of magnitude of kidney stone prevalence (upper) and obesity prevalence (lower) .....	9
Figure 5 Urinary citrate level in Thai healthy individuals and patient with urolithiasis. ...	11
Figure 6 Amorphous CaOx nanoparticle. ....	13
Figure 7 Effect of COD and COM on Vero cell death.....	15
Figure 8. Principle of citrate detection by Mrx IDA .....	19
Figure 9 Structure of citric acid and Calcit .....	21
Figure 10 FTIR of CalCit. ....	21
Figure 11 Structure of phenolic acid.....	22
Figure 12. Standard curve of Mrx IDA using $\text{Ca}_3\text{Cit}_2$ (0.2-2.0 mM) as standard material. ....	27
Figure 13. Relationship between Limit of Blank (LoB), Limit of Detection (LoD), Limit of Quantitation (LoQ) .....	29
Figure 14. A ROC curve .....	32
Figure 15. The decision matrix (2x2 Table) for diagnosing stone condition .....	34
Figure 16. The absorbance of $\text{Ca}_3\text{Cit}_2$ Std by Mrx IDA. ....	36
Figure 17 Selectivity of the Mrx IDA reaction (part 1). ....	42
Figure 18. Selectivity of the Mrx IDA reaction (part 2). ....	43

Figure 19. Selectivity of the Mrx IDA reaction (part 3).....	44
Figure 20. Selectivity of the Mrx IDA reaction (part 4).....	45
Figure 21. Selectivity of the Mrx IDA reaction (part 5).....	46
Figure 22. FTIR analysis of precipitated CalCit. ....	48
Figure 23 Levels of precipitated CalCit measured by the Mrx IDA method compared between stone (ST) and non-stone (NS) groups. ....	50
Figure 24. The dynamic changing of absorbance after adding citrate.....	55
Figure 25. (supplement S1) FTIR analysis (part 1). ....	68
Figure 26. (supplement S2) FTIR analysis (part 2). ....	69
Figure 27. (supplement S3) Histogram, demonstrating urinary precipitated CalCit level from non-stone and stone group.....	77



## Chapter 1 Background and Rationales

Urolithiasis or urinary stone disease is one of the main urologic health problems worldwide <sup>(1)</sup>. Most urinary stones are formed in the kidneys and called kidney stone. Globally, prevalence of kidney stone is progressively increasing <sup>(2)</sup>. Kidney stone is highly recurrent, and the recurrence rate is reported up to 66.9% in 2022 <sup>(3)</sup>. Kidney stone potentially causes serious consequences because it progressively damages kidneys and increases the risk of chronic kidney disease. Furthermore, the economic burden of kidney stone management is substantial <sup>(4)</sup>. Therefore, development of diagnostic tests for identifying people at risk of kidney stone development is required to prevent kidney stone formation and recurrence.

The risk factors of kidney stone formation include dietary habits, genetic predisposition, and environmental factors <sup>(5, 6)</sup>. According to the mineral composition of stones, the most common type of stones is calcium oxalate (CaOx, 75%-90%), followed by uric acid, calcium phosphate (CaP), struvite, apatite, and cystine stones <sup>(5)</sup>. Calcium and oxalate (Ox) are the main CaOx stone promoters whereas citrate is the most potent inhibitor of CaOx stone. Hypocitraturia and hyperoxaluria are well accepted as the crucial metabolic risk factors of CaOx stone formation and recurrence <sup>(6, 7)</sup>. In 2006, Youngjermchan et al. reported that hypocitraturia was the most frequent metabolic risk factor found in Thai stone patients <sup>(8)</sup>. Additionally, in 2009, Saepoo et al. also confirmed that hypocitraturia is the main metabolic risk factor observed in Thai patients <sup>(9)</sup>. Therefore, measurement of urinary citrate is necessary to estimate the risk of kidney stone development. The common techniques for measuring urinary citrate concentration include high performance liquid chromatography (HPLC), proton nuclear magnetic resonance (<sup>1</sup>H-NMR) spectroscopy, enzymatic assay, and liquid chromatography with tandem mass spectrometry (LC-MS/MS). Generally, these methods are time-consuming, expensive and require qualified operation skill.

Citrate is the well-known inhibitor of CaOx stone because it binds with calcium to produce a water-soluble calcium citrate (CaCit) compound. In contrast, the reaction of calcium and oxalate yields an insoluble CaOx compound/ crystal that further acts as a seed for CaOx stone formation. Citrate also inhibits growth and aggregation of CaOx crystals. Basically, CaOx (CaC<sub>2</sub>O<sub>4</sub>) stone formation is divided into 2 phases: early phase of aggregation, and later phase of crystallization and/or transformation <sup>(10)</sup>. Citrate exhibits its inhibitory role in both phases. In addition, citrate also has an important protective

role to renal tubular cells by preventing the crystal transformation from calcium oxalate dihydrate (COD) to calcium oxalate monohydrate (COM) <sup>(11)</sup>. We thought that the more citrate existing in urine would produce a more soluble CalCit complex that further prevent CaOx stone development. Therefore, we proposed that measurement of urinary CalCit might be an alternative method to be used for estimating the risk of CaOx urolithiasis development or for separating CaOx stone patients from non-stone subjects.

Since the formation of lithogenic crystals, specifically CaOx, calcium phosphate (CaP) and uric acid, is initial step in lithogenesis, measurement of the relative supersaturation of CaOx, CaP and uric acid are widely used for estimating the risk of kidney stone development. The likelihood of CaOx kidney stone formation increases with higher supersaturation of CaOx and CaP <sup>(12)</sup>. In contrast, CalCit supersaturation and CalCit crystal formation, that is an inhibitory force for CaOx stone development, has never been investigated in kidney stone disease. Generally, urine citrate concentration in CaOx stone patients is lower than in healthy subjects. We proposed that after challenging urine sample with excessive calcium the formation of urinary CalCit complex in CaOx stone patients was lower than in non-stone subjects. Development of method to measure this CalCit complex should be a reflective of urinary citrate, and might be able to distinguish CaOx stone patients from the healthy population.

Based on literature review and our preliminary study, we proposed to measure the precipitated CalCit from urine by a simple colorimetric indicator displacement assay (IDA) using murexide (Mrx) as an indicator. Mrx is a purple indicator that reacts with copper ions ( $\text{Cu}^{2+}$ ) and yields a yellow complex (maximum absorption at 457 nm). After adding citrate<sup>3-</sup>, Mrx is displaced by citrate<sup>3-</sup>, and the stable complexes of citrate- $\text{Cu}^{2+}$  are formed <sup>(13)</sup>, leaving free Mrx in the solution and turning the color of solution to purple. The purple signal (maximum absorption at 522 nm) of the free Mrx dye is proportionated to the amount of citrate in the solution, and the displacement time is considerably rapid that is completely displaced within less than 1 minute <sup>(13)</sup>. Mrx IDA had been used as a tool for measuring citrate esterification property <sup>(14, 15)</sup>, calcium level <sup>(16, 17)</sup>, and phenolic acid level <sup>(18)</sup> in many food samples. Some urinary phenolic acids can also displace Mrx, and they might interfere the CalCit measurement <sup>(18)</sup>. Therefore, measuring CalCit in urine sample directly by Mrx IDA is not recommended. To decrease this interfering effect, we proposed to induce CalCit supersaturation in

urine sample first by adding excessive calcium and precipitate CalCit using ethanol. Then, the precipitated CalCit was re-dissolved before measurement of CalCit by the Mrx IDA.

In this study, we aimed to develop a new in-house method for measuring the total amount of CalCit precipitated in 24-h urine sample using the Mrx IDA. CalCit supersaturation in urine sample was induced by addition of excessive calcium chloride. The urinary CalCit was precipitated by the ethanol precipitation, and the precipitated CalCit was re-dissolved in HCl for further measuring citrate by Mrx IDA. Method validation to demonstrate the suitability of our new test for measuring CalCit precipitates in urine was performed, and the method validation parameters including selectivity, linearity, limit of blank (LoB), limit of detection (LoD), limit of quantitation (LoQ), precision, accuracy, reproducibility was calculated and reported. Finally, diagnostic accuracy testing of our new test was carried out in 24-h urine samples obtained from CaOx urolithiasis patients and non-stone subjects. Diagnostic values of the new test including sensitivity, specificity, accuracy, positive predict value, and negative predict value were calculated and reported. To our knowledge this was the first study proposed to measure CalCit precipitation in urine as a CaOx stone prevention indicator. We did hope that it could provide a clinical usefulness for screening or estimating the risk of CaOx urolithiasis development.

**Keywords:** Kidney stone, Calcium oxalate, Calcium citrate, Murexide, Indicator displacement assay, Screening test

#### Research questions

Could measurement of CalCit precipitation in urine using Mrx IDA be successfully established, and be useful for screening CaOx kidney stone disease?

#### Hypotheses

1. The urinary CalCit precipitation measurement using Mrx IDA could be successfully developed.
2. The newly established method was validated to be suitable for measuring CalCit precipitation in urine samples.



3. The urinary CalCit precipitation measurement by Mrx IDA had a good performance to identify people at risk of CaOx stone formation.

#### Objectives

1. To develop the Mrx IDA for measuring CalCit precipitation in 24-h urine samples.
2. To perform the method validation of the newly established Mrx IDA for measuring urinary CalCit precipitation.
3. To evaluate the diagnostic accuracy, precision, positive and negative predict value of the newly established Mrx IDA for CaOx urolithiasis.

#### Expected benefits

1. The measurement of CalCit precipitation in urine using Mrx IDA was successfully established.
2. A new Mrx IDA for measurement of urinary CalCit precipitation that had a high accuracy for diagnosing CaOx urolithiasis.

#### Conceptual framework

CaOx is the most common type of kidney stone. Citrate is the best-known inhibitor of CaOx stone formation and recurrence. To help estimate the risk of CaOx stone formation and recurrence, citrate concentration in urine must be determined. Although HPLC is widely used for determination of urinary citrate concentration with a high accuracy, it is time-consuming and costly. In addition, sophisticated instrument, high technical skill, and complicated sample preparation are required. We propose here a new Mrx IDA-based method for measurement of precipitated CalCit in urine that could be indirectly reflected the concentration of urinary citrate. We believe that this new method is robust, quick, simple, inexpensive, and be able to be use as a screening test for CaOx urolithiasis.

This study consisted of three main parts; 1) developing the Mrx IDA for measurement of CalCit precipitated in urine, 2) performing the method validation to evaluate the suitability of the newly established method for CalCit measurement, and 3) conducting the clinical validation to investigate the diagnostic performance of the new test for CaOx urolithiasis. The conceptual framework and the schematic workflow of the proposed study are shown in Figure 1 and Figure 2, respectively.

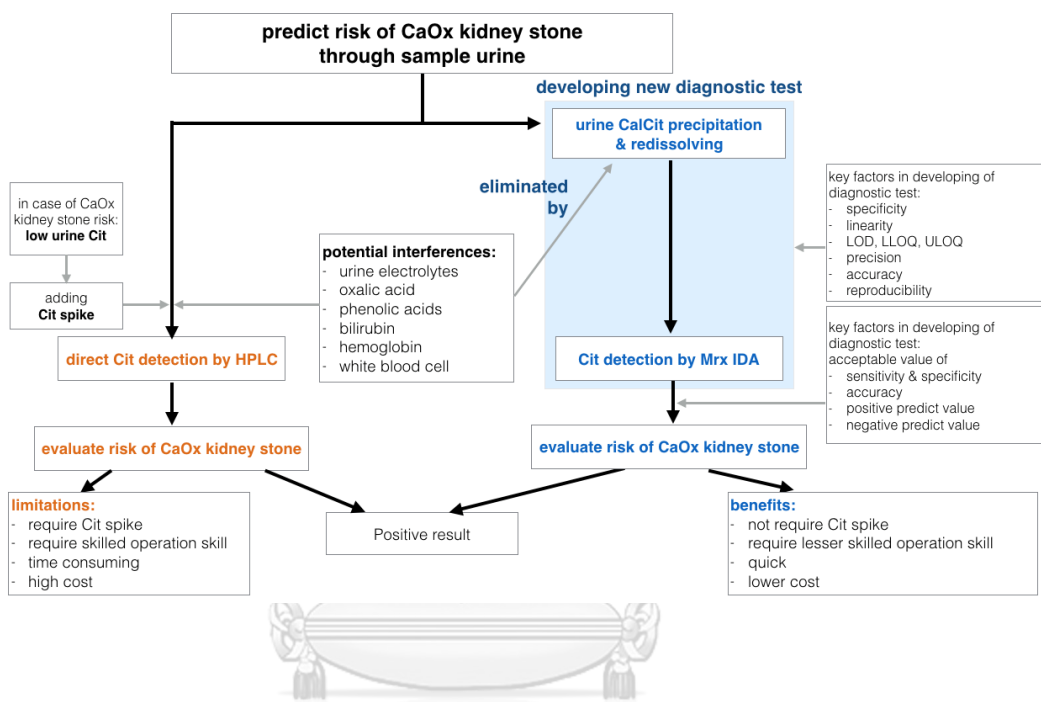


Figure 1. Conceptual framework of the present study.

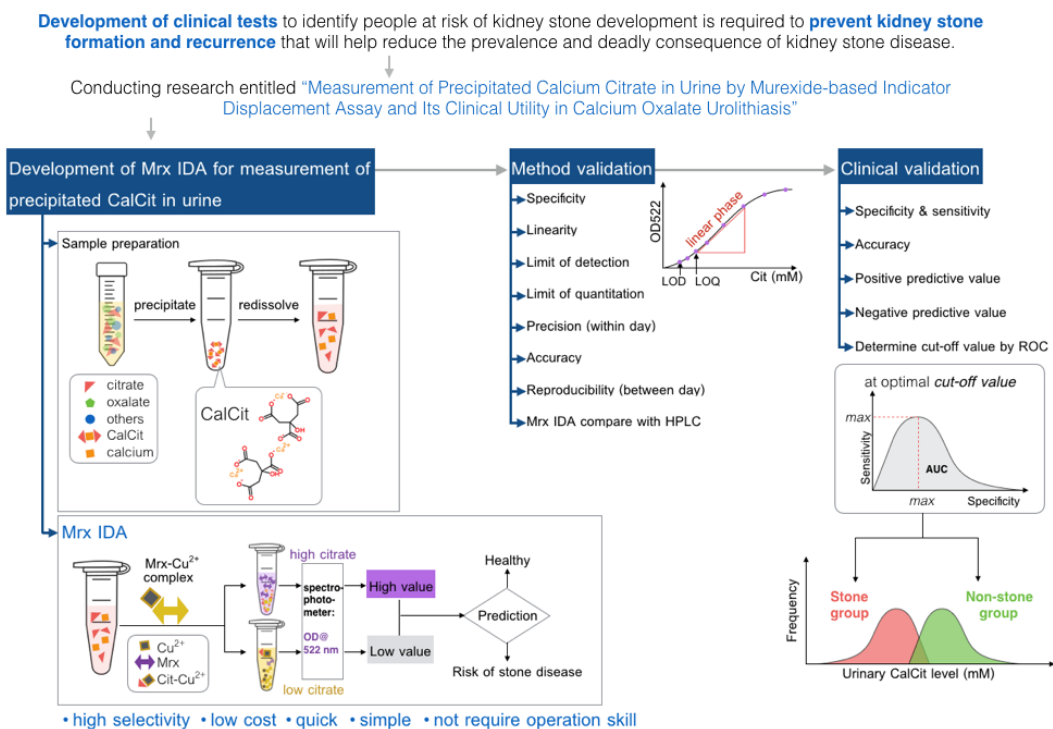


Figure 2 Schematic workflow of the present study.

## Chapter 2 Review related literature

### 2.1 Urinary stone disease epidemiology

Urolithiasis is a condition with calcified masses, called stones, formed in the urinary tract. Most urinary stones are formed inside the kidneys, called kidney stones. Kidney stones progressively impair kidney function and eventually cause chronic kidney disease and end-stage renal disease <sup>(19-21)</sup>. Several evidences demonstrate that kidney stone disease closely relates to metabolic syndrome <sup>(3, 21-24)</sup>. It increases the risk of cardiovascular disease, diabetes, obesity, and hypertension <sup>(20)</sup>, and vice versa <sup>(1)</sup>. Unsurprisingly, the global prevalence of both metabolic syndrome and kidney stone is continuously rising <sup>(25, 26)</sup>. The study by Qian et al. showed that kidney stone prevalence increased by 48.57% <sup>(25)</sup>. The incident cases of kidney stone increases from 77.78 million in 1990 to 115.55 million in 2019 <sup>(25)</sup>. In 2018, the kidney stone prevalence was reported at 5%-19.1% in the West, Southeast, and South Asia <sup>(5)</sup>. Thailand is also in the “stone belt region” (Figure 3) and increased prevalence of kidney stone is corresponded well with the increased obesity prevalence (Figure 4) <sup>(27, 28)</sup>. The disease may present with symptoms such as chronic, episodic flank pain, hematuria, or may even be asymptomatic <sup>(29)</sup>. Stone disease is highly recurrent. The high recurrence rate of kidney stone was reported in 2022 at 66.9% <sup>(3)</sup>. The earlier studies reported the 5-year recurrence rate at 50% <sup>(30, 31)</sup>. The study in 2019 reported that majority of recurrent kidney stone patients present with an underlying diseases such as overweight/ obesity, hyperlipidemia, hyperuricemia and hyperglycemia <sup>(32)</sup>.

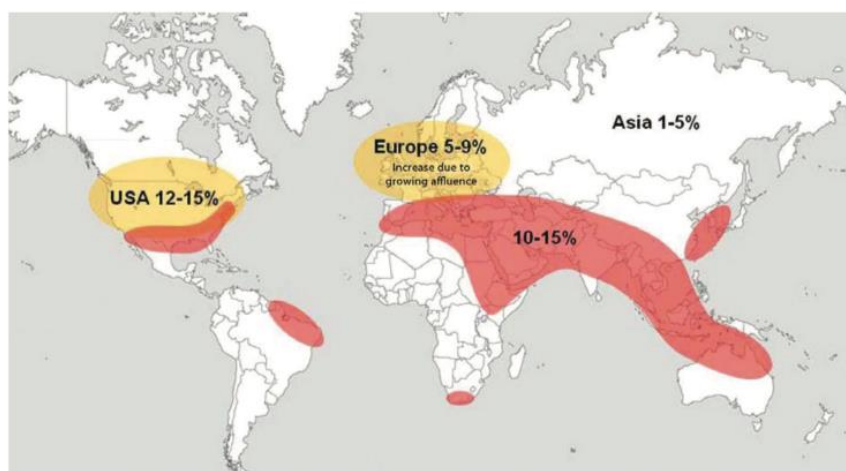


Figure 3 Stone belt (red) extends all the way around the world (adapted with permission from the publication by Fisang and colleagues) <sup>(27)</sup>.



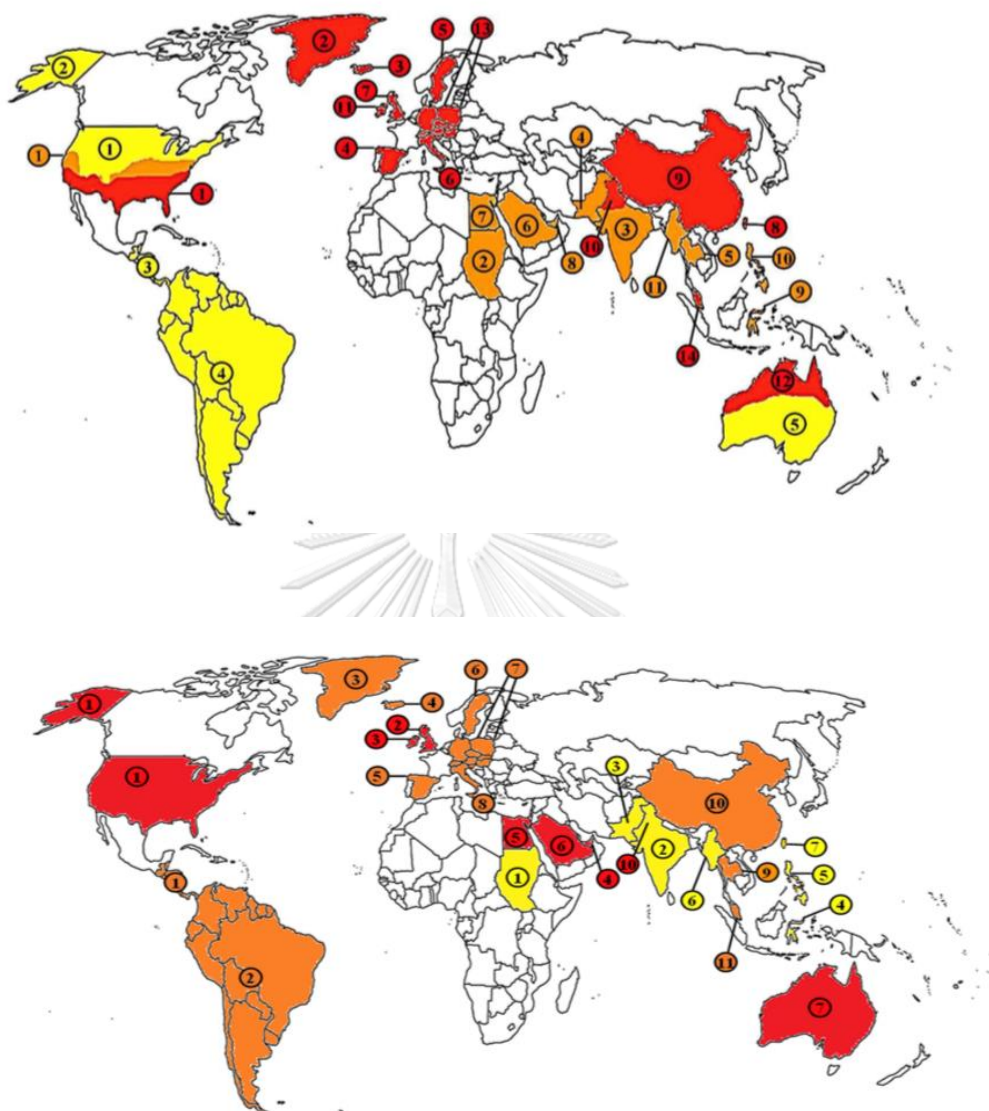


Figure 4 Comparison of world map projection of magnitude of kidney stone prevalence (upper) and obesity prevalence (lower) <sup>(28)</sup>. Magnitude of prevalence: high (red), medium (orange), low (yellow).

## 2.2 Types of kidney stones

The stone was formed from urinary component. The stone consists of over 90% mineral and less than 10% organic compounds <sup>(33)</sup>. Most (62.6%) stone composition are heterogenous <sup>(34)</sup>. Stones are normally classified into calcium stone and non-calcium stone. The most common type of stone is CaOx (75-90% of cases), followed by calcium phosphate (CaP, 20% of cases) or a mixture of CaOx and CaP. The non-calcium stone includes uric acid, struvite (magnesium ammonium phosphate), and cystine. These uncommon stone types can be found more, and they are usually related to disease conditions, such as obesity, diabetes, bacterial infection <sup>(23)</sup>. Some types of stones relate to urinary pH. CaP and struvite stone associates with urinary pH >7, while uric acid stone associates to urinary pH <5 <sup>(19)</sup>. Generally, in western patient with CaOx stone, the hypercalciuria, hyperoxaluria and hypocitraturia are frequently found. Urinary calcium is more than 250 mg per day in female, and more than 300 mg/day in male, while the urinary oxalate is more than 40 mg per day. Furthermore, the urinary citrate is less than 325 mg per d <sup>(35)</sup>. In Thailand, the CaOx stone is the most common type (70%) <sup>(36)</sup>. In 2006, Youngjermchan et al. reported that hypocitraturia was the most frequent metabolic risk factor found in Thai stone patients <sup>(8)</sup>. Additionally, in 2009, Saepoo et al. also confirmed that hypocitraturia is the main metabolic risk factor observed in Thai patients <sup>(9)</sup>. Thai patient with hypocitraturia was reported at <200 mg per day (Figure 5) <sup>(8,9)</sup>.

The CaOx stone is initially formed in urine supersaturation, then forming a CaOx crystallization (or nucleation), followed by crystal growth and aggregation, and further becoming a stone. The CaOx crystallization has 3 forms: CaOx monohydrate (COM;  $\text{CaC}_2\text{O}_4 \cdot \text{H}_2\text{O}$ ), dihydrate (COD;  $\text{CaC}_2\text{O}_4 \cdot 2\text{H}_2\text{O}$ ), and trihydrate (COT;  $\text{CaC}_2\text{O}_4 \cdot 3\text{H}_2\text{O}$ ). COM or COD is common form found in CaOx stone <sup>(37)</sup>.

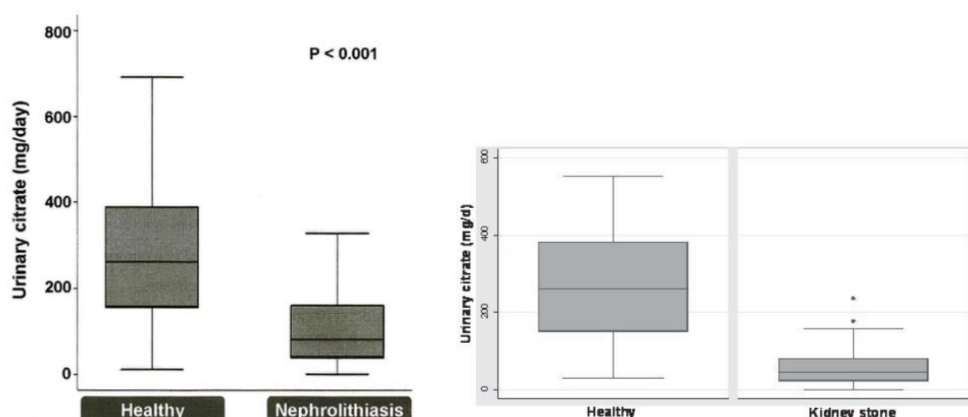


Figure 5 Urinary citrate level in Thai healthy individuals and patient with urolithiasis. Left) from study of Youngjermchan et al. (2006)<sup>(8)</sup>, and from study of Saepoo et al (2009)<sup>(9)</sup>.

### 2.3 Cause and risks factor of kidney stone disease

The etiology of stone formation is multifactorial involving both intrinsic and extrinsic factors. The intrinsic factors include age, gender, body mass index, and genetic background while the extrinsic factors include dietary intake, lifestyle, climate, occupation, drugs, and stress<sup>(5,6)</sup>.

The kidney stone prevalence normally begins after 20 years old<sup>(38)</sup>. The peak of prevalence was reported in between the age of 40 and 60 years old in males<sup>(38)</sup>. In females, the incidence rate is higher at almost 30 years old and lower rate after 50 years old<sup>(38,39)</sup>. The human gene polymorphism study indicated that homozygous GG of rs11567842 SNP in *NaDC-1* gene has a protective role for hypocitraturia, while the homozygous AA of this SNP has a higher risk for kidney stone recurrence<sup>(6)</sup>. The arid climate, outdoor-occupation, and high temperature-related work increase risk of dehydration leading to urine supersaturation which is the initial step of kidney stone formation<sup>(19)</sup>. Interestingly, several mechanisms of chronic metabolic disease have been proposed to relate to kidney stone formation. The increased urinary secretion of calcium, uric acid, phosphorus, and oxalate in hyperglycemic patients may lead to further stone formation<sup>(24)</sup>. The vascular dysfunction may cause the formation of calcium plaque on interstitial tissue of the renal papilla<sup>(24)</sup>. The change in blood pressure in hypertension may affect the urinary microbiome and promote kidney stone formation<sup>(3)</sup>. Oxidative stress has a vital role in CaOx stone formation<sup>(40,41)</sup>. Dietary factors that lead to urine



supersaturation, hyperoxaluria and hypocitraturia, such as inadequate fluid intake, too much oxalate intake, too low citrate intake, and/or low anti-oxidant diet, are the major causes of stone formation and recurrence. Our study indicated that consumption of HydroZitLa, which mainly contains citrate and antioxidants, can prevent CaOx stone formation in both *in vitro* and *in vivo* models <sup>(4)</sup>.

#### 2.4 Citrate and CaOx stone formation

The best-known inhibitor of CaOx stone formation and recurrence is citrate. Citrate can prevent CaOx stone in both pre-crystallization and crystal transformation phases.

At the pre-crystallization stage, citrate ion competitively binds to free  $\text{Ca}^{2+}$  ion, which delays oxalate ion ( $\text{C}_2\text{O}_4^{2-}$ ) binding to  $\text{Ca}^{2+}$  ion. Additionally, carboxylate group of citrates can bind to calcium at surfaces of CaOx species (such as,  $\text{CaHC}_2\text{O}_4^+$  or  $\text{CaC}_2\text{O}_4^0$ ) to form the negatively charged outer shell (zeta potential =  $-39.2 \pm 2.0$  mV) of amorphous CaOx (a non-crystalline stage with unclear shape) (Figure 6). The citrate shell prevents a transition from CaOx nucleation to aggregation. Without citrate CaOx has zeta potential close to zero that promptly leads to aggregation <sup>(10)</sup>.

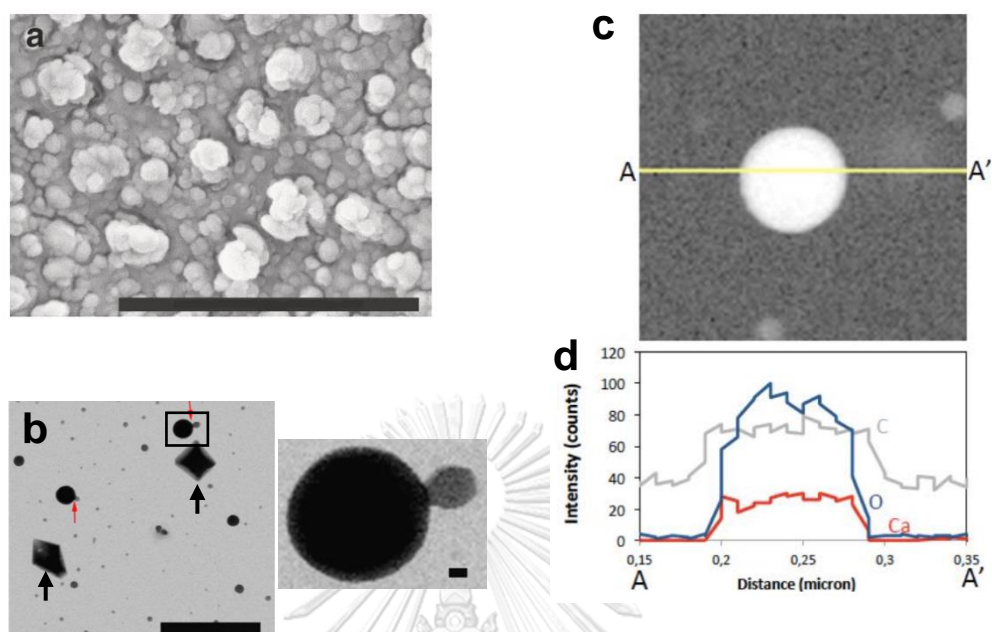


Figure 6 Amorphous CaOx nanoparticle. a) Cryo-ESEM image of shape of CaOx precipitated with citrate. b) TEM image CaOx precipitated with citrate. The rounded nanoparticles seem to grow by aggregation of smaller nanoparticles. The diamond-shaped of CaOx crystals (COD) are also showed (black arrow). Scale bar: 200 nm, 10 nm (inset). c) TEM image of the edge of an amorphous CaOx nanoparticle displaying about 20 nm thick rim. d) line-profile of energy-dispersive X-ray spectroscopy analysis (along the line A-A' depicted in the TEM image) showing an increase in C (carbon, from carboxylic group) in the outer part of the sphere <sup>(10)</sup>.

Citrate also has an important role to protect renal cell damage by inhibiting COD-to-COM transformation. During the CaOx crystal transformation, enough amount of citrate can attract more water molecules to facilitate COD formation, and citrate can also stabilize COD and inhibit CaOx growth. COD is a precursor of COM transformation, and it is more soluble than COM<sup>(33, 42)</sup>. COD is the most commonly CaOx crystals found in healthy urine. In contrast, kidney stone urine contains COM more than COD<sup>(43)</sup>. COD shows a lower affinity to renal epithelial cells than COM. Therefore, COD is routinely flushed out by the urinary flow. Study showed that the COD exhibits a lower cell toxicity than COM with same crystal size (Figure 7)<sup>(43)</sup>. The proposed mechanism is that COD induces expression of osteopontin (the crystal adhesion molecule) lower than COM that further causes lesser crystal adhesion and lesser cell membrane injury<sup>(7, 43)</sup>. Furthermore, exposure of COM to renal tubular cells causes several cellular changes such as, increased production of hyaluronic acid, osteopontin, and fibronectin, enhanced cell injury, activated inflammatory response, and increased reactive oxygen species production<sup>(44)</sup>. In conclusion, citrate protects renal epithelial cell damage from CaOx crystals by stabilizing COD and inhibiting COM growth and aggregation.

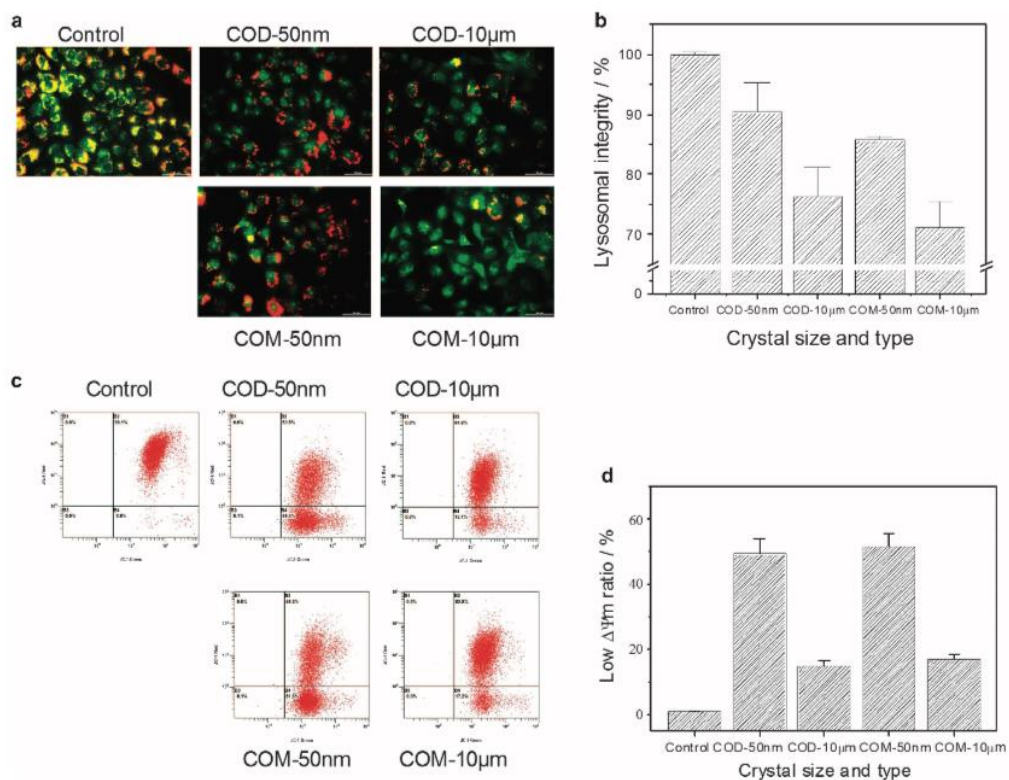


Figure 7 Effect of COD and COM on Vero cell death<sup>(43)</sup>. a) Fluorescence microscope observation of live cell (green), dying cell (yellow), and dead cell (red). b) Lysosomal integrity in Vero cells, detected by red fluorescence, which represented unruptured lysosomes. c) Flow cytometric data of mitochondrial membrane potential and d) quantitative histogram of that.

**2.5 Measurement of urinary citrate** Urinary citrate level is clinically useful for screening, and prediction of kidney stone formation. There are many techniques used to measure urine citrate such as high-performance liquid chromatography (HPLC), proton nuclear magnetic resonance ( $^1\text{H-NMR}$ ) spectroscopy, enzymatic assay, or liquid chromatography with tandem mass spectrometry (LC-MS/MS). However, these methods are time-consuming, and require qualified operation skill, expensive kits and sophisticated instruments. The new method that is simple, time-and-cost-effective, and highly specific to citrate must be developed. HPLC has been widely used for urinary citrate measurement with high specificity and high sensitivity <sup>(45-47)</sup>. However, there are complicated steps for sample preparation and derivatization such as addition of barium hydroxide, tri-n-octylamine-chloroform/phosphoric acid, and sulfuric acid. In our experience, the urinary citrate levels in kidney stone urine samples are very low. It needs to spiked with known concentration of citrate to be able to detect, and it is not much practical.  $^1\text{H-NMR}$  spectroscopy can measure profile of organic compounds with rapid, specific, and nondestructive measurement. It has been used to measure urine citrate and other compounds in several studies <sup>(48-52)</sup>. However, urinary citrate was analyzed together with other metabolites, such as hippurate, which is a derivative from citrate cycle. Therefore, the amount of urinary citrate may be disturbed from other metabolites, especially those metabolites related to gut microbiota <sup>(48, 52)</sup>.  $^1\text{H-NMR}$  spectroscopy also needs qualified operation skill, and sophisticated instruments. However,  $^1\text{H-NMR}$  is claimed that it needs lesser sample preparation and has a lower operating cost than the LC-MS/MS <sup>(48)</sup>. จุฬาลงกรณ์มหาวิทยาลัย

Urine citrate level have been measured by coupled enzymatic assay <sup>(53, 54)</sup>. The citrate is first converted to oxalacetate by citrate lyase. The coupling enzymes, e.g., L-malate dehydrogenase, oxaloacetate decarboxylate, and L-lactate dehydrogenase, further convert oxalacetate into other products, in parallel with a use of NADH. The level of NADH consumption is used to calculate the level of citrate. The reference value of urinary citrate level determined by enzymatic assay was  $<1.2 \text{ mM}/12\text{-h}$  <sup>(55)</sup>. The enzymatic test is highly specific, but it is still expensive <sup>(45, 56)</sup>. Furthermore, it yields a low recovery rates, because it is interfered by phosphate and sulphates <sup>(45)</sup>.

LC-MS/MS has been developed to measure urine citrate and oxalate <sup>(57, 58)</sup>. However, LC-MS/MS is still time-consuming <sup>(59)</sup>. Accuracy and reproducibility of LC-MS/MS are less than 3% <sup>(45)</sup>. It is reliable but very expensive. Summary of methods for urinary citrate measurement is shown in Table 1.

Table 1. Comparison of urine citrate measurement among various methods.

	Directly measurement to urinary citrate	Purified citrate from sample urine	Time consuming	Cost consuming	Sophisticated instruments	Need qualified operation skill
	No, added up					
HPLC	by many chemicals or citrate spike	No	High	High	Yes	Yes
<sup>1</sup> H-NMR	Yes	No	High	High	Yes	Yes
Enzymatic assay	No	No	High	Extremely high	Probably, no	Yes
LC-MS/MS	Yes	No	High / low	High	Yes	Yes
Mrx IDA in this study (expected benefit)	Yes	Yes	Low	Low	No	No

## 2.6 Measurement of citrate<sup>3-</sup> in the form of CalCit by colorimetric assay.

There is a study that detect urinary citrate by the production of Fe<sup>3+</sup>-citrate complex <sup>(56)</sup>. However, that study had a limitation that the reaction must be maintained at pH 2 while the three pKa of citrate are at 3.13, 4.76, and 6.40 <sup>(60, 61)</sup>. There is another colorimetric method that measure citrate<sup>3-</sup> in the HEPES buffer, pH 8. That is Mrx IDA, detecting citrate<sup>3-</sup> based on indicator displacement assay. Mrx or murexide is also called ammonium purpurate, ammonium salt of purpuric acid (ammonium 2, 6-dioxo-5-[(2, 4, 6-trioxo-5-hexahydropyrimidinylidene)amino]-3H-pyrimidin-4-olate). Mrx acts as the purple indicator. When combined with Cu<sup>2+</sup>, it generates a yellow Mrx-Cu<sup>2+</sup> complex (Figure 7). Citrate<sup>3-</sup> used its chelating activity to bind to Cu<sup>2+</sup> in HEPES buffer, pH 8. The purple Mrx was replaced by citrate<sup>3-</sup> in dose-dependent manner. The citrate<sup>3-</sup>-Cu<sup>2+</sup> complex was stable and the reaction was very rapid, within less than 1 minute <sup>(13)</sup>. In an early study by Graffmun et al. in 1974, Mrx was used as an indicator of Cu<sup>2+</sup>-citrate<sup>3-</sup> titration procedure <sup>(62)</sup>. Later, Mrx was utilized as an indicator in the Mrx-Ni<sup>2+</sup>-based IDA for detecting histidine in the study by Sun et al. <sup>(63)</sup>. Mrx-Cu<sup>2+</sup>-based IDA had been used as the tool to measure citrate esterification property <sup>(14, 15)</sup>, calcium level <sup>(16, 17)</sup>, and phenolic acid levels <sup>(18)</sup> in food studies. This Mrx IDA has a low detection limit at 19.1 nM, and operating range between 0.2 and 8.2 μM. The purple signal of displaced Mrx was detected at 522 nm, while the yellow Mrx-Cu<sup>2+</sup> complex was measured at 457 nm. The specificity of Mrx IDA to citrate was tested among several urine co-existing minerals (cations), including K<sup>+</sup>, Mg<sup>2+</sup>, Fe<sup>3+</sup>, Ca<sup>2+</sup>, Zn<sup>2+</sup>, Na<sup>+</sup> <sup>(13)</sup>. However, the effect of phenolic compounds to interfere the Mrx IDA have not been explored. The phenolic compound was reported in human urine, such as gallic acid <sup>(64)</sup>. Many phenolic compounds, including catechin, gallic acid, epigallocatechin-3-gallate (Figure 11) had suggested that they have a benefit in preventing of kidney stone development <sup>(65-67)</sup>.

According to our preliminary study, phenolic compounds (gallic acid and catechin) can also displace Mrx from the Mrx-Cu<sup>2+</sup> complex, acting as interfering substance in the CalCit measurement by Mrx IDA.

The Mrx IDA was applied in the part of microfluidic paper-based analysis for detecting citrate<sup>3-</sup> in kidney stone urine <sup>(68)</sup>. The urine sample was not modified and was directly dropped on analytic paper. The interference from co-existing phenolic acid may be not concerned and excluded in that study.

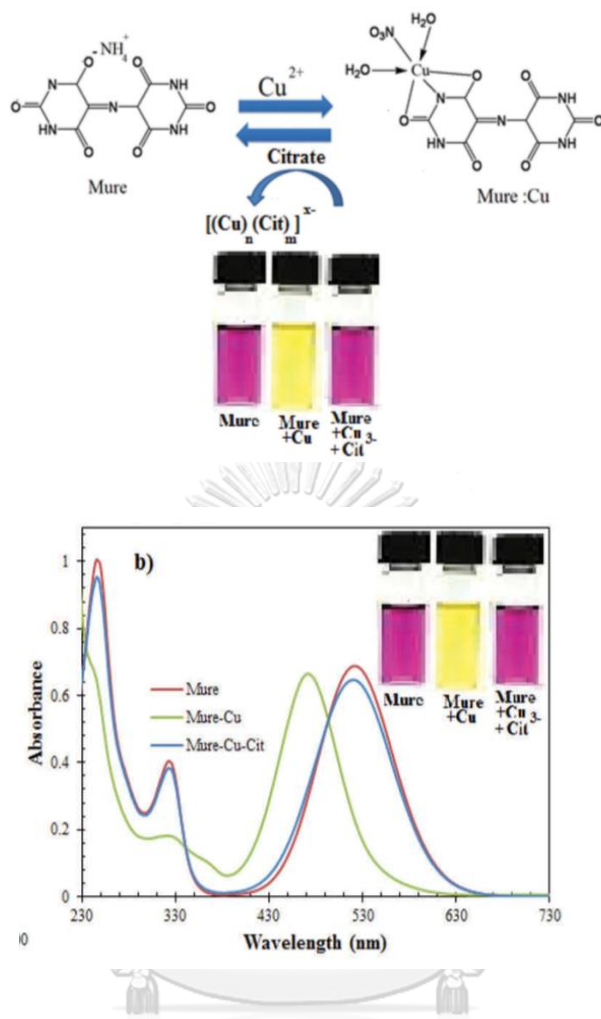


**Figure 8.** Principle of citrate detection by Mrx IDA<sup>(13)</sup>. The Mrx was combined with  $\text{Cu}(\text{NO}_3)_2$ , in 10 mM, HEPES buffer, pH 8. Citrate<sup>3-</sup> in basic buffer chelated  $\text{Cu}^{2+}$  from the yellow  $\text{Mrx}-\text{Cu}^{2+}$  complex (maximum absorbance at 457 nm). The purple color of displaced Mrx was proportioned to the concentration of citrate (maximum absorbance at 522 nm).



## 2.7 Calcium citrate precipitation

Citrate<sup>3-</sup> in the urine sample was extracted by precipitation of calcium citrate (CalCit) crystal (Figure 8). FTIR spectrum of CalCit is shown in Figure 9. Citric acid is the well-known organic chemical in Krebs's cycle. It also had a wide application in food additives, cosmetics, buffering, chelating agents, pharmaceuticals<sup>(69)</sup>. The various method to extract citrate<sup>3-</sup> and/or citric acid from liquid were reviewed, for example: extracting by 1-octanol/n-heptane solutions of trialkylamine<sup>(70)</sup>, tri-n-octylamine which associated with chloroform, or methyl isobutyl ketone<sup>(71)</sup>. However, the simplest way seemed precipitation citrate with calcium.

In citric acid fermentation industry processing, citric acid was precipitated into CalCit through calcium carbonate in base conditions<sup>(69, 72)</sup>. The traditional method to re-dissolve CalCit was the use of H<sub>2</sub>SO<sub>4</sub>. The harmful byproduct such as calcium sulfate, was produced. In addition, the process was costly and complex. CalCit was also used as a calcium source for bone grafting. In biomaterial studies, CalCit was precipitated by EtOH<sup>(72, 73)</sup>. EtOH can change the free energy of reaction and establish supersaturation of solution that led to CalCit nucleation and further growth. The ratio of EtOH per water was critical for the shape and amount of CalCit precipitates<sup>(72, 74)</sup>. The EtOH was extensively used as a desolvating agent in nanoparticle fabrication studies<sup>(75, 76)</sup>. The desolvation procedure was based on the same principle described above. EtOH generated supersaturation condition and led to initiation of nanoparticle formation. The study by Chalermnon et al. fabricated CalCit nanoparticle by EtOH desolvation to be used for encapsulating metformin derivatives<sup>(77)</sup>. In this study, we expected that urinary CalCit was extracted by excessive Ca<sup>2+</sup> challenging and EtOH precipitation. By doing so, interfering effect of phenolic compounds in Mrx IDA can be avoided.

Taken together, this is the first study to measure urinary CalCit precipitation by Mrx IDA, and this method could be used to indirectly detect urine citrate<sup>3-</sup> level indirectly, which indicates CaOx stone prevention indicator.

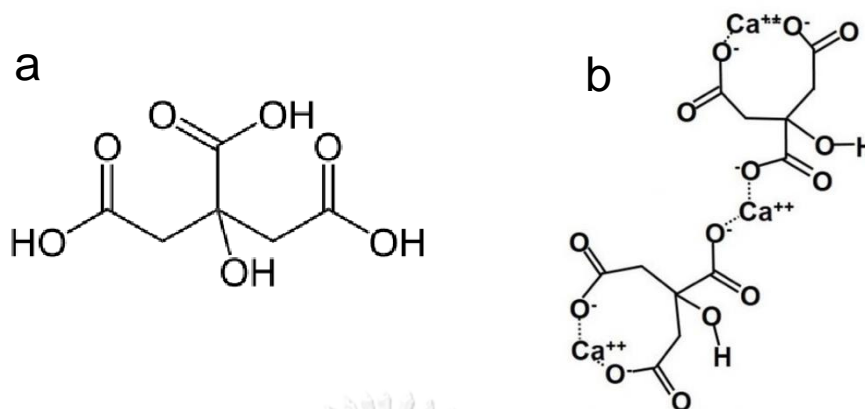


Figure 9 Structure of citric acid and Calcit. a) citric acid <sup>(78)</sup> and b) CalCit <sup>(79)</sup>.

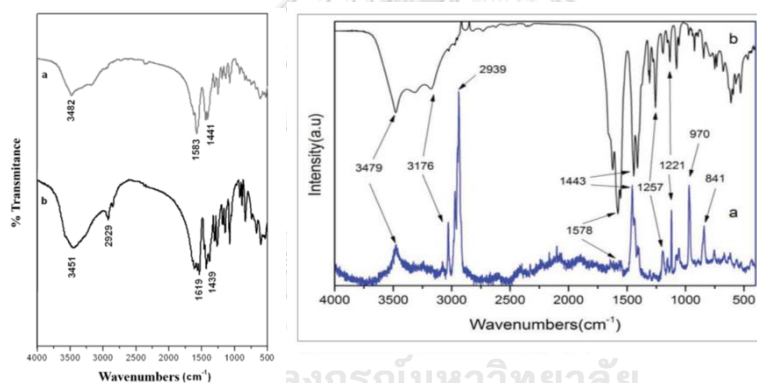


Figure 10 FTIR of CalCit. left) The FTIR of CalCit standard (a) and tablet (b) <sup>(80)</sup>. right) The FTIR (black line) and RAMAN (blue line) spectrum of CalCit precipitated by EtOH <sup>(72)</sup>. The specific absorption of Ca-O bond (bonding between Ca and carboxylic groups of citrates) was indicated by the peak range of 1439-1443  $\text{cm}^{-1}$  (symmetric stretching vibration) and of 1578-1619  $\text{cm}^{-1}$  (anti-symmetric stretching vibration).

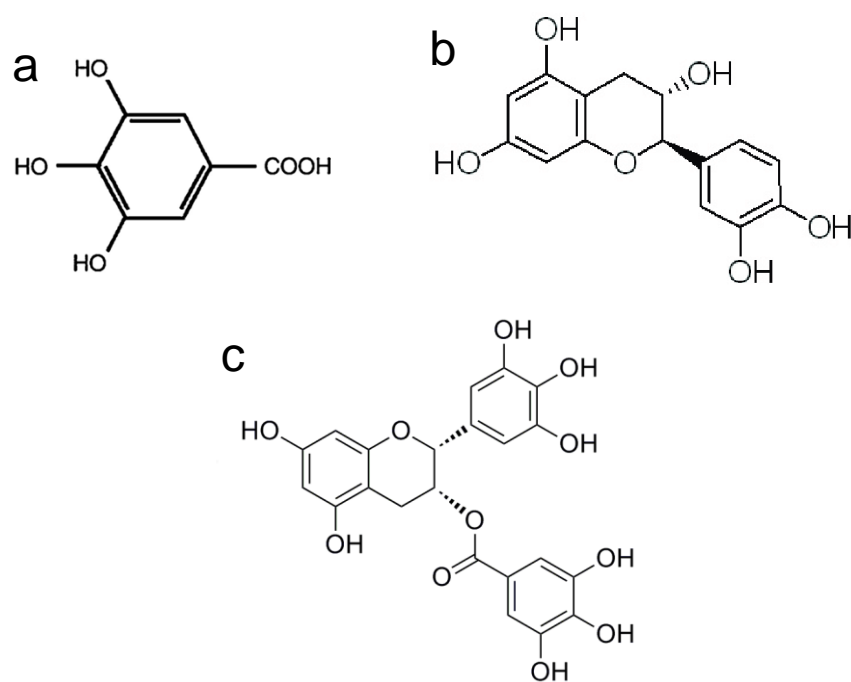


Figure 11 Structure of phenolic acid. a) gallic acid <sup>(81)</sup>, b) catechin <sup>(82)</sup>, c) epigallocatechin-3-gallate

<sup>(83)</sup>

## Chapter 3 Research methodology

### 3.1 Study design

This study was divided into three parts. Part 1 was involved development of method for measuring precipitated CalCit in urine sample based on IDA principle. Part 2 was a method validation study to evaluate whether the newly developed analytical method was suitable for the intended use. Part 3 was a cross-sectional study to measure precipitated CalCit in 24-h urine samples from non-stone forming individuals and urolithiasis patients. The IDA-based method for measurement of precipitated CalCit in urine developed in this study used Mrx dye as an indicator. Therefore, it was called Mrx IDA test. In part 3, the clinical performance of the Mrx IDA for separating CaOx urolithiasis from non-stone subjects was investigated.

### 3.2 Urine specimen collection

The 24-h urine samples used in this study were from our previous project, entitled “Test accuracy of urinary calcium oxalate crystallization index (COCI) for diagnosis of urolithiasis, and development of an innovative quantum dot nanoparticle-based method for determination of urinary oxalate” (IRB:286/59). The urine samples had been stored at  $-20^{\circ}\text{C}$  until testing. The 24-h urine samples were collected from non-stone forming healthy individuals ( $n = 122$ ) who resided in the Kaedam District, Mahasarakham province and urolithiasis patients ( $n = 141$ ) who admitted to Mahasarakham Hospital, during 2017 and 2018. The stone condition was confirmed by computed tomography (CT) scan. The stone type was identified by Fourier-transform infrared spectroscopy (FTIR). Forty-five stone patients were diagnosed with CaOx stone.

### 3.3 24-h urine sample preparation

The frozen 24-h urine samples were thawed and filtered through the 0.22  $\mu\text{m}$  membrane before testing.

**Part 1:** Development of Mrx IDA method for measuring precipitated CalCit in urine samples

### 3.4 CalCit precipitation

For the experiment, 800  $\mu\text{l}$  of urine sample or artificial urine (AU) with a known concentration at 0.6 and 1.2 mM of  $\text{Ca}_3\text{Cit}_2$  (positive control/ control material) was placed into a 1.5-ml tube. The positive control was prepared from stock  $\text{Ca}_3\text{Cit}_2$  solution (20 mM, dissolved in HCl, and diluted with HEPES buffer). The AU was prepared from chemicals shown in table 2, and the pH was adjusted to 6.2. Citrate has 3 pKa, and the third pKa ( $\text{pKa}_3$ ) were 6.4<sup>(60, 61)</sup>. Therefore, if the urine sample pH was below 6.4<sup>(84)</sup>, citrate will be in the protonated form, and it would not be completely combined with calcium ions and it would not be completely precipitated. In our precipitation procedure, urine samples with pH below 6.4 were added with 16  $\mu\text{l}$  of 1 N NaOH in order to increase the pH of urine samples. To induce CalCit precipitation, 50  $\mu\text{l}$  of 1M  $\text{CaCl}_2$  solution was added to the sample, 800  $\mu\text{l}$ ). The first sediment (potentially contained CaOx) was formed, and it was removed through centrifugation at 14,000  $\text{xg}$  for 5 minutes at room temperature. The first supernatant (contained soluble CalCit) was transferred to a 15-ml tube pre-filled with 3.4 ml of 100% ethanol (EtOH). The final concentration of EtOH was 80% (v/v) that caused CalCit in the solution precipitated. This second sediment (contained CalCit crystals) was collected by centrifugation at 20,000  $\text{xg}$  for 10 minutes at 4°C. The second supernatant (contained EtOH) was discarded. The remaining EtOH in the 2<sup>nd</sup> precipitate was removed by heating at 90°C for 10 minutes. The dried CalCit-containing sediment was kept at -20°C for further testing. Since the precipitated CalCit sediment was not soluble in water, but dissolved well in acid solution  $\text{pH} < 2$ <sup>(85)</sup>, it was re-dissolved in 0.04 N HCl (100  $\mu\text{l}$ ,  $\text{pH} < 1$ ) and then diluted with DI water to the original volume of urine sample (800  $\mu\text{l}$ ). To be completely dissolved, the re-dissolved CalCit was sonicated using the water bath sonicator (Elmasonic S30H, 37kHz) for 1-5 minutes at room temperature.

**Table 2.** Formula of artificial urine is modified from the AU-siriraj<sup>(86)</sup>. Citrate and oxalate were not added. The pH of the AU was adjusted to 6.2.

Composition	Chemical used	concentration
Urea	Urea	200 mM
Uric acid	Uric acid	1 mM
Creatinine	Creatinine	4 mM
NaCl	Sodium chloride	54 mM
KCl	Potassium chloride	30 mM
NH <sub>4</sub> Cl	Ammonium chloride	15 mM
CaCl <sub>2</sub>	Calcium chloride dihydrate	3 mM
MgSO <sub>4</sub>	Magnesium sulfate heptahydrate	2 mM
NaHCO <sub>3</sub>	Sodium carbonate	2 mM
Na <sub>2</sub> SO <sub>4</sub>	Sodium sulfate anhydrous	9 mM
NaH <sub>2</sub> PO <sub>4</sub>	Sodium dihydrogen phosphate monohydrate	3.6 mM
Na <sub>2</sub> HPO <sub>4</sub>	Disodium hydrogen phosphate anhydrous	0.4 mM



### 3.5 Mrx IDA and $\text{Ca}_3\text{Cit}_2$ standard preparation

The Mrx- $\text{Cu}^{2+}$  solution was freshly prepared. It consisted of Mrx dye and  $\text{Cu}(\text{NO}_3)_2$  dissolved in 10 mM HEPES buffer. This HEPES buffer was identified as the most suitable buffer for citrate measurement using the Mrx IDA <sup>(13, 87)</sup>. The Mrx-to- $\text{Cu}^{2+}$  concentration ratio was set at 1:1 <sup>(13)</sup>. The concentration of both Mrx and  $\text{Cu}^{2+}$  solution was 2.22 mM. Calcium citrate ( $\text{Ca}_3\text{Cit}_2$ ) was used as standard material to generate the standard curve. The concentrations were ranged from 0.2 to 2 mM. The  $\text{Ca}_3\text{Cit}_2$  standard material of each concentration was prepared by diluting a stock of 20 mM  $\text{Ca}_3\text{Cit}_2$  solution with HEPES buffer. The final pH of the standard  $\text{Ca}_3\text{Cit}_2$  were fallen between 3 and 7.

The Mrx IDA reaction was performed in a microplate wells. 20  $\mu\text{l}$  of standard  $\text{Ca}_3\text{Cit}_2$  (or precipitated CalCit sample) was mixed with 180  $\mu\text{l}$  of Mrx- $\text{Cu}^{2+}$  solution. The final concentrations of both Mrx and  $\text{Cu}^{2+}$  after adding the sample were 2 mM, and the total reaction volume was 200  $\mu\text{l}$ . The reaction was finished within 1 minute. The maximum absorption of displaced Mrx dye (purple) was measured at 522 nm by the UV-vis spectrometer (Multiskan™ GO Microplate Spectrophotometer, Skanit Software 4.1 Research Edition). The measurement was done in 5 replicates. The HEPES buffer was used as the blank control. The standard curve of  $\text{Ca}_3\text{Cit}_2$  is shown in Figure 11.  $\text{Ca}_3\text{Cit}_2$  concentrations over 1.4 mM reached the plateau phase because their OD at 522 nm were not significantly increased.

in 200  $\mu$ l of reaction  
 Final conc. Mrx-Cu<sup>2+</sup> = 2 mM, reacted with  
 Ca<sub>3</sub>Cit<sub>2</sub> Standard (in HEPES):

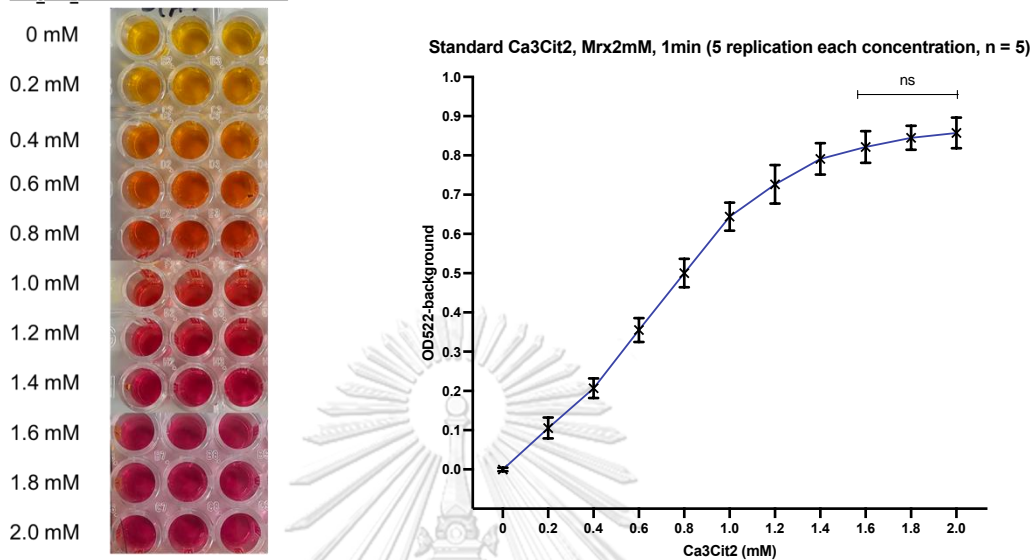


Figure 12. Standard curve of Mrx IDA using Ca<sub>3</sub>Cit<sub>2</sub> (0.2-2.0 mM) as standard material. Ca<sub>3</sub>Cit<sub>2</sub> concentrations over 1.4 mM reached the plateau phase because their OD at 522 nm were not significantly (ns) changed. The graph displays in mean. Error bars indicate standard deviation.



## Part 2: method validation study

### 3.6 Method validation

Principally, once a new analytical test was developed or established, method validation must be performed to show the test suitability. This involved assessing the accuracy, uncertainty, and traceability of the measurement assay. The method validation of the Mrx IDA for determining the precipitated CalCit level had be performed, including: <sup>(88, 89)</sup>

#### 1) Precision: repeatability (within-day precision) and reproducibility (within-laboratory precision)

The standard  $\text{Ca}_3\text{Cit}_2$  solutions (11 concentrations: 0, 0.2, 0.4, 0.6, 0.8, 1.0, 1.2, 1.4, 1.6, 1.8, 2.0 mM) were prepared in HEPES buffer, and then tested by Mrx IDA. The five replicates of each  $\text{Ca}_3\text{Cit}_2$  concentration were prepared, and performed with Mrx IDA for 5 days. The mean of OD522 of Mrx detection, mean with blank subtraction, standard deviation, % of relative standard deviation (RSD) was documented. The RSD is the absolute value of the % coefficient of variation (%CV) <sup>(90)</sup>. The standard curve was plotted and the linear phase was defined, through regression equation, slope, y-axis intercepts, and coefficient of determination ( $R^2$ ) which this value was  $\geq 0.99$  <sup>(91)</sup>. The repeatability (or within-day precision), and reproducibility (or within-laboratory) precision were determined by %CV was acceptable at <5% and <10%, respectively <sup>(91)</sup>.

#### 2) Accuracy and %yield of precipitation test

The two concentrations of  $\text{Ca}_3\text{Cit}_2$  within the linear range were prepared at 0.6, 1.2 mM as the material controls, as well as positive control. The 2 concentrations of  $\text{Ca}_3\text{Cit}_2$  in HEPES buffer were directly measurement. Parallely, these concentrations of  $\text{Ca}_3\text{Cit}_2$  in artificial urine, which underwent pH adjustment to pH 8, followed by precipitation before measurement. The Mrx IDA measurement of control materials was carried out. The observed values of  $\text{Ca}_3\text{Cit}_2$  were calculated based on the  $\text{Ca}_3\text{Cit}_2$  standard curve to obtain %CV, and %recovery. The acceptable criteria was %recovery within the range of 90-110% of the expected  $\text{Ca}_3\text{Cit}_2$  concentration <sup>(91)</sup>. Parallely, the observed values of direct measurement of  $\text{Ca}_3\text{Cit}_2$  in HEPES and precipitated CalCit from AU were compared, to test %yield of precipitation.

3) Linearity: detection capability & sensitivity, including limit of blank (LoB), limit of detection (LoD), limit of quantitation (LoQ)

The detection capability and sensitivity were calculated from the accumulated data of the linearity test of  $\text{Ca}_3\text{Cit}_2$ , with 5 replications for each standard concentration over 5 days as a dataset. The LoB, LoD, and LoQ were then calculated from this whole dataset. The LoB, the highest concentration of standard  $\text{Ca}_2\text{Cit}_3$  which was determined as a blank, was calculated using the following equation <sup>(92)</sup>:

$$\text{LoB} = \text{mean}_{\text{blank}} + 1.645 * (\text{SD}_{\text{blank}})$$

The LoD, the lowest concentration of standard  $\text{Ca}_2\text{Cit}_3$  which was clearly distinguish from concentration of LoB and practically detected, was calculated using the following equation <sup>(92)</sup>:

$$\text{LoD} = \text{LoB} + 1.645 * (\text{SD}_{\text{low concentration sample}})$$

The LoQ, the lowest concentration of standard  $\text{Ca}_2\text{Cit}_3$ , which its %CV was below 20% <sup>(92)</sup>.

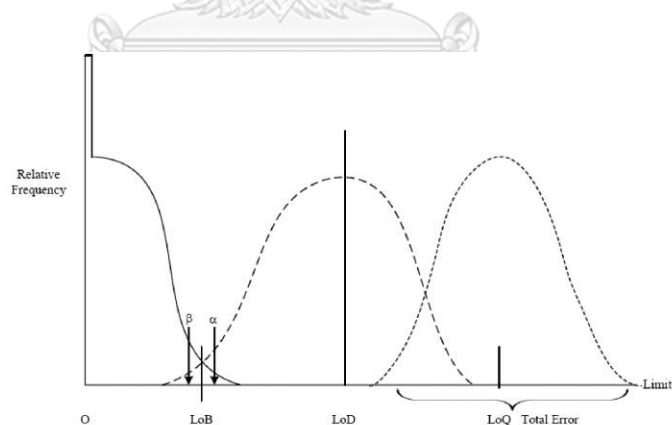


Figure 13. Relationship between Limit of Blank (LoB), Limit of Detection (LoD), Limit of Quantitation (LoQ), original image by Armbruster et al. <sup>(92)</sup>. Probability of false positive result ( $\alpha$ ) was 0.05.

Probability of false negative result ( $\beta$ ) was 0.05. SD: standard deviation.

#### 4) Selectivity

The selectivity of Mrx IDA indicated the specificity of its detection for  $\text{Ca}_3\text{Cit}_2$  (or CalCit). Mrx IDA was performed in the direct measurement of a 1 mM  $\text{Ca}_3\text{Cit}_2$  solution, and pellet of 2<sup>nd</sup> precipitated CalCit from a 1 mM  $\text{Ca}_3\text{Cit}_2$  solution, which were considered as control. Both controls were prepared with and without potential interfering substances (including common urinary ions, oxalate, catechin, gallic acid, lactic acid, tartaric acid, malic acid, bilirubin, and hemoglobin) within the physiological range of these interferences. The list of interferences was shown in Table 3. Most of chemicals were prepared in DI water. Uric acid was firstly prepared in 50 mM, KOH solution, then diluted by DI water. Bilirubin was firstly prepared in dimethyl sulfoxide (DMSO), then diluted by DI water. Catechin was firstly prepared in absolute EtOH, then diluted by DI water. Hemoglobin was lysed from bovine RBC by DI water. Its protein debris was filtered. Hemoglobin concentration was measured by bicinchoninic acid (BCA) assay, according to manufactural recommended protocol.

Additionally, to ensure that CalCit was truly precipitated at 2<sup>nd</sup> pellet of precipitation, the precipitated 2<sup>nd</sup> pellet from a urine sample of ST group was dried and subjected to FTIR analysis to identify mineral composition. For sample preparation, the 2<sup>nd</sup> precipitate sample was mixed and well-grounded with dried KBr powder (avoid wetness). The mixed powder was pressed into tablet for FTIR analysis. FTIR was performed at the absorbance spectrum of mid-infrared range (4000-400  $\text{cm}^{-1}$ )<sup>(93)</sup>. FTIR analysis of the chemicals (AR grade) including  $\text{Ca}_3\text{Cit}_2$ , CaOx, and  $\text{K}_2\text{HPO}_4$  were also performed to compare their spectra with the spectrum of the urinary 2<sup>nd</sup> precipitate pellet, as control.

Table 3. Potential urine interference, within Mrx IDA reaction.

Chemicals	Physiological range in urine	Prepared concentration (for adding to CalCit control)
Urea	167 – 583 mM <sup>(94)</sup>	50, 100, 200, 400, 800 mM
Uric acid	1.79 – 4.17 mM <sup>(94)</sup>	1, 2, 3, 4, 5 mM
Creatinine	0 - 1.33 mM <sup>(94)</sup>	0.15, 0.3, 0.6, 1.2, 2.4 mM
NH <sub>4</sub> <sup>+</sup> (from NH <sub>4</sub> Cl)	10 – 105 mM <sup>(94)</sup>	7, 14, 28, 56, 112 mM
SO <sub>4</sub> <sup>2-</sup> (from Na <sub>2</sub> SO <sub>4</sub> )	1.7 – 10 mM <sup>(94)</sup>	1, 2, 4, 8, 16 mM
HCO <sub>3</sub> <sup>-</sup> (from NaHCO <sub>3</sub> )	artificial urine: 2 mM <sup>(86)</sup>	0.5, 1, 2, 4, 8 mM
PO <sub>4</sub> <sup>3-</sup> (from K <sub>2</sub> HPO <sub>4</sub> )	8.9 – 28.9 mM <sup>(95)</sup>	8, 30, 32 mM
Ox <sup>2-</sup> (from Na <sub>2</sub> Ox)	normal: 0.07 – 0.3 mM hyperoxaluria: 0.67 – 2.67 mM <sup>(96)</sup>	0.25, 0.5, 1, 2, 4 mM
catechin	0.008 mM from ingestion <sup>(97)</sup>	0.001, 0.01, 0.1, 1, 10 mM
Gallic acid	0.05 mM from ingestion <sup>(98, 99)</sup>	0.001, 0.01, 0.1, 1, 10 mM
Lactic acid	0-0.6 mmol/mmol creatinine <sup>(100)</sup>	0.001, 0.01, 0.1, 1, 10 mM
Tartaric acid	0.04-0.11 mmol/mmol creatinine <sup>(101, 102)</sup>	0.001, 0.01, 0.1, 1, 10 mM
Malic acid	0.112 mM <sup>(103)</sup>	0.001, 0.01, 0.1, 1, 10 mM
Bilirubin	(6 mg/dL) 0.103 mM <sup>(104)</sup>	0.025, 0.05, 0.1, 0.2, 0.4 mM
Hemoglobin (from lysed bovine RBC)	13.02 – 18.63 mg/ml <sup>(105)</sup>	2, 4, 8, 16, 32 mg/ml

### Part 3: clinical validation study

#### 3.7 Diagnostic accuracy validation

The established Mrx IDA was used to measure precipitated CalCit in 24-hour urine samples from the NS group (n = 122) and the kidney stone (ST) group (n = 141). Receiver Operating Characteristic (ROC) curve analysis was performed to assess the overall diagnostic performance of Mrx IDA for total urolithiasis cases. Following the selection of an appropriate cut-off value, a 2x2 table was created, and diagnostic values were calculated <sup>(106)</sup>.

Basically, the ROC curve was a functional curve between “1-specificity” (or false positive rate) as the x-axis and “sensitivity” as the y-axis, at all cut-off values (Figure 13). The specificity was the proportion of the urine samples that did not have stone, which were tested negative (higher CalCit level). The sensitivity was the proportion of urine samples that had stone, which were tested positive (lower CalCit level). The area under the ROC curve (AUC) were determined as the diagnostic accuracy of the Mrx IDA. The ideal AUC was = 1, when sensitivity = 1, and specificity = 1 (false positive rate = 0), which was the best diagnostic performance. Practically, AUC of the meaningful (good or acceptable) diagnostic assay was over 0.8, as shown in Table 4.

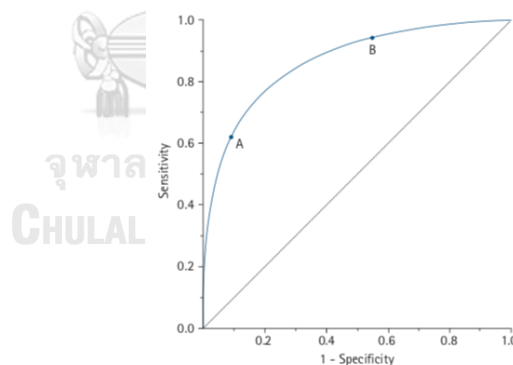


**Figure 14.** A ROC curve connected coordinates point between “1-specificity” (false positive rate) and “sensitivity” at all cut-off values, which were measured from the test. Point A represents the more inflexible cut-off value than that of point B. The 45° diagonal line was the reference line of condition, when true negative and true positive groups had normal distribution and considerable overlap <sup>(106)</sup>

Table 4. The interpretation of the AUC from ROC analysis <sup>(106)</sup>.

Area under the curve (AUC)	Interpretation
$0.9 \leq \text{AUC}$	Excellent
$0.8 \leq \text{AUC} < 0.9$	Good
$0.7 \leq \text{AUC} < 0.8$	Fair
$0.6 \leq \text{AUC} < 0.7$	Poor
$0.5 \leq \text{AUC} < 0.6$	Fail

For a diagnostic test to be meaningful, the AUC must be greater than 0.5. Generally, an  $\text{AUC} \geq 0.8$  is considered acceptable.

Considering that kidney stone disease is not highly serious in terms of mortality and the cost of the Mrx IDA procedure is not expensive, the optimal cut-off value was determined based on a greater importance of sensitivity than specificity <sup>(106)</sup>. After selecting optimal cut-off value, the decision matrix, which was the 2x2 table of predicted stone condition (tested positive or negative, determined from citrate level by Mrx IDA) and true stone condition (stone positive or negative, determined by CT scanning) was generated. A CT scan result was used as a gold standard reference. The diagnostic accuracy parameters which were including: sensitivity (or positive percent agreement, PPA), specificity (or negative percent agreement, NPA), accuracy (or overall rates of agreement, ORA), positive predictive value (PPV), negative predictive value (NPV), positive likelihood ratio ( $\text{LH}^+$ ), and negative likelihood ratio ( $\text{LH}^-$ ) were calculated using the following formulas:

- % sensitivity =  $(\text{true positive tested number} / \text{total CT positive number}) * 100$
- % specificity =  $(\text{true negative tested number} / \text{total CT negative number}) * 100$
- % accuracy =  $[(\text{true positive} + \text{true negative tested number}) / \text{total number}] * 100$
- % positive predictive value =  $(\text{true tested positive number} / \text{total Mrx IDA positive number}) * 100$
- % negative predictive value =  $(\text{true tested negative number} / \text{total Mrx IDA negative number}) * 100$
- positive likelihood ratio =  $\text{sensitivity} / (1 - \text{specificity})$
- negative likelihood ratio =  $(1 - \text{sensitivity}) / \text{specificity}$

		CT scan		
		True stone positive (+)	True stone negative (-)	
Mrx IDA	Tested positive (+) (lower CalCit)	True positive tested number	False positive tested number	Total Mrx IDA positive number
	Testes negative (-) (higher CalCit)	False negative tested number	True negative tested number	Total Mrx IDA negative number
		Total CT positive number	Total CT negative number	Total number

Figure 15. The decision matrix (2x2 Table) for diagnosing stone condition by the test result of Mrx IDA using CT scan result as gold standard method.

### 3.8 Statistical analysis

The method validation of Mrx IDA for measurement of urinary precipitated CalCit was performed and the parameters including selectivity, linearity, LoB, LoD, LoQ, accuracy, within-day and within-laboratory precision were reported. Data of CalCit level was reported as mean  $\pm$  standard error of mean (SEM). The difference of CalCit level between NS and ST groups was tested by two-sample *t*-test. ROC analysis was performed to evaluate how well the Mrx IDA could be used for urolithiasis screening, and the diagnostic values including sensitivity, specificity, accuracy, PPV, NPV,  $LH^+$ , and  $LH^-$  were calculated. The GraphPad Prism Software version 9.0 (GraphPad Software, Inc, California) was used for all statistical calculations. P-value  $<0.05$  was considered statistically significant.

### 3.9 Ethical consideration

The 24-h urine samples of healthy individuals and kidney stone patients were collected from Kaedam District and Mahasarakham Hospital, during 2017 and 2018, from our previous project “Test accuracy of urinary calcium oxalate crystallization index (COCI) for diagnosis of urolithiasis, and development of an innovative quantum dot nanoparticle-based method for determination of urinary oxalate” (IRB:286/59). These urine samples had been kept at  $-20^{\circ}\text{C}$ . The personal information including consent form was confidentiality by using code. There were clear inclusion and exclusion criteria. This project did not seek benefit from any individual. This study aimed to provide new knowledge about the benefit of calcium citrate precipitation for implementing in CaOx stone screening. When the results of the research were published, the information of participants was always concealed.





## Chapter 4 Results

### 4.1 Scanning spectrum of displaced Mrx in $\text{Ca}_3\text{Cit}_2$ concentration-dependent manner

To confirm the concentration-dependent of citrate<sup>3-</sup> displacement of the Mrx-Cu<sup>2+</sup> complex, the  $\text{Ca}_3\text{Cit}_2$  standard at 0, 0.2, 0.4, 0.6, 0.8, 1.0, 1.2, 1.4, 1.6, 1.8, 2.0 mM (20  $\mu\text{l}$ ) were introduced to the Mrx-Cu<sup>2+</sup> complex (180  $\mu\text{l}$ ) (set at 2 mM ratio). After incubation for 1 min, the absorbance spectrum (400-600 nm) of the yielding product (Mrx-Cu<sup>2+</sup> complex and the displaced Mrx dye) was scanned, and the result is shown in Figure 16 (left panel). The maximum absorption of the Mrx-Cu<sup>2+</sup> complex was at around 470 nm, while the maximum absorption of the displaced Mrx dye was at around 510 nm. A gradual decrease in OD470 and increase in OD510 were well corresponded with the  $\text{Ca}_3\text{Cit}_2$  concentration. In this work, we opted to measure the reaction product (displaced Mrx dye) at 522 nm (13). The scatter plot of  $\text{Ca}_3\text{Cit}_2$  concentrations against OD522 was created from mean and SD of 5 replicate measurements for 5 days (Figure 16, right panel). The plateau phase was observed at concentration of 1.6, 1.8, 2.0 mM, indicated by a non-significant change in their absorbance (p-value >0.07) (Table 5).

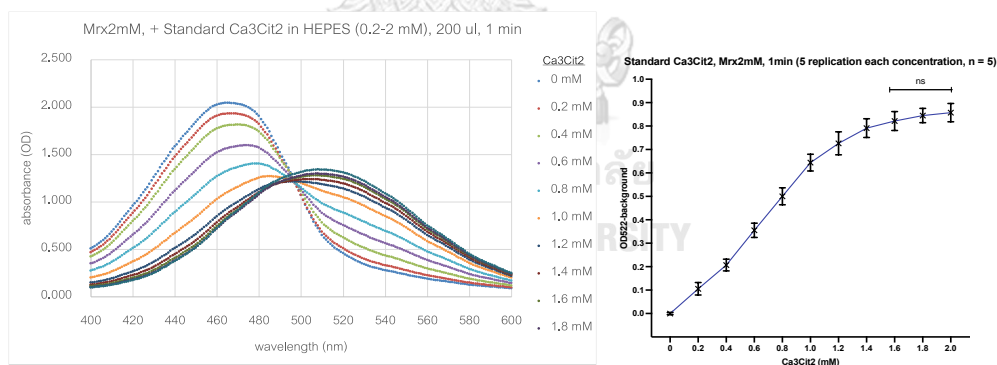


**Figure 16.** The absorbance of  $\text{Ca}_3\text{Cit}_2$  Std by Mrx IDA. (left) The absorbance spectrum obtained from the reaction of  $\text{Ca}_3\text{Cit}_2$  standard at 0, 0.2, 0.4, 0.6, 0.8, 1.0, 1.2, 1.4, 1.6, 1.8, 2.0 mM within Mrx-Cu<sup>2+</sup> complex (n = 5). (right) The scatter plot between  $\text{Ca}_3\text{Cit}_2$  concentrations and OD522. Error bars indicate standard deviation.

**Table 5.** Comparison of absorbance of each  $\text{Ca}_2\text{Cit}_3$  standard with the previous concentration.

$\text{Ca}_3\text{Cit}_2$	OD522 (mean-background)	SD	comparison OD between	p-value
0 mM	0.000	0.005		
0.2 mM	0.106	0.027	0 mM to 0.2 mM	<0.0001
0.4 mM	0.207	0.025	0.2 mM to 0.4 mM	<0.0001
0.6 mM	0.355	0.030	0.4 mM to 0.6 mM	<0.0001
0.8 mM	0.500	0.036	0.6 mM to 0.8 mM	<0.0001
1.0 mM	0.644	0.036	0.8 mM to 1.0 mM	<0.0001
1.2 mM	0.726	0.049	1.0 mM to 1.2 mM	<0.0001
1.4 mM	0.791	0.040	1.2 mM to 1.4 mM	<0.0001
1.6 mM	0.821	0.040	1.4 mM to 1.6 mM	0.0770
1.8 mM	0.845	0.030	1.6 mM to 1.8 mM	0.3543
2.0 mM	0.857	0.039	1.8 mM to 2.0 mM	0.9723

#### 4.2 Linearity, LoB, LoD, LoQ

To determine the linearity of  $\text{Ca}_3\text{Cit}_2$  standard, the absorbance of  $\text{Ca}_3\text{Cit}_2$  was plotted for further defining the regression equation and slope. The y-axis intercept was set at 0 mM (pass through origin). The mean, SD, %CV, and %recovery of  $\text{Ca}_3\text{Cit}_2$  level is shown in Table 6. The LoD, LoD, and were determined, as previously mentioned in section 3. The linear range that was practical for measurement precipitated  $\text{CaCit}$  form urine was defined through lower limit of LoQ (LLoQ) and upper limit of LoQ (ULoQ). These parameters are shown in Table 7. In this study, the linear range of  $\text{Ca}_3\text{Cit}_2$  standard was between 0.4 and 1.4 mM.

**Table 6.** Comparison of  $\text{Ca}_2\text{Cit}_3$  level of each  $\text{Ca}_2\text{Cit}_3$  standard and their %CV and %recovery values used for calculating LoB, LoD, and LoQ.

targeted $\text{Ca}_3\text{Cit}_2$ level	mean of $\text{Ca}_3\text{Cit}_2$ observed level (mM)	SD	%CV	%recovery
0 mM	0.00	0.01		
0.2 mM	0.18	0.04	21.3	89
0.4 mM	0.35	0.04	11.8	87
0.6 mM	0.60	0.04	6.4	100
0.8 mM	0.84	0.05	5.4	105
1.0 mM	1.08	0.03	3.2	108
1.2 mM	1.22	0.03	2.2	102
1.4 mM	1.33	0.03	2.2	95
1.6 mM	1.38	0.03	2.0	86
1.8 mM	1.42	0.03	2.4	79
2.0 mM	1.44	0.03	2.0	72

**Table 7.** The formulas and values of LoB, LoD, and LoQ of  $\text{Ca}_2\text{Cit}_3$  standard <sup>(96)</sup>.

definition	equation or criteria	determined value (mM)
LoB	limit of blank $\text{mean}_{\text{blank}} + (1.645 * \text{SD}_{\text{blank}})$	0.018
LoD	limit of detection $\text{LoB} + (1.645 * \text{SD}_{\text{low concentration sample}})$	0.08
LLoQ	lower limit of quantiation lowest concentration that %CV <15%	0.4
ULoQ	upper limit of quantiation highest concentration that %recovery >90%	1.4

#### 4.3 Precision and accuracy test

The linear range of  $\text{Ca}_3\text{Cit}_2$  standard was in the range of 0.4-1.4 mM. Therefore,  $\text{Ca}_3\text{Cit}_2$  level of control material should be within this range. The  $\text{Ca}_3\text{Cit}_2$  concentrations of control materials were 0.6 and 1.2 mM, and their %recovery of >90% were obtained (Table 8). The precisions test, including repeatability (within-run precision) and reproducibility (within-laboratory precision) was indicated by %CV, whereas the accuracy of test was indicated by %recovery. The acceptable %CV of repeatability and reproducibility were <5% and <10%, respectively. The acceptable %recovery was within 90-110%. The precision and accuracy data of the Mrx IDA test are shown in Table 8. Our findings indicated that the Mrx IDA test is well precise and accurate.

**Table 8.** The observed  $\text{Ca}_3\text{Cit}_2$  values of control material and their %CV and %recovery.

targeted $\text{Ca}_3\text{Cit}_2$ value (mM)	mean of observed $\text{Ca}_3\text{Cit}_2$ value (mM)	precision test		accuracy test
		repeatability (within day) (%CV)	reproducibility (within laboratory) (%CV)	%recovery
0.6	0.60	4.53	6.85	99.57
1.2	1.22	1.85	2.36	101.63
acceptable value:		<5	<10	90-110

#### 4.4 %yield of $\text{Ca}_3\text{Cit}_2$ precipitation

The positive control material of  $\text{Ca}_3\text{Cit}_2$  at 0.6 and 1.2 mM were prepared in HEPES for Mrx IDA direct measurement. The other set of positive control material was parallelly prepared in AU for CalCit precipitation. The pH of AU after adding  $\text{Ca}_3\text{Cit}_2$  was at around 4-5, and they were adjusted to pH 8-9 by adding 1N NaOH (16  $\mu\text{l}$ ). The precipitation procedure was performed like precipitation of CalCit in urine sample. The pellet of first precipitation by adding excessive calcium chloride was clearly visible, and then it was removed. The supernatant (potentially consisted of CalCit) was transferred to new tube that contained 80% EtOH to precipitate CalCit. This pellet was collected and dried, then was re-dissolved by 0.04N HCl (100  $\mu\text{l}$ ), followed by adding HEPES buffer (700  $\mu\text{l}$ ) to get the original sample volume of 800  $\mu\text{l}$ . These precipitated CalCit of 0.6 and 1.2 mM control material, were measured for 5 replications for 5 days. The observed concentrations were compared with the targeted  $\text{Ca}_3\text{Cit}_2$  value, and %yield of CalCit precipitation was calculated, as shown in Table 9. The %yield showed that CalCit precipitation process constantly pellet CalCit at around 70-80% of the targeted  $\text{Ca}_3\text{Cit}_2$  concentrations. The %CV for repeatability was found at <5%, and for reproducibility was at <10%, indicated that the method had a good precision.

**Table 9.** The observed  $\text{Ca}_3\text{Cit}_2$  values of control material and %recovery after CalCit precipitation (%yield of CalCit precipitation).

targeted $\text{Ca}_3\text{Cit}_2$ value (mM)	mean of observed $\text{Ca}_3\text{Cit}_2$ value (mM)	precision test		%yield test	
		repeatability (within-day) (%CV)	reproducibility (within-laboratory) (%CV)	%yield	%loss
0.6	0.48	4.75	7.79	79.79	20.21
1.2	0.89	1.59	5.64	74.28	25.72
acceptable value:		<5	<10		

#### 4.5 Selectivity of Mrx IDA

Selectivity of the Mrx IDA was tested by comparing the signal of 1 mM  $\text{Ca}_3\text{Cit}_2$  with interferences at various concentrations with the signal of  $\text{Ca}_3\text{Cit}_2$  control without interferences ( $n = 3$ ). In both direct and post-precipitation measurements, common urinary ions ( $\text{NH}_4^-$ , urea,  $\text{SO}_4^{2-}$ ,  $\text{HCO}_3^-$ ), creatinine, and bilirubin did not interfere with the Mrx signal for CalCit detection (Figure 17a-f). However, oxalate at high concentration tended to increase the Mrx signal, but it was not statistically significant (Figure 18a). In contrast, malic acid and tartaric acid exhibit significant interfering signal in the direct measurement. However, in post-precipitation measurement, the Mrx signal of 2<sup>nd</sup> pellet sample were decreased for both malic acid and tartaric acid at high concentration, and this phenomenon was also observed in from the case of lactic acid (Figure 18b-d). Hemoglobin at high concentration (13-18.6 mg/L) also showed a significant interfering effect in both direct measurement and post-precipitation measurement (Figure 18e). Perhaps, it was due to the high opacity at high hemoglobin concentration and might be from the denaturation of hemoglobin during the drying process. For uric acid, it significantly interfered the Mrx signal of the 2<sup>nd</sup> pellet sample, especially at the high concentration. It was possibly due to the formation of calcium urate in the CalCit precipitation process (Figure 18f). The interference signal from  $\text{PO}_4^{3-}$  was not significant in direct measurement. However, it significantly decreased the CalCit signal in the 2<sup>nd</sup> pellet sample at high concentration of  $\text{PO}_4^{3-}$  (Figure 19a). Furthermore, the signal of citrate was detected significantly higher in 1<sup>st</sup> pellet of precipitation, when CalCit was mixed with  $\text{PO}_4^{3-}$  (Figure 19b). This signal could be from CaP, which also formed during precipitation process. The citrate<sup>3-</sup> may be entrapped within CaP or coated on the CaP crystals. To ensure this, the dry weight of 1<sup>st</sup> pellet of precipitation of  $\text{PO}_4^{3-}$  was performed with presence or absence of CalCit. The result showed that dry weight of 1<sup>st</sup> pellet of precipitation of  $\text{PO}_4^{3-}$  was significantly increased, with presence of CalCit (Figure 19c, right panel). The volume of pellet also was remarkable noticed (Figure 19c, left panel).

For phenolic compounds, the interferences from both gallic acid and catechin were highly significant, especially at high concentrations (Figure 20, 21). However, these interfering signals were eliminated through the EtOH precipitation step. The signal from both gallic acid and catechin were detected within supernatant of 2<sup>nd</sup> precipitation, but not in the 2<sup>nd</sup> pellet (Figure 20, 21).

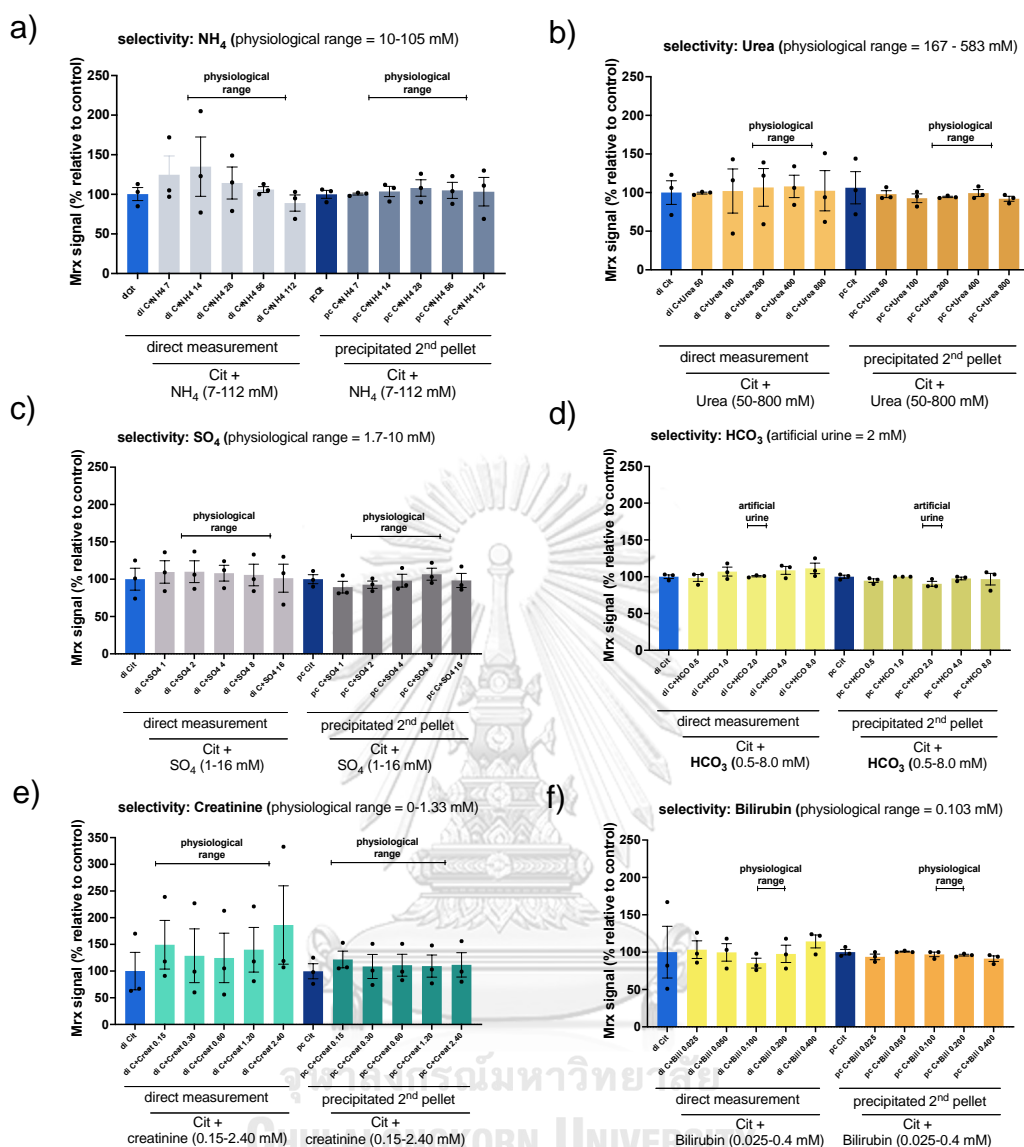


Figure 17 Selectivity of the Mrx IDA reaction (part 1). The % relative Mrx signal of 1 mM  $\text{Ca}_3\text{Cit}_2$  with a)  $\text{NH}_4^-$ , b) urea, c)  $\text{SO}_4^{2-}$ , d)  $\text{HCO}_3^-$ , e) creatinine, and f) bilirubin at various concentrations, which compared to their control without interferences (light blue bars: direct measurement control, dark blue bars: precipitated control) was presented as the mean with SEM (n =3).

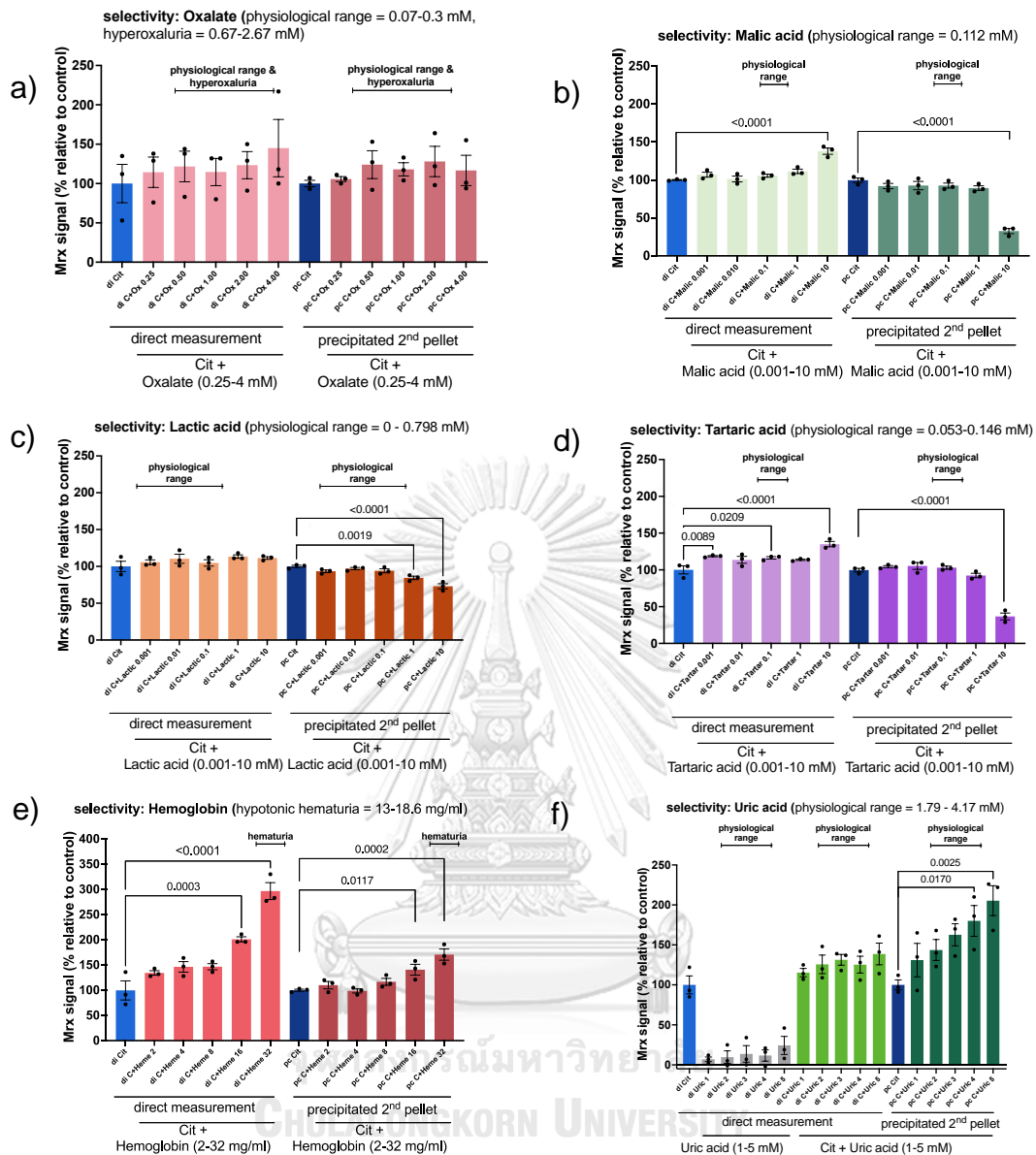


Figure 18. Selectivity of the Mrx IDA reaction (part 2). The % relative Mrx signal of 1 mM  $\text{Ca}_3\text{Cit}_2$  with a) oxalate, b) malic acid, c) lactic acid, d) tartaric acid, e) hemoglobin, and f) uric acid at various concentrations, which compared to their control without interferences (light blue bars: direct measurement control, dark blue bars: precipitated control) was presented as the mean with SEM ( $n = 3$ ).



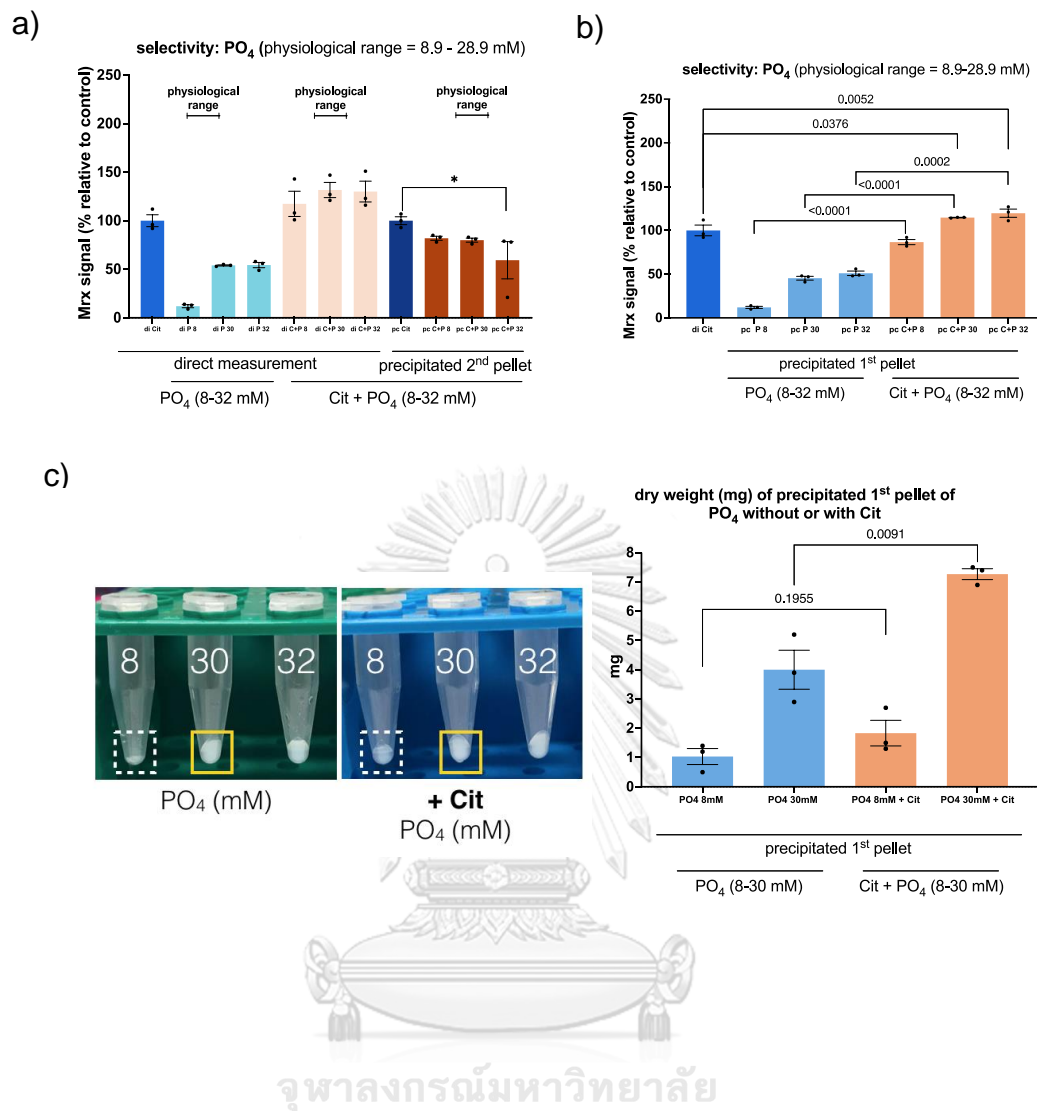


Figure 19. Selectivity of the Mrx IDA reaction (part 3). a, b) The % relative Mrx signal of 1 mM  $\text{Ca}_3\text{Cit}_2$  with  $\text{PO}_4^{3-}$  at various concentrations, which compared to their control without interferences (light blue bars: direct measurement control, dark blue bars: precipitated control) was presented as the mean with SEM ( $n=3$ ). a)  $\text{PO}_4^{3-}$  interference was demonstrated in 2<sup>nd</sup> pellet of CalCit precipitation. b)  $\text{PO}_4^{3-}$  interference was demonstrated in 1<sup>st</sup> pellet of CalCit precipitation. c) (left) images of 1<sup>st</sup> pellet of CalCit precipitation and (right) bar graph, demonstrating the dry weight (mg) of 1<sup>st</sup> pellet of CalCit precipitation with  $\text{PO}_4^{3-}$ .

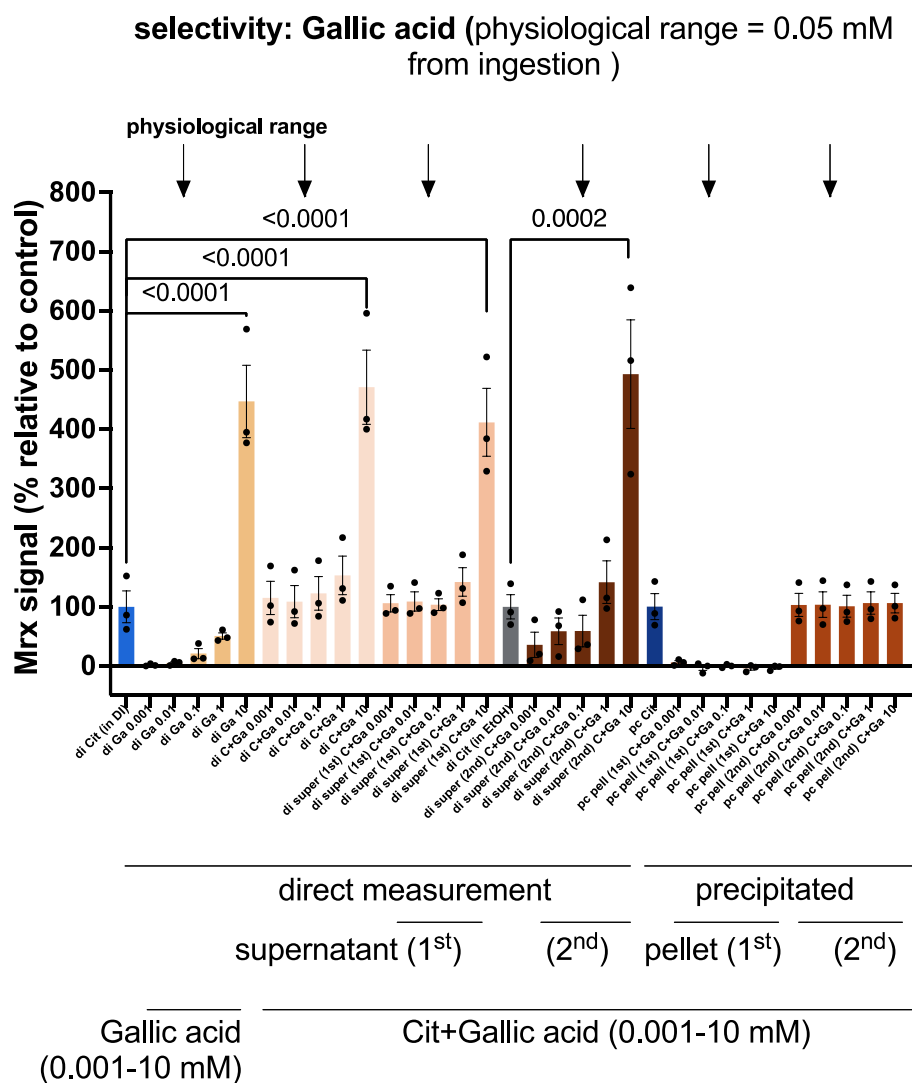


Figure 20. Selectivity of the Mrx IDA reaction (part 4). The % relative Mrx signal of 1 mM  $\text{Ca}_3\text{Cit}_2$  with gallic acid at various concentrations, which compared to their control without interferences (light blue bar: direct measurement control in DI water, grey bar: direct measurement control in EtOH, dark blue bar: precipitated control) was presented as the mean with SEM ( $n = 3$ ). The bar graph demonstrated all fractions during precipitation procedure.

**selectivity: Catechin** (physiological range = 0.008 mM from ingestion)

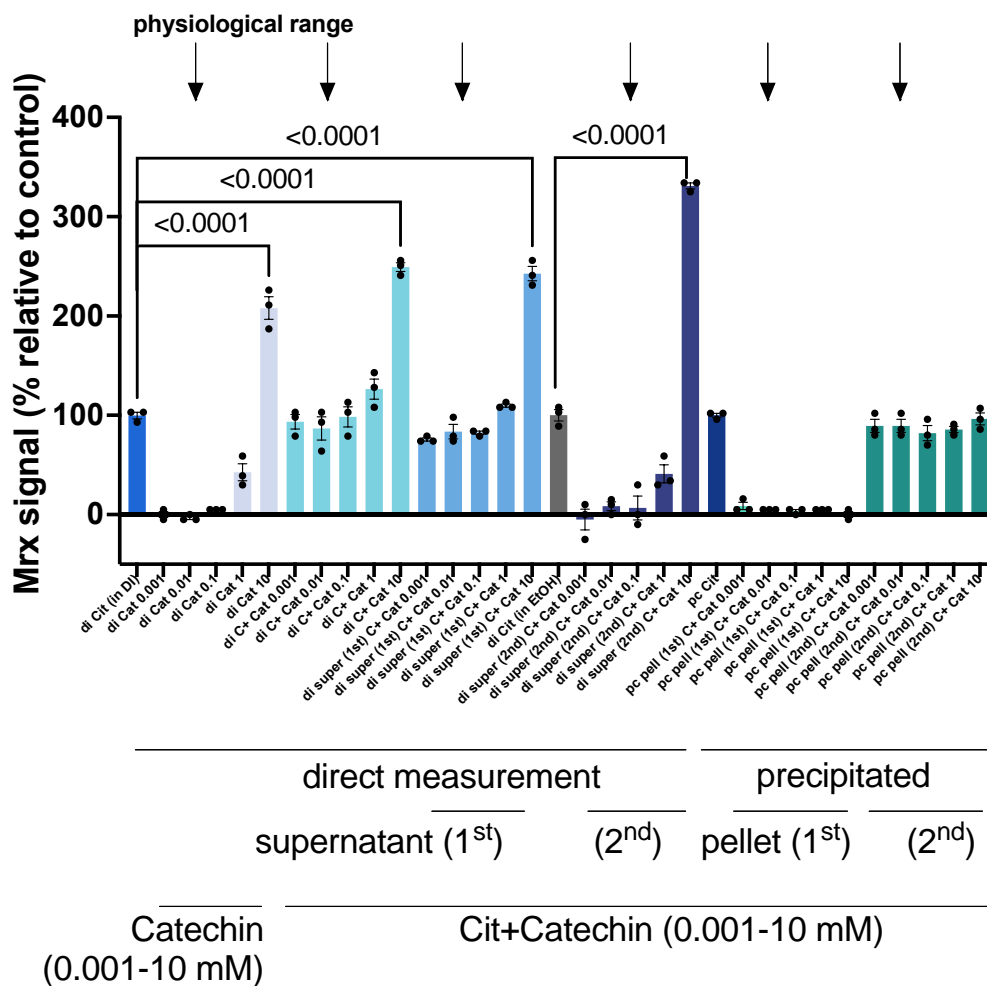


Figure 21. Selectivity of the Mrx IDA reaction (part 5). The % relative Mrx signal of 1 mM  $\text{Ca}_3\text{Cit}_2$  with catechin at various concentrations, which compared to their control without interferences (light blue bar: direct measurement control in DI water, grey bar: direct measurement control in EtOH, dark blue bar: precipitated control) was presented as the mean with SEM ( $n = 3$ ). The bar graph demonstrated all fractions during precipitation procedure.

#### 4.6 FTIR analysis of the 2<sup>nd</sup> pellet sample precipitated urine sample of urolithiasis patients

FTIR analysis of CalCit pellet sample (the 2<sup>nd</sup> precipitate) from urine sample of ST patients was performed. It exhibited the presence of CalCit, as indicated by the peak range of 1439-to-1443  $\text{cm}^{-1}$  and of 1578-to-1619  $\text{cm}^{-1}$  similar to the peaks observed in  $\text{Ca}_3\text{Cit}_2$  control (Figure 22a, b). There was also another peak at 1096  $\text{cm}^{-1}$  that which was similar to the specific absorption of  $\text{K}_2\text{HPO}_4$  control (Figure 22a, c). These specific absorption peaks indicated that the 2<sup>nd</sup> precipitate from ST urine sample was not a pure CalCit composition. There was CaP co-precipitated together with CalCit in the excessive calcium condition. Therefore,  $\text{PO}_4^{3-}$  could be precipitated as CaP in both 1<sup>st</sup> and 2<sup>nd</sup> pellet during the CalCit precipitation process (Figure 18, 20).



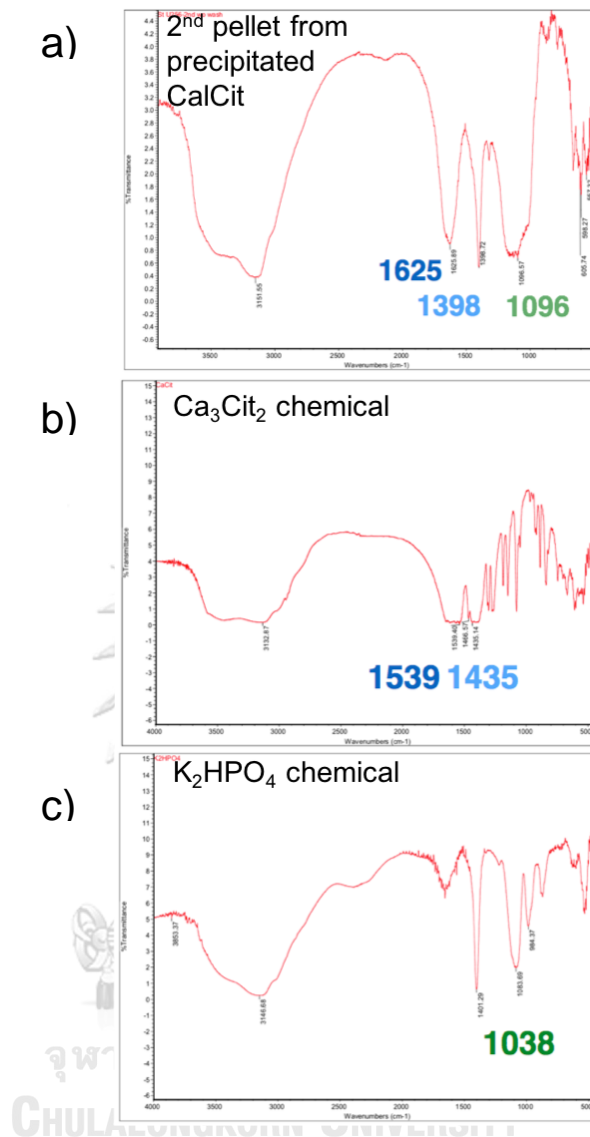


Figure 22. FTIR analysis of precipitated CalCit. a) CalCit pellet sample (2<sup>nd</sup> precipitate) from urine sample of ST patients, b) Ca<sub>3</sub>Cit<sub>2</sub> standard chemical, and c) K<sub>2</sub>HPO<sub>4</sub> standard chemical.

#### 4.7 Clinical validation: ROC curve analysis and its parameters

The method validation of the Mrx IDA test for measuring precipitated CalCit in urine samples was completely conducted. The LoD of the test was 0.08 mM, and the reliable quantitative linear was ranged between 0.4 (LLoQ) and 1.4 mM (ULoQ). The % yield of CalCit precipitation was >70%. The precision and accuracy of the Mrx IDA test was well acceptable.

Clinical validation was conducted. The Mrx IDA test was performed in real 24-h urine samples obtained from healthy subjects (non-stone, NS, n = 122) and kidney stone patients (ST, n = 141). In urine samples with pH <6.4 (n = 34), their pH was adjusted to 7-12 with 1N NaOH before testing. After precipitation, the pH of redissolved CalCit solutions were at around pH 2-7, and pH adjustment before performing Mrx IDA reaction was not required. The data of pH of urine samples, OD522 from Mrx IDA, observed CalCit value, and 24-h urine volume are shown in supplementary table S19. The number of cases that the detected OD522 were or were not fallen within the range of linearity (0.4-1.4 mM) are displayed in supplementary table S21.

The precipitated CalCit concentrations (values) were reported in 4 units including  $\mu\text{M}$ , mg/L,  $\mu\text{mol}$  per day, and mg per day. They result showed that the precipitated CalCit values in ST group was significantly lower than NS groups for all 4 units (p-value <0.0001).

Based on ROC analysis result, CalCit value in the unit of  $\mu\text{M}$  demonstrated the highest AUC value (0.7879, 95%CI: 0.7325-0.8433), indicated that the test had a fair diagnostic accuracy for distinguishing stone cases (all stone type) from non-stone cases.

Of 141 stone patients, 45 were diagnosed with CaOx stone (CaOx stone (n = 17), CaOx mixed with CaP stone (n =17), and CaP mixed with CaOx stone (n = 11). The level of urinary precipitated CalCit in the ST group was significantly lower than in the NS group. ROC analysis revealed an AUC of 0.8227 (95% CI: 0.7522-0.8931). This indicated that the Mrx IDA test had a good diagnostic accuracy for separating CaOx stone cases from non-stone cases (Figure 23, Table 10).

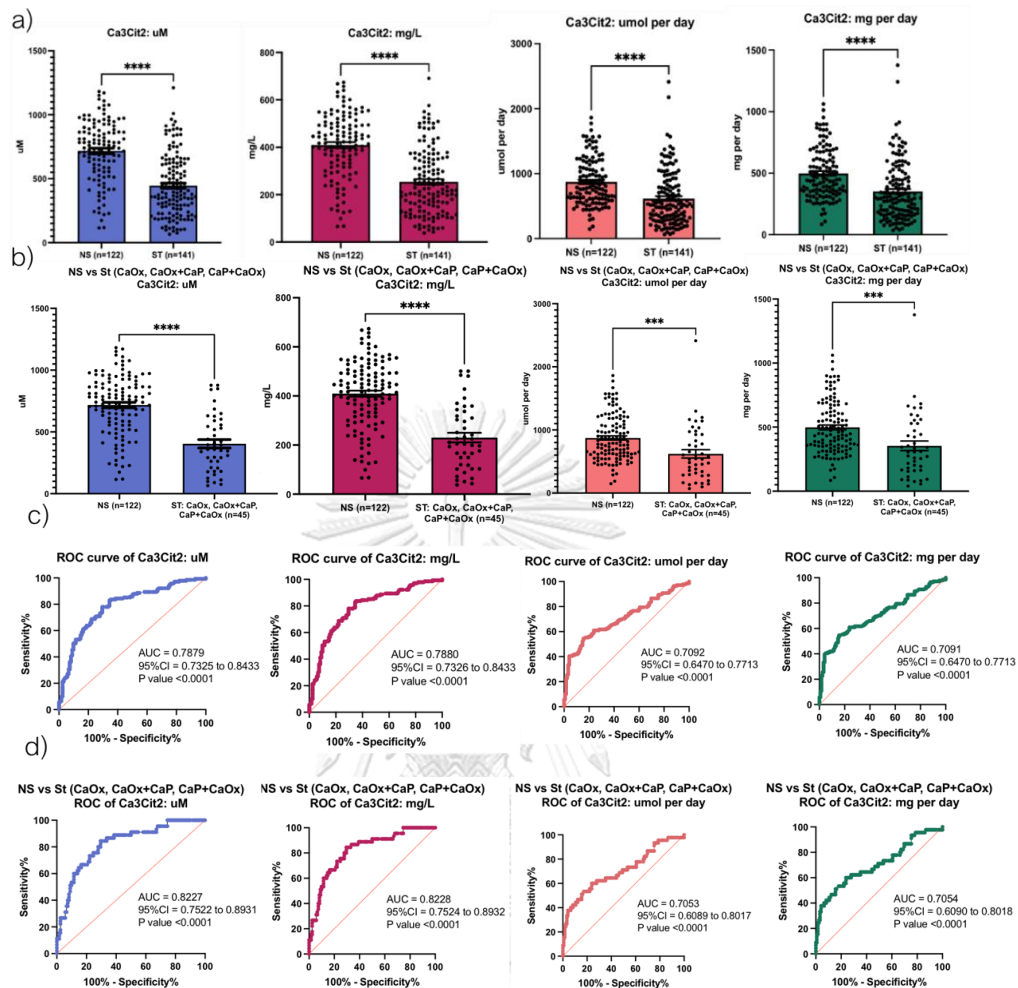


Figure 23 Levels of precipitated CaCit measured by the Mrx IDA method compared between stone (ST) and non-stone (NS) groups. The precipitated CaCit levels were expressed in the units of  $\mu\text{M}$ , mg/L,  $\mu\text{mol per day}$ , and mg per day. a) Precipitated CaCit levels compared between 122 NS subjects and 141 stone patients. b) Precipitated CaCit levels compared between 122 NS subjects and 45 CaOx urolithiasis patients. c) ROC curves for separating NS subjects from all ST patients. d) ROC curves for distinguishing NS subjects from CaOx stone formers. Bars indicate means and SEMs.

Table 10. Comparison of precipitated CalCit values between NS group and ST groups.

	NS group	ST group, all stone types	ST group, CaOx type
n	122	141	45
CalCit values: mean (SD)			
μM	717 (239)	445 (243)	404 (239)
mg/L	409 (136)	254 (139)	230 (131)
μmol per day	873 (364)	616 (415)	621 (440)
mg per day	498 (208)	352 (237)	354 (251)
compare to NS group			
<i>t</i> -test: p-value			
μM		<0.0001	<0.0001
mg/L		<0.0001	<0.0001
μmol per day		<0.0001	0.0002
mg per day		<0.0001	0.0002
compare to NS group			
ROC curve:			
AUC (95%CI)			
μM		0.7879 (0.7325-0.8433)	0.8227 (0.7522-0.8931)
mg/L		0.7880 (0.7326-0.8433)	0.8228 (0.7524-0.8932)
μmol per day		0.7092 (0.6470-0.7713)	0.7053 (0.6089-0.8017)
mg per day		0.7091 (0.6470-0.7713)	0.7054 (0.6090-0.8018)



The cutoff value of the precipitated CalCit level in the unit of  $\mu\text{M}$  was selected, because the  $\mu\text{M}$  unit provided the best diagnostic performance according to the ROC analysis (Figure 23d). The cutoff values for overall stone and CaOx cases were 663.5 and 632.0  $\mu\text{M}$ , respectively. The 2x2 table was created and the diagnostic values including: sensitivity (or PPA), specificity (or NPA), accuracy (or ORA), PPV, NPV,  $\text{LH}^+$ , and  $\text{LH}^-$  were calculated. These calculated diagnostic values are showed in Table 11.

**Table 11.** Cutoff values of urinary precipitated CalCit and diagnostic values for separating NS subjects from ST patients.

	NS group vs ST group, overall stone types	NS group vs CaOx ST group, CaOx and CaP types
CalCit ( $\mu\text{M}$ )		
ROC curve: AUC	0.7879	0.8227
95% CI	0.7325 to 0.8433	0.7522 to 0.8931
Cutoff value	663.5 $\mu\text{M}$	632.0 $\mu\text{M}$
sensitivity (or positive percent agreement)	82.98%	84.44%
specificity (or negative percent agreement)	65.57%	70.49%
accuracy (or overall rates of agreement)	74.90%	74.25%
positive predictive value	73.58%	51.35%
negative predictive value	76.92%	92.47%
positive likelihood ratio	2.41	2.86
negative likelihood ratio	0.26	0.22

## Chapter 5 Discussion

Urinary stones are heterogeneous, primarily they composed of CaOx. The most frequent component mixed with CaOx is CaP. CaOx crystal formation is an initial step of CaOx stone formation. Citrate<sup>3-</sup> is the best-known CaOx stone inhibitor. Mechanistically, citrate inhibits CaOx formation through 3 main mechanisms: 1) it competes oxalate to bind to Ca<sup>2+</sup> ion, and hence reducing the saturation of CaOx, 2) it prevents CaOx aggregation and growth by forming the citrate shell on CaOx crystals and keeping the crystal surface high zeta negative potential<sup>(10)</sup>, and 3) it prevents the adhering of CaOx crystals onto kidney epithelium by promoting the formation of COD instead of COM<sup>(11)</sup>. Therefore, measurement of urinary citrate level is beneficial for estimating the risk of CaOx stone formation. However, routine measurement of urinary citrate is not common. In the past, methods like HPLC, 1H-NMR, LC-MS/MS, or enzymatic assays were recommended for directly determining urinary citrate levels. Nevertheless, these approaches have numerous limitations, involving multiple steps in urine preparation, complex instrumentation, and high operating cost. To overcome these issues, we proposed to use the Mrx IDA method for measuring CalCit precipitated in the supersaturated urine. It is a simple colorimetric assay measuring citrate<sup>3-</sup> in the form of CalCit that can indirectly be a reflective of urinary citrate level.

Our newly developed Mrx IDA method measured precipitated CalCit from supersaturated urine samples instead of directly determining urinary citrate content. The urine sample was induced to be at the state of supersaturation by challenging with excessive calcium chloride. Under the supersaturated condition, both CalCit and CaOx were formed simultaneously. The CalCit complexes were separated by precipitation with ethanol, and the content of citrate was determined by the Mrx IDA. The higher level of CalCit found in urine could be interpreted as the preventive factor against the formation of CaOx stone, as citrate competed with oxalate to react with calcium forming more soluble CalCit compounds. To date, the measurement of urinary CalCit have not been investigated. In this study, we aimed to develop the Mrx IDA method for measurement the urinary CalCit and sked if it had a clinical potential for screening CaOx urolithiasis.

Recently, an index for screening CaOx stone formation, called urinary iCOCl test, was developed<sup>(107)</sup>. The urinary Mrx IDA for precipitated CalCit measurement developed in this study shares a similar concept with iCOCl that involves an addition of excessive Ca<sup>2+</sup> ion to induce crystallization. In the process of urine sample preparation, it was possible to obtain both the urinary CaOx and CalCit pellets.

The CaOx pellet could be collected during the first precipitation in water, while the CalCit was still soluble in the supernatant. Subsequently, CalCit was precipitated by ethanol to yield the second pellet,<sup>(72, 74)</sup>. Beneficially, the precipitation of CalCit by ethanol enabled the elimination of potential urinary phenolic acids, such as catechin and gallic acid, that interfered with the detection of CalCit by Mrx IDA<sup>(18)</sup>. However, the CalCit obtained in the second precipitate was not solely pure. Based on the present findings, some urine components, such as bilirubin was also precipitated together with CalCit as well as CaP. Our FTIR result demonstrated the presence of specific spectrum of  $\text{PO}_4^{3-}$  in the 2<sup>nd</sup> pellet of urine samples. The occurrence of CalCit in the precipitation process could enhance the precipitation of CaP<sup>(108)</sup>. We found that the 1<sup>st</sup> precipitate contained CaP, and the precipitation was more pronounced in the presence of CalCit. Moreover, the Mrx signal of the 1<sup>st</sup> precipitate was faultily high in the presence of  $\text{PO}_4^{3-}$ . Although CaP or  $\text{PO}_4^{3-}$  ion could not displace the Mrx dye like the CalCit or citrate<sup>3-</sup> did, CaP might have the ability to entrap some of the citrate<sup>3-</sup>. As shown in our finding, the precipitation of CalCit consistently yielded around 70-80%, rather than reaching a full 100%.

CalCit was precipitated by forming a complex with  $\text{Ca}^{2+}$  ion, and citrate could displace the Mrx dye from the Mrx- $\text{Cu}^{2+}$  complex. This occurs only under the condition that the pH of urine or CalCit solution is around 6-7, which corresponded to the  $\text{pK}_{a_3}$  (6.4) of citric acid<sup>(60, 61)</sup>. At pH 7, citrate<sup>3-</sup> ion exists about 75%<sup>(61)</sup> among other citrate ions (citrate<sup>-</sup> or citrate<sup>2-</sup>). At pH 7.5, citrate<sup>3-</sup> exists more than 90%<sup>(61)</sup>. In the process of CalCit precipitation from urine or AU, pH was always checked and adjusted to be basic by 1 N NaOH. The HEPES buffer, pH 8 was highly recommended to prepare the Mrx- $\text{Cu}^{2+}$  solution<sup>(26)</sup> because it had buffer capacity to maintain the pH of the precipitated CalCit solution or  $\text{Ca}_3\text{Cit}_2$  standard material within the range of 7-8. These basic conditions ensured that citrate<sup>3-</sup> in urine sample was mostly precipitated and Mrx was always clearly displaced by citrate<sup>3-</sup>.

Citrate<sup>3-</sup> effectively displaces the Mrx dye from Mrx- $\text{Cu}^{2+}$  complex due to the higher affinity and stability of  $\text{Cu}^{2+}$ -citrate<sup>3-</sup> complex compared to the Mrx- $\text{Cu}^{2+}$  complex<sup>(13)</sup>. The absorbance of displaced Mrx (maximum absorbance at 522 nm) was gradually increased after adding citrate, together with a gradual decrease in absorbance of Mrx- $\text{Cu}^{2+}$  complex (maximum absorbance at 457 nm). The signal increased in the dose-dependent manner. This was similar to the study of Tavallai et al. in 2019<sup>(13)</sup> (Figure 23).

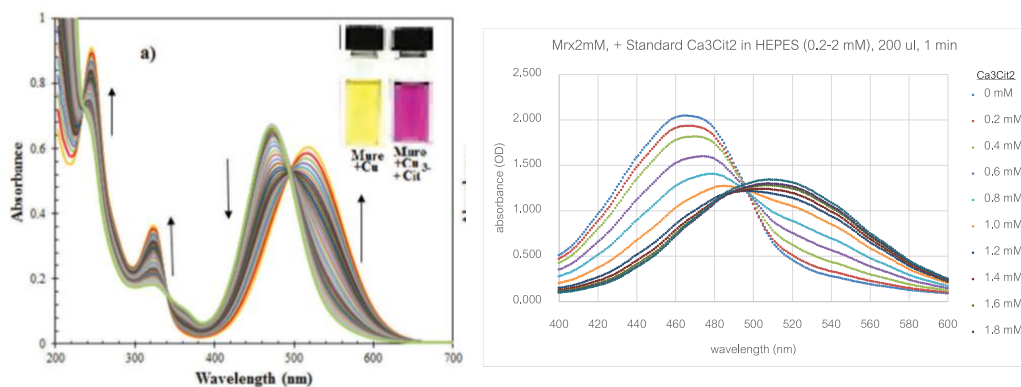
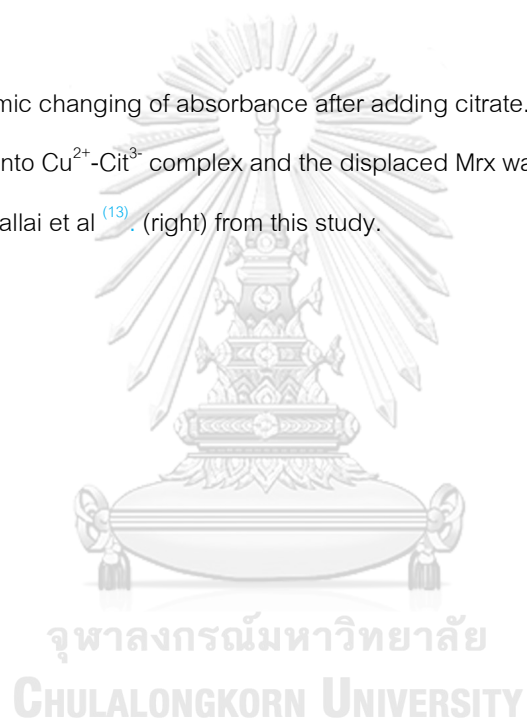


Figure 24. The dynamic changing of absorbance after adding citrate. It indicated the transformation of  $\text{Mrx-Cu}^{2+}$  complex into  $\text{Cu}^{2+}\text{-Cit}^{3-}$  complex and the displaced Mrx was released into the solution. (left) from work of Tavallai et al <sup>(13)</sup>. (right) from this study.



The measurement of urinary CalCit precipitate levels could be carried out using the Mrx IDA method. Based on method validation and clinical validation data, it was suggested that the urinary Mrx IDA test could be the screening test for ruling out the CaOx urolithiasis. The method validation of the Mrx IDA was proved that the test did not only have a good precision (repeatability at <5% CV and reproducibility at <10% CV), but it also had a good accuracy (achieving 90-110% recovery). The analytical measurement interval was determined at the range between LLoQ and ULoQ (linear range of 0.4-1.4 mM) that had covered most urinary CalCit level in both NS and ST groups. In the ST group, the urinary CalCit level was lower than that in the NS group, as expected. The urinary CalCit level of some cases in ST group was lower than 0.4 mM or lower than the LLoQ (about 15% of total stone case, Table S3). According to this limitation, the accurate measurement of urinary precipitated CalCit, was not clearly achievable. Consequently, the practical application of the Mrx IDA test was recommended for the use as a qualitative test (positive or negative) rather than as a quantitative method. The cutoff value for urinary precipitated CalCit was established based on the ROC analysis. Urine samples with precipitated CalCit levels below this cutoff were classified as a positive test result. Urine samples with CalCit levels above the cutoff were tagged as negative test result.

The clinical validation of the Mrx IDA test demonstrated the potential of the test to screen the CaOx urolithiasis with a good diagnostic accuracy (an AUC of 0.8277 (95%CI: 0.7522-0.8931) <sup>(106)</sup>. The diagnostic performance of the Mrx IDA test for all stone types was only fair. The cutoff value of CalCit level for screening CaOx risk urine was 632  $\mu\text{M}$ , provided the sensitivity (or PPA) and specificity (or NPA) of 84.44% and 70.49%, respectively. This indicated that there were an 84% probability to get the positive test result (urinary CalCit level below 632  $\mu\text{M}$ ) in CaOx stone cases. However, there was an 16% possibility that patients with CaOx stone might be undetected by the Mrx IDA test. The PPV of the test was 51.35%, suggested that individuals with positive test result (CalCit levels below 632  $\mu\text{M}$ ) has about 51% chance of getting CaOx stone condition. Additional confirmation tests, such as CT scan, should be recommended for further testing.

On the other side, the Mrx IDA test provided a specificity of 70.49%. This means that people who have no stone condition have about 70% chance to be tested negative, and about 30% probability to be faultily tested positive.

Interestingly, the NPV of the Mrx IDA test was 92.47%. This means that people who tested negative have about 92% of chance to be healthy or free of CaOx stone condition. Therefore, the Mrx IDA test developed in this study had a clinical potential to be used as a urinary screening test for ruling out CaOx urolithiasis.

Likelihood ratios serve as alternative statistics to summarize diagnostic accuracy, predict the risk of disease, and offer clinical guidance to either confirm or exclude the disease, regardless of the disease prevalence <sup>(109)</sup>. It is widely acknowledged that an  $LH^+$  of 10 or higher and an  $LH^-$  of 0.1 or lower indicates an excellently informative screening test <sup>(110)</sup>. In this study, we obtained an  $LH^-$  of 0.22 for predicting CaOx stone. This implies that individuals with a negative result (their CalCit level was higher than 632  $\mu\text{M}$ ) have a 4.5-fold ( $1/0.22$ ) decrease in the odds of developing CaOx stones. For preventing CaOx stone development, ensuring adequate water intake, reducing high-oxalate food consumption, and increasing high-citrate food intake (such as HydroZitla <sup>(4)</sup>), are strongly recommended.

The limitations of the study should be mentioned. The studied cohort in this study was known non-stone and stone cases. It is worthwhile to further conduct the diagnostic accuracy study in urine samples taken before diagnosis in order to minimize the bias and to obtain the more realistic diagnostic values. Collection of 24-h urine specimens is complicated and relatively hard. It is interesting to further investigate whether this Mrx IDA test can be applied to spot urine or first morning urine samples.

Conclusions, we successfully developed the Mrx IDA test for measurement of precipitated CalCit in 24-h urine samples. The test had a clinical potential to be used as a screening test for ruling out the CaOx stone disease. This Mrx IDA test is quick, simple, and robust that does not require a special training skill to perform the test. Based on our current data, it is recommended to implement this test in the real clinical setting.

## Supplement data

Table 12. (supplement S1). List of chemicals used in this study.

Chemical	Full name	Company	Country
BCA assay	Pierce™ BCA protein assay	Thermo Scientific	Ohio, USA
Bilirubin	bilirubin	TCI	Tokyo, Japan
Ca <sub>3</sub> Cit <sub>2</sub> *4H <sub>2</sub> O	calcium citrate tetrahydrate	Sigma aldrich	Damstadt, Germany
CaCl <sub>2</sub> *2H <sub>2</sub> O	calcium chloride dihydrate	Merck	Damstadt, Germany
CaOx*xH <sub>2</sub> O	calcium oxalate hydrate	Sigma aldrich	UK
Catechin	(+)-catechin hydrate	TCI	Tokyo, Japan
Creatinine	creatinine anhydrous	Sigma aldrich	Damstadt, Germany
Cu(NO <sub>3</sub> ) <sub>2</sub> *2.5H <sub>2</sub> O	copper (II) nitrate hemi(pentahydrate)	Sigma aldrich	Damstadt, Germany
DMSO	dimethyl sulfoxide	Merck	Damstadt, Germany
EtOH	ethyl alcohol 99.9%	QR&C	New Zealand
Gallic acid	gallic acid hydrate	TCI	Tokyo, Japan
HCl	hydrochloric acid fuming 37%	Merck	Damstadt, Germany
HEPES	2-[4-(2-hydroxyethyl)-1-piperazinyl]ethanesulfonic acid	TCI	Shanghai, China
K <sub>2</sub> HPO <sub>4</sub>	potassium phosphate (dibasic, anhydrous)	Bio basic	Ontario, Canada
KCl	potassium chloride	Bio basic	Ontario, Canada
KOH	potassium hydroxide	Merck	Damstadt, Germany
Lactic acid	lactic acid 88%	LOBA chemie	Maharashita, India
Malic acid	malic acid	Chemipan	Thailand
MgSO <sub>4</sub> *7H <sub>2</sub> O	magnesium sulfate heptahydrate	Merck	Massachusetts, USA
Murexide	murexide	TCI	Tokyo, Japan
Na <sub>2</sub> HPO <sub>4</sub>	di-sodium hydrogen phosphate	Merck	Damstadt, Germany
Na <sub>2</sub> SO <sub>4</sub>	sodium sulfate anhydrous	RCI Labscan	Thailand
Na <sub>3</sub> Ox	sodium oxalate	Sigma aldrich	Missouri, USA
NaCl	sodium chloride	Merck	Damstadt, Germany
NaH <sub>2</sub> PO <sub>4</sub> *H <sub>2</sub> O	sodium dihydrogen phosphate monohydrate	Merck	Damstadt, Germany

$\text{NaHCO}_3$	sodium carbonate	Merck	Damstadt, Germany
NaOH	sodium hydroxide	Merck	Damstadt, Germany
$\text{NH}_4\text{Cl}$	ammonium chloride	Merck	Damstadt, Germany
Tartaric acid	tartaric acid	Chemipan	Thailand
Urea	urea	Bio basic	Ontario, Canada
Uric acid	uric acid	Acros organics	New Jersey, USA





Table 13. (supplement S2) List of equipment used in this study.

Equipment	Model	Company	Country
96-well plate	96-well microtitre plate, flat bottom, non sterile	Thermo Scientific	Ohio, USA
Autoclave	HICLAVE HVA-110	Hirayama	Saitama, Japan
Autopipette	10, 100, 200, 1000 $\mu$ l	Axygen	California, USA
Autopipette	multi channel, 300 $\mu$ l	Cleaver Scientific	Warwickshire, UK
Beaker	50, 200, 1000 ml	BOECO	Germany
Centrifuge	mini spin plus (eppendorf)	Marshall scientific	New Hampshire, USA
Centrifuge (refrigerated)	Centrifuge 5910 R (eppendorf)	Marshall scientific	New Hampshire, USA
Distilled water maker	MicroPure	Thermo Scientific	Ohio, USA
Four decimal analytical balances	ME Precision ME303 Balance	Mettler Toledo	Switzerland
Freezer	-20°C, -80°C	Sanyo Electric	Osaka, Japan
Freezer	4°C	Panasonic	Japan
FTIR	FT-IR Nicolet iS50	Thermo Scientific	Ohio, USA
Heat block	ELITE DRY BATH INCUBATOR, dual unit	Major science	Taoyuan, Taiwan
Hot air oven		Memmert	Germany
Magnetic stirrer	IKA big-squid	IKA	Baden-Württemberg, Germany
Microcentrifuge tubes	1.5, 2 ml	Axygen	California, USA
Microcentrifuge tubes	15 ml	TARSONS	Kolkata, India
Microcentrifuge tubes	50 ml	GenFollwer Biotech	Zhejiang, China
pH meter	edge HI2002	Hanna Instrument	UK
pH-indicator strips	pH 0-14 universal indicator	Merck	Darmstadt, Germany
Pipette controller	S1 pipet filler	Thermo Scientific	Ohio, USA
Sero pipette	BRAND <sup>®</sup> graduated pipette serological, 10 ml	Merck	Darmstadt, Germany
Syring filter	nylon 13 mm., 0.22 $\mu$ m	Ageia Technologies	USA
UV-vis spectrophotometer	Multiskan™ GO Microplate Spectrophotometer	Thermo Scientific	Ohio, USA
Vortex mixer	VORTEX-2 GENIE	Scientific Industries	USA

Water bath sonicator	Elmasonic S30H, 37kHz	Distrelec	Germany
----------------------	-----------------------	-----------	---------



**Table 14.** (supplement S3) Artificial urine recipe which is modified from the AU-siriraj<sup>(86)</sup>. Citrate and oxalate are not added.

Chemicals	MW.	Concentration (mM)	mg
Urea	60.06	200	12,000
Uric acid	168.11	1	168
Creatinine	113.2	4	452
NaCl	58.4	54	3,156
KCl	74.55	30	2,236
NH <sub>4</sub> Cl	53.49	15	802
CaCl <sub>2</sub> *2H <sub>2</sub> O	147.01	3	442
MgSO <sub>4</sub> *7H <sub>2</sub> O	246.48	2	496
NaHCO <sub>3</sub>	84.0	2	168
Na <sub>2</sub> SO <sub>4</sub>	142.04	9	1,278
NaH <sub>2</sub> PO <sub>4</sub> *H <sub>2</sub> O	137.99	3.6	496
Na <sub>2</sub> HPO <sub>4</sub>	141.96	0.4	56
DI water			up to 1L*
total			1L

**Note.** \*adjust pH to 6.2 by NaOH or HCl solution, keep at -4°C.

**Table 15.** (supplement S4) 2 N HCl solution recipe.

Chemicals	ml
hydrochloric acid fuming 37% (12N)	10
DI water	50
total	60

**Table 16.** (supplement S5) 0.04 N HCl solution recipe.

Chemicals	ml
2 N HCl solution	1
DI water	49
total	50

**Table 17.** (supplement S6) 10 mM, HEPES buffer recipe.

Chemicals	MW.	mg
HEPES (2-[4-(2-hydroxyethyl)-1-piperazinyl]ethanesulfonic acid)	238.3	2,383
DI water		up to 1L*
total		1L

**Note.** \*adjust pH to 8 by NaOH or HCl solution.

**Table 18.** (supplement S7) 10 mM, Mrx solution recipe, fresh preparation before measuring.

Chemicals	MW.	mg
murexide dye	284.19	2.84
10 mM, HEPES buffer		1 ml
total		1 ml

**Table 19.** (supplement S8) 10 mM, 10 mM, Cu<sup>2+</sup> solution recipe, fresh preparation before measuring.

Chemicals	MW.	mg
Cu(NO <sub>3</sub> ) <sub>2</sub> *2.5H <sub>2</sub> O	232.69	2.32
10 mM, HEPES buffer		1 ml
total		1 ml

**Table 20.** (supplement S9) 4.44 mM, Mrx solution, fresh preparation before measuring.

Chemicals	ml
10 mM, Mrx solution	0.888
10 mM, HEPES buffer	19.112
total	20*

**Note.** \*the absorbance of solution at OD522 must be set at ~3.25, 200 µl.

**Table 21.** (supplement S10) 4.44 mM, Cu<sup>2+</sup> solution, fresh preparation before measuring.

Chemicals	ml
10 mM, Cu <sup>2+</sup> solution	0.888
10 mM, HEPES buffer	19.112
total	20

**Table 22.** (supplement S11) 2.22 mM Mrx-Cu<sup>2+</sup> solution recipe ( for measuring at 2 mM, about 100 reactions), fresh preparation before measuring.

Chemicals	ml
4.44 mM, Mrx solution	10*
4.44 mM, Cu <sup>2+</sup> solution	10*
total	20

**Note.** \*the ratio of Mrx solution-to-Cu<sup>2+</sup> solution must be adjusted; such as at 1:1, 0.9:1, or 0.85:1 ratio to give linear curve of Ca3Cit2 standard at R<sup>2</sup> of ≥0.99

**Table 23.** (supplement S12) 200 mM,  $\text{Ca}_3\text{Cit}_2$  solution recipe.

Chemicals	MW.	mg
$\text{Ca}_3\text{Cit}_2 \cdot 4\text{H}_2\text{O}$	570.49	5,704
2N, HCl solution		50 ml
total		50 ml

**Note.** keep at  $-4^\circ\text{C}$ .

**Table 24 .** (supplement S13) 20 mM,  $\text{Ca}_3\text{Cit}_2$  solution recipe.

Chemicals	ml
200 mM, $\text{Ca}_3\text{Cit}_2$ solution	5
10 mM, HEPES buffer	45
total	50

**Note.** aliquot and keep at  $-4^\circ\text{C}$ .

**Table 25.** (supplement S14) 20 mM,  $\text{Ca}_3\text{Cit}_2$  solution recipe, fresh preparation before measuring.

$\text{Ca}_3\text{Cit}_2$ Standard solution (mM)	20 mM, $\text{Ca}_3\text{Cit}_2$ solution	10 mM, HEPES buffer
0.2	5 $\mu\text{l}$	495 $\mu\text{l}$
0.4	10 $\mu\text{l}$	490 $\mu\text{l}$
0.6	15 $\mu\text{l}$	485 $\mu\text{l}$
0.8	20 $\mu\text{l}$	480 $\mu\text{l}$
1.0	25 $\mu\text{l}$	475 $\mu\text{l}$
1.2	30 $\mu\text{l}$	470 $\mu\text{l}$
1.4	35 $\mu\text{l}$	465 $\mu\text{l}$
1.6	40 $\mu\text{l}$	460 $\mu\text{l}$
1.8	45 $\mu\text{l}$	455 $\mu\text{l}$
2.0	50 $\mu\text{l}$	450 $\mu\text{l}$

Table 26. (supplement S15)  $\text{CaCl}_2$ , 1 M solution.

Chemicals	MW.	mg
$\text{CaCl}_2 \cdot 2\text{H}_2\text{O}$	147.01	7,350
DI water		50 ml
total		50 ml

Table 27. (supplement S16) NaOH, 1 N solution.

Chemicals	MW.	mg
NaOH	40.0	2,000
DI water		50 ml
total		50 ml

Table 28 (supplement S17) KOH, 50 mM solution.

Chemicals	MW.	mg
KOH	56.1	140.25
DI water		50 ml
total		50 ml

Table 29. (supplement S18.) Working solution recipe of potential interferences of Mrx IDA.

Chemicals	MW.	Working concentration	mg	Diluent, ml	Designed concentration for testing*
Urea	60.06	1,600 mM	960	DI water, 10 ml	50, 100, 200, 400, 800 mM
Uric acid	168.11	24 mM	40.32	50 mM, KOH, 10 ml	1, 2, 3, 4, 5 mM
Creatinine	113.2	4.8 mM	5.424	DI water, 10 ml	0.15, 0.3, 0.6, 1.2, 2.4 mM
NH <sub>4</sub> <sup>+</sup> (from NH <sub>4</sub> Cl)	53.49	224 mM	118.72	DI water, 10 ml	7, 14, 28, 56, 112 mM
SO <sub>4</sub> <sup>2-</sup> (from Na <sub>2</sub> SO <sub>4</sub> )	142.04	32 mM	45.44	DI water, 10 ml	1, 2, 4, 8, 16 mM
HCO <sub>3</sub> <sup>-</sup> (from NaHCO <sub>3</sub> )	84.0	16 mM	13.44	DI water, 10 ml	0.5, 1, 2, 4, 8 mM
PO <sub>4</sub> <sup>3-</sup> (from K <sub>2</sub> HPO <sub>4</sub> )	174.2	64 mM	111.36	DI water, 10 ml	8, 30, 32 mM
Ox <sup>2-</sup> (from Na <sub>2</sub> Ox)	134.0	8 mM	10.72	DI water, 10 ml	0.25, 0.5, 1, 2, 4 mM
Catechin	290.26	20 mM	58.05	EtOH, 10 ml	0.001, 0.01, 0.1, 1, 10 mM
Gallic acid	170.12	20 mM	34.0	DI water, 10 ml	0.001, 0.01, 0.1, 1, 10 mM
Lactic acid 88% (11.7 M)	-	20 mM	0.017 ml	DI water, up to 10 ml	0.001, 0.01, 0.1, 1, 10 mM
Tartaric acid	150.087	20 mM	30.0	DI water, 10 ml	0.001, 0.01, 0.1, 1, 10 mM
Malic acid	134.087	20 mM	26.8	DI water, 10 ml	0.001, 0.01, 0.1, 1, 10 mM
Bilirubin	584.66	0.8 mM	1.8	DMSO, 4 ml	0.025, 0.05, 0.1, 0.2, 0.4 mM
Hemoglobin (from lysed bovine red blood cell)	-	100 mg/ml	-	DI water	2, 4, 8, 16, 32 mg/ml

Note. \*diluted from working solution to designed concentrations by DI water



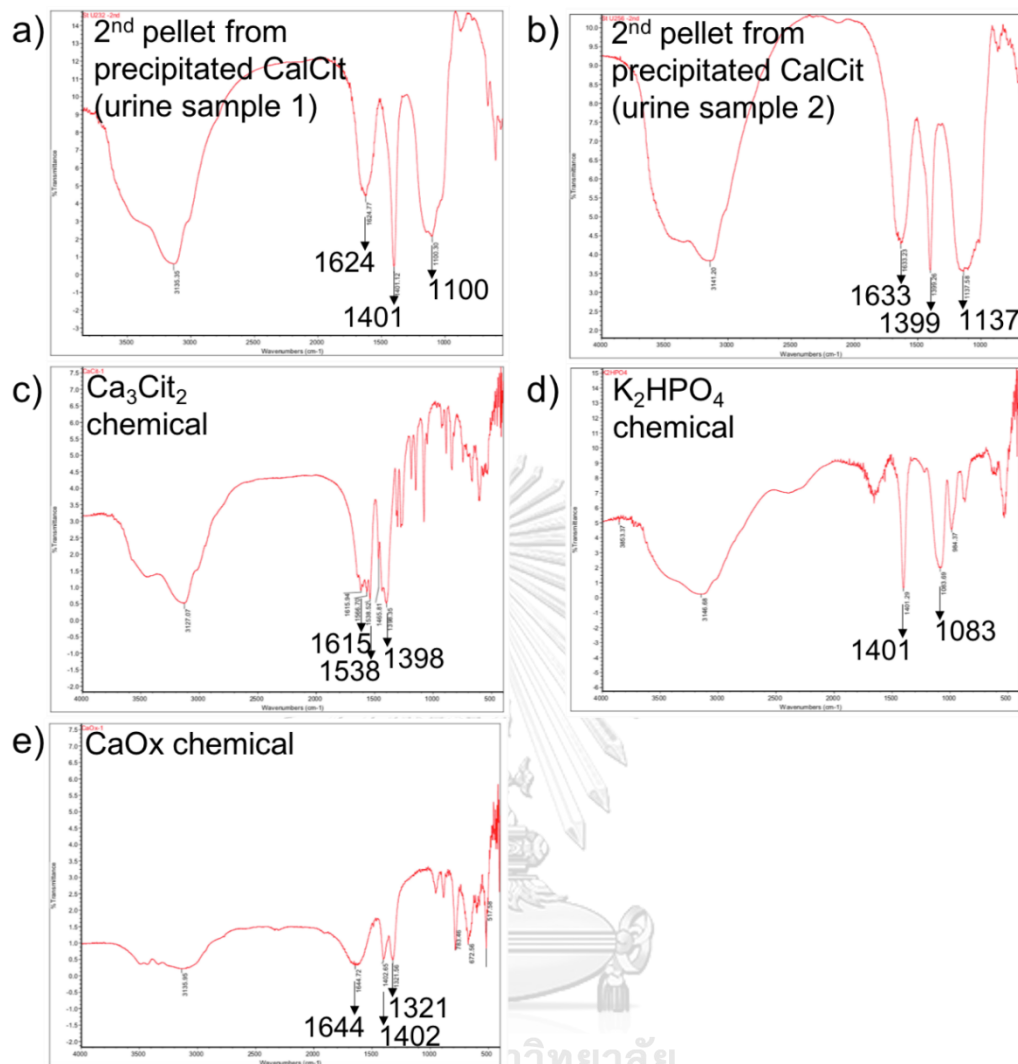


Figure 25. (supplement S1) FTIR analysis (part 1). demonstrating spectra peak of a, b) 2<sup>nd</sup> pellet of precipitation from 2 urine samples, c)  $\text{Ca}_3\text{Cit}_2$ , d)  $\text{K}_2\text{HPO}_4$ , e)  $\text{CaOx}$  chemicals.

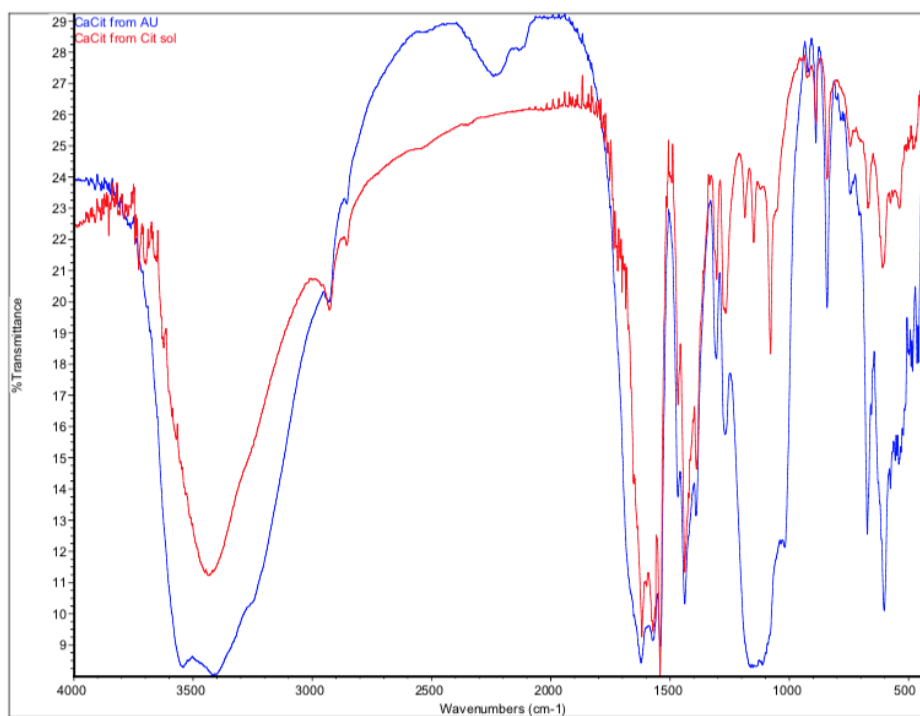


Figure 26. (supplement S2) FTIR analysis (part 2). Demonstrating spectra peak of precipitated CaCit from citrate<sup>3-</sup> in DI water (red line) and CaCit from citrate<sup>3-</sup> in artificial urine (blue line).

Table 30 (supplement S19) Data of urine samples. Note that non-stone urine (0) and stone urine (1) were collected from diagnosed individuals by CT scanning.

No.	NS or ST	Stone Type	urine volume (ml)	urine pH	urine pH, after pH adjustment by 1N, NaOH	pH of precipitated Ca/Cit solution before Mx/IDA	R <sup>2</sup>	slope (range: 0.4-1.4 mM)	OD-blank (sample)	observed Ca/Cit value			
										μM	mg/L	μmol per day	mg per day
1	0		870	7.08		5	0.9980	0.5691	0.492	864	493	751	429
2	0		780	7.01		5	0.9980	0.5691	0.389	684	390	533	304
3	0		3800	7.62		4	0.9980	0.5691	0.224	393	224	1492	851
4	0		720	6.25		5	0.9980	0.5691	0.361	634	362	457	261
5	0		1100	7.38		5	0.9980	0.5691	0.285	500	285	550	314
6	0		460	6.48		6	0.9980	0.5691	0.673	1182	674	544	310
7	0		730	6.75		5-10-6	0.9980	0.5691	0.539	946	540	691	394
8	0		1800	6.82		5	0.9980	0.5691	0.334	567	335	1056	603
9	0		430	6.58		5-10-6	0.9980	0.5691	0.476	836	477	360	205
10	0		1610	5.58	9	4	0.9980	0.5691	0.443	778	444	1253	715
11	0		1690	7.60		5	0.9980	0.5691	0.348	611	348	1032	589
12	0		500	6.06	10	5	0.9980	0.5691	0.667	1171	668	586	334
13	0		2570	5.84	10	3	0.9980	0.5691	0.277	487	278	1251	714
14	0		2640	6.34		3	0.9980	0.5691	0.065	115	66	304	173
15	0		800	6.20		5	0.9980	0.5691	0.363	638	364	510	291
16	1		700	6.08	10	3	0.9980	0.5691	0.180	333	190	233	133
17	0		460	6.73		5	0.9980	0.5691	0.548	963	549	443	253
18	0		1240	7.03		5	0.9980	0.5691	0.493	865	494	1073	612
19	0		2400	6.68		4	0.9980	0.5691	0.130	228	130	546	312
20	0		1300	9.03		8	0.9980	0.5691	0.433	761	434	989	564
21	0		1010	4.67	10	5	0.9980	0.5691	0.487	855	488	863	493
22	0		1280	6.23		5	0.9980	0.5691	0.280	491	280	629	359
23	1		440	5.29	10	5	0.9980	0.5691	0.689	1211	691	533	304
24	0		750	6.95		5	0.9980	0.5691	0.446	783	447	587	335
25	0		700	5.94	7	3	0.9980	0.5691	0.455	800	456	560	319
26	0		630	7.41		5	0.9980	0.5691	0.398	699	399	441	251
27	0		990	7.27		6	0.9980	0.5691	0.557	978	558	968	552
28	0		1220	8.83		6	0.9980	0.5691	0.415	729	416	890	508
29	1		560	7.86		5	0.9980	0.5691	0.297	521	297	292	166
30	1		810	7.14		5	0.9980	0.5691	0.374	656	374	532	303
32	1		410	8.29		3	0.9980	0.5691	0.185	325	185	133	76
33	1		2210	7.85		4	0.9980	0.5691	0.354	621	354	1373	783
34	1		950	5.16	9	4	0.9980	0.5691	0.539	947	540	900	513
35	1		2010	6.25		5	0.9980	0.5691	0.374	656	374	1319	753
36	1		820	5.67	9	2	0.9980	0.5691	0.098	172	98	141	81
37	1		2050	9.02		6	0.9980	0.5691	0.059	103	59	211	120
38	1		1300	7.47		3	0.9980	0.5691	0.093	163	93	211	121
39	1		850	6.45		3	0.9980	0.5691	0.118	207	118	176	101
40	1		1480	6.38		4	0.9980	0.5691	0.219	384	219	568	324
41	1		600	6.80		5	0.9980	0.5691	0.417	732	418	439	251

42	1		650	6.94		5	0.9980	0.5691	0.255	447	255	291	166
43	1		1870	7.35		4	0.9980	0.5691	0.209	367	210	687	392
44	1		2400	7.60		3	0.9980	0.5691	0.131	230	131	552	315
45	1		880	6.77		5	0.9980	0.5691	0.228	401	229	353	201
46	1		620	5.57	8	3	0.9980	0.5691	0.351	616	351	382	218
47	1		850	6.36		4	0.9980	0.5691	0.159	279	159	237	135
48	1		2200	8.06		3	0.9980	0.5691	0.329	577	329	1270	724
49	1		980	4.60	9	3	0.9980	0.5691	0.575	1010	576	990	565
50	1		1450	6.30		5	0.9980	0.5691	0.279	489	279	710	405
51	1		1700	8.20		3	0.9980	0.5691	0.166	292	166	496	283
52	1		2700	7.32		3	0.9980	0.5691	0.110	193	110	522	298
53	1		1600	8.40		3	0.9980	0.5691	0.060	105	60	167	95
54	1		1550	8.11		3	0.9980	0.5691	0.130	228	130	354	202
55	1		2400	7.48		4	0.9980	0.5691	0.120	211	120	506	289
56	1		1200	8.98		6	0.9980	0.5691	0.372	653	372	783	447
57	1		400	7.33		5-10-6	0.9980	0.5691	0.382	671	383	268	153
58	1		1850	8.84		6	0.9980	0.5691	0.180	316	180	585	334
59	1		1880	7.46		5	0.9980	0.5691	0.248	436	249	819	467
60	1		2600	6.27		5-10-6	0.9980	0.5691	0.477	837	478	2177	1242
61	1		1400	6.74		5-10-6	0.9980	0.5691	0.427	750	428	1050	599
62	1		1950	8.84		6	0.9980	0.5691	0.262	459	262	896	511
64	1		800	5.66	9	4	0.9980	0.5691	0.549	965	550	772	440
65	1		850	7.13		5-10-6	0.9980	0.5691	0.432	759	433	645	368
66	1		1300	8.36		3	0.9980	0.5691	0.162	284	162	369	210
67	1		1300	8.65		6	0.9980	0.5691	0.153	268	153	348	199
68	1		900	6.28		5-10-6	0.9980	0.5691	0.378	663	378	597	341
69	1		850	8.52		6	0.9980	0.5691	0.267	469	268	399	228
70	1		720	8.82		6	0.9980	0.5691	0.403	708	404	510	291
71	1		3300	6.47		5	0.9980	0.5691	0.173	304	173	1003	572
72	1		1250	8.93		6	0.9980	0.5691	0.129	227	129	283	162
73	1		730	8.56		6	0.9980	0.5691	0.251	440	251	321	183
74	1		920	6.67		6	0.9980	0.5691	0.298	523	296	461	274
75	1		770	9.08		6	0.9980	0.5691	0.066	116	66	89	51
76	1		1100	8.69		6	0.9980	0.5691	0.352	619	353	680	388
77	1		1940	8.80		6	0.9980	0.5691	0.372	654	373	1268	723
78	1		2290	9.15		6	0.9980	0.5691	0.261	458	261	1048	598
79	1		750	8.75		5-10-6	0.9980	0.5691	0.204	358	204	269	153
80	1		420	8.39		5	0.9980	0.5691	0.504	886	505	372	212
81	1		1300	8.66		6	0.9980	0.5691	0.212	373	213	484	276
83	1		580	8.56		5	0.9980	0.5691	0.311	546	311	316	181
84	1		1350	9.00		6	0.9980	0.5691	0.068	119	68	161	92
86	1		2350	9.12		6	0.9980	0.5691	0.287	503	287	1183	675
87	1		900	9.02		3	0.9980	0.5691	0.136	239	136	215	123
88	1		850	9.18		6	0.9980	0.5691	0.176	308	176	262	150
90	1	Uric acid	1800	8.81		6	0.9980	0.5691	0.108	190	108	342	195
91	1	CaP+CaOX	2000	8.83		6	0.9980	0.5691	0.102	178	102	357	203

92	1	CaOx+CaP	2100	8.64		6	0.9980	0.5691	0.168	295	168	620	354
93	1		1720	6.45		3	0.9980	0.5691	0.116	204	116	351	200
94	1		1200	6.96		5	0.9980	0.5691	0.347	610	346	732	417
96	1		1240	9.16		6	0.9980	0.5691	0.104	183	104	227	129
97	1	CaOx	700	8.45		5	0.9980	0.5691	0.232	408	233	285	163
98	1	CaOx+CaP	800	8.87		6	0.9980	0.5691	0.199	350	199	280	160
100	1		1440	9.14		6	0.9980	0.5691	0.171	300	171	431	246
102	1		2850	4.55	9	3	0.9980	0.5691	0.320	561	320	1600	913
103	1		610	8.77		6	0.9980	0.5691	0.201	353	201	215	123
104	1		1900	7.31		3	0.9980	0.5691	0.109	191	109	362	207
107	1		2410	8.98		6	0.9980	0.5691	0.170	299	170	720	411
108	1		1620	8.36		6	0.9980	0.5691	0.306	537	306	870	496
110	0		1820	9.00		6	0.9980	0.5691	0.139	243	139	443	253
111	0		2150	7.42		4	0.9980	0.5691	0.416	731	417	1572	897
112	1		1800	4.70	9	5	0.9980	0.5691	0.438	770	439	1385	790
113	0		1900	6.93		5	0.9980	0.5691	0.450	790	451	1501	856
114	0		780	6.97		5-10-6	0.9980	0.5691	0.639	1122	640	875	499
115	0		1260	6.89		6	0.9980	0.5691	0.408	716	408	902	515
116	0		1500	6.11	9	6	0.9980	0.5691	0.363	638	364	957	546
117	0		770	7.08		5-10-6	0.9980	0.5691	0.656	1152	657	887	506
118	0		840	6.05	10	3	0.9980	0.5691	0.315	554	316	465	265
119	0		1080	7.30		5-10-6	0.9980	0.5691	0.600	1053	601	1138	649
120	0		1580	7.32		5	0.9980	0.5691	0.299	525	300	830	474
121	0		1650	7.86		5	0.9980	0.5691	0.545	958	546	1580	901
122	0		1740	7.34		5-10-6	0.9980	0.5691	0.514	903	515	1572	897
123	0		2090	5.96	9	3	0.9980	0.5691	0.187	329	187	687	392
124	0		2310	5.27	9	3	0.9980	0.5691	0.292	512	292	1183	675
125	0		1300	8.21		5	0.9980	0.5691	0.528	927	529	1205	687
126	0		1900	4.89	10	4	0.9980	0.5691	0.421	739	422	1404	801
127	0		1440	6.28		5-10-6	0.9980	0.5691	0.323	567	323	816	466
128	0		1090	5.76	10	6	0.9934	0.5529	0.551	996	568	1086	619
129	0		780	7.27		6	0.9934	0.5529	0.465	877	500	664	390
130	0		1010	6.07	9	3	0.9934	0.5529	0.384	694	396	701	400
131	0		1700	8.34		6	0.9934	0.5529	0.283	512	292	671	497
132	1		3030	6.62		5	0.9934	0.5529	0.259	468	267	1418	809
133	0		2160	6.55		6	0.9934	0.5529	0.454	821	469	1774	1012
134	0		1410	5.70	10	3	0.9934	0.5529	0.249	450	257	634	362
135	0		1100	7.31		6	0.9934	0.5529	0.476	860	491	946	540
136	0		1060	7.37		6	0.9934	0.5529	0.505	913	521	968	552
137	0		890	6.09	9	4	0.9934	0.5529	0.336	607	346	540	308
138	1		900	5.76	7	6	0.9934	0.5529	0.494	893	509	804	458
139	0		950	8.26		5	0.9934	0.5529	0.420	760	434	722	412
140	1		1610	6.88		3	0.9934	0.5529	0.103	187	106	301	171
141	1		1270	7.07		5	0.9934	0.5529	0.344	622	355	789	450
142	0		800	6.17	9	5	0.9934	0.5529	0.470	850	485	680	388
143	0		2030	7.24		5	0.9934	0.5529	0.379	686	391	1392	794

144	1		1000	6.72		5	0.9934	0.5529	0.365	660	376	660	376
145	0		1170	6.54		6	0.9934	0.5529	0.613	1109	633	1298	740
146	0		1620	7.17		5	0.9934	0.5529	0.216	391	223	633	361
147	0		1550	6.83		6	0.9934	0.5529	0.391	708	404	1097	626
148	0		1500	6.29		5-10-6	0.9934	0.5529	0.551	996	568	1494	852
149	0		2870	6.94		5	0.9934	0.5529	0.149	270	154	774	442
150	0		1620	8.07		5	0.9934	0.5529	0.438	793	452	1284	732
151	1		2060	7.90		3	0.9934	0.5529	0.215	388	222	800	456
152	0		670	5.62	8	5-10-6	0.9934	0.5529	0.448	811	462	543	310
153	0		1460	7.25		5-10-6	0.9934	0.5529	0.533	964	550	1408	803
154	0		1890	5.90	12	5	0.9934	0.5529	0.231	417	238	789	450
155	0		1590	6.87		3	0.9934	0.5529	0.065	118	67	187	107
156	0		850	6.32		5	0.9934	0.5529	0.322	582	332	495	282
157	0		850	6.84		3	0.9934	0.5529	0.086	174	99	148	84
158	0		1670	8.87		7	0.9934	0.5529	0.401	726	414	1212	691
159	0		1290	7.25		5-10-6	0.9934	0.5529	0.375	679	387	875	499
161	0		1490	7.32		5	0.9934	0.5529	0.227	411	234	612	349
162	0		2240	7.17		4	0.9934	0.5529	0.162	293	167	657	375
163	1		810	7.31		5-10-6	0.9934	0.5529	0.327	592	338	479	273
164	0		970	6.08	10	3	0.9934	0.5529	0.256	463	264	449	256
165	0		950	6.15	10	4	0.9934	0.5529	0.358	648	370	615	351
166	0		760	6.54		5	0.9934	0.5529	0.372	673	384	512	292
167	0		660	6.55		5-10-6	0.9934	0.5529	0.512	926	528	611	349
168	0		780	6.99		5-10-6	0.9934	0.5529	0.557	1007	574	785	448
169	0		540	5.78	8	5-10-6	0.9934	0.5529	0.478	864	493	467	266
170	1		1250	6.87		5-10-6	0.9934	0.5529	0.509	920	525	1150	656
171	0		960	7.17		5-10-6	0.9934	0.5529	0.543	982	560	943	538
172	0		1060	8.28		5	0.9934	0.5529	0.382	691	394	733	418
173	0		2130	5.40	10	3	0.9934	0.5529	0.307	555	316	1182	674
174	0		920	8.67		5	0.9934	0.5529	0.287	519	296	477	272
175	0		1360	6.75		5	0.9934	0.5529	0.433	783	446	1064	607
176	0		1130	6.74		4	0.9934	0.5529	0.307	555	316	627	358
177	0		1430	7.02		5-10-6	0.9934	0.5529	0.492	889	507	1272	726
178	0		870	7.03		5-10-6	0.9934	0.5529	0.380	705	402	613	350
179	0		940	7.34		5	0.9934	0.5529	0.448	811	462	762	435
180	0		1570	6.45		5-10-6	0.9934	0.5529	0.536	969	553	1521	868
181	0		320	5.92	8	5-10-6	0.9934	0.5529	0.498	901	514	288	164
182	0		1180	7.26		5	0.9934	0.5529	0.355	642	366	757	432
183	0		670	6.69		5-10-6	0.9934	0.5529	0.528	955	545	640	365
184	0		930	6.65		5	0.9934	0.5529	0.576	1041	594	968	552
185	0		1260	6.74		5	0.9934	0.5529	0.466	842	481	1061	605
186	0		1010	6.64		5-10-6	0.9934	0.5529	0.489	884	504	893	509
187	0		1000	8.43		4	0.9934	0.5529	0.360	651	371	651	371
188	0		1600	7.47		3	0.9934	0.5529	0.201	364	208	582	332
189	0		970	6.76		5-10-6	0.9934	0.5529	0.433	783	446	759	433
190	0		750	6.50		5-10-6	0.9934	0.5529	0.596	1077	615	808	461

191	0		2200	7.14		4	0.9934	0.5529	0.121	219	125	482	275
192	0		1670	8.00		4	0.9934	0.5529	0.478	865	493	1444	824
193	1		800	6.45		3	0.9934	0.5529	0.212	363	216	306	175
194	0		740	6.99		5-10-6	0.9934	0.5529	0.418	755	431	559	319
195	0		4130	7.49		3	0.9934	0.5529	0.129	233	133	961	548
196	0		950	6.70		4	0.9934	0.5529	0.376	680	388	646	368
197	0		860	5.87	7	5	0.9934	0.5529	0.410	741	423	637	364
198	1		1360	7.70		3	0.9934	0.5529	0.104	188	108	256	146
199	0		1290			4	0.9934	0.5529	0.194	350	200	452	258
200	0		1000	6.24		5-10-6	0.9934	0.5529	0.435	787	449	787	449
201	0		880	6.58		5-10-6	0.9934	0.5529	0.445	805	459	709	404
202	0		1150	6.01	9	4	0.9934	0.5529	0.323	585	333	672	384
203	0		1850	7.54		4	0.9934	0.5529	0.367	664	379	1229	701
204	0		1090	7.33		5-10-6	0.9934	0.5529	0.525	949	541	1034	590
205	0		1700	7.86		4	0.9934	0.5529	0.389	704	402	1197	683
206	0		1440	7.16		5-10-6	0.9934	0.5529	0.239	433	247	623	355
207	1		1600	6.94		5-10-6	0.9934	0.5529	0.433	783	446	1252	714
208	0		2430	6.63		5-10-6	0.9934	0.5529	0.424	766	437	1862	1062
209	0		2160	7.97		4	0.9934	0.5529	0.427	773	441	1669	952
210	0		1610	8.23		4	0.9934	0.5529	0.404	731	417	1177	671
211	0		1560	7.77		5-10-6	0.9934	0.5529	0.474	857	489	1337	762
212	0		790	6.87		5-10-6	0.9934	0.5529	0.538	973	555	789	439
213	0		1280	6.55		5-10-6	0.9934	0.5529	0.531	961	546	1230	702
214	0		1130	6.33		5-10-6	0.9934	0.5529	0.593	1073	612	1212	692
215	0		760	6.61		5-10-6	0.9934	0.5529	0.516	933	532	709	404
216	1		1470	7.74		5	0.9934	0.5529	0.490	886	505	1302	743
217	0		2000	7.89		4	0.9934	0.5529	0.433	783	446	1565	893
218	0		2350	7.97		3	0.9934	0.5529	0.230	416	238	978	558
219	0		760	7.68		5	0.9934	0.5529	0.449	812	463	617	352
220	1	CaP+CaOx	800	7.72		3	0.9934	0.5529	0.188	340	194	272	155
221	1	CaOx+CaP	2750	7.62		5-10-6	0.9934	0.5529	0.485	878	501	2413	1377
223	1	CaOx	1800	6.73		5	0.9934	0.5529	0.233	422	241	759	433
224	1	CaOx	2100	7.30		5	0.9934	0.5529	0.244	441	251	926	528
225	1	CaOx	1300	8.51		5-10-6	0.9934	0.5529	0.070	126	72	164	93
226	1	Uric acid	1000	6.88		4	0.9934	0.5529	0.276	499	284	499	284
227	1	CaOx+CaP	2000	8.40		5	0.9934	0.5529	0.359	649	370	1298	740
228	1	Uric acid	1500	6.40		5	0.9934	0.5529	0.191	345	197	517	295
229	1	CaP	1350	7.59		4	0.9934	0.5529	0.198	358	205	484	276
230	1	Uric acid	1200	8.05		4	0.9934	0.5529	0.186	337	192	404	231
231	1	CaOx+CaP	1450	7.39		4	0.9934	0.5529	0.205	370	211	537	306
232	1	CaOx	1410	?		5	0.9934	0.5529	0.470	850	485	1198	683
233	1	CaOx+CaP	1850	8.71		7	0.9934	0.5529	0.348	630	359	1165	665
234	1	CaP	1380	8.05		3	0.9934	0.5529	0.208	377	215	520	296
235	1	CaP	1230	7.64		4	0.9934	0.5529	0.467	845	482	1039	593
236	1	CaP+CaOx	1680	9.19		6	0.9934	0.5529	0.199	359	205	604	344
237	1	CaOx	1400	8.43		6	0.9934	0.5529	0.191	345	197	483	275

238	1	CaOx+CaP	1550	6.63		5	0.9934	0.5529	0.347	627	358	972	554
239	1	CaOx+CaP	1880	8.40		5-10-6	0.9934	0.5529	0.100	181	103	341	194
240	1	CaP	2700	6.31		3	0.9934	0.5529	0.120	217	124	567	335
241	1	CaOx+CaP	1760	6.38		5	0.9934	0.5529	0.308	557	318	981	560
242	1	Uric acid	2270	7.20		4	0.9934	0.5529	0.126	227	130	516	294
243	1	CaOx	1750	6.21		5	0.9934	0.5529	0.327	591	337	1034	590
244	1	CaOx	1520	6.69		5	0.9934	0.5529	0.415	751	428	1141	651
245	1	Uric acid	1950	6.06	9	3	0.9934	0.5529	0.191	346	197	674	385
246	1	CaOx+CaP	1800	6.82		4	0.9934	0.5529	0.117	211	120	380	217
247	1	Uric acid	1850	8.04		2	0.9934	0.5529	0.056	102	58	188	107
248	1	CaOx	1700	8.16		3	0.9934	0.5529	0.050	90	51	153	87
249	1	CaOx	1350	8.79		6	0.9934	0.5529	0.219	396	226	534	305
250	1	CaOx	1760	8.22		3	0.9934	0.5529	0.062	112	64	196	112
251	1	CaOx+CaP	1530	6.77		5-10-6	0.9934	0.5529	0.379	685	391	1048	598
252	1	CaP+CaOX	1760	8.85		4	0.9934	0.5529	0.171	309	176	543	310
254	1	CaOx	550	8.73		7	0.9934	0.5529	0.145	262	149	144	82
255	1	CaOx+CaP	1130	6.86		5	0.9934	0.5529	0.293	530	303	599	342
257	1	CaOx	2500	8.03		3	0.9934	0.5529	0.145	262	149	654	373
259	1	CaP+CaOX	1480	8.80		6	0.9934	0.5529	0.218	395	225	584	333
260	1	CaP+CaOX	1060	9.06		6	0.9934	0.5529	0.037	66	38	70	40
261	1	CaOx	1250	8.90		6	0.9934	0.5529	0.198	358	204	447	255
262	1	CaP+CaOX	1320	9.20		6	0.9934	0.5529	0.041	75	43	98	56
263	1	CaOx+CaP	1100	6.64		5-10-6	0.9934	0.5529	0.466	843	481	928	529
264	1	CaP+CaOX	1400	8.99		6	0.9934	0.5529	0.162	292	167	409	234
265	1	CaP+CaOX	650	6.44		5	0.9934	0.5529	0.561	1015	579	660	376
266	1	Uric acid	1550	6.11		5	0.9934	0.5529	0.253	457	261	708	404
267	1	CaP+CaOX	1230	8.17		4	0.9934	0.5529	0.333	603	344	741	423
268	1	CaOx+CaP	1000	9.21		7	0.9934	0.5529	0.161	292	166	292	166
269	1	Uric acid	2000	5.76	9	3	0.9934	0.5529	0.280	506	289	1012	577
270	1	CaP+CaOX	1350	6.99		5-10-6	0.9934	0.5529	0.521	943	538	1273	726
272	1	CaOx+CaP	1300	6.81		5	0.9934	0.5529	0.485	878	501	1141	651
273	1	CaOx+CaP	1650	5.12	10	4	0.9934	0.5529	0.260	471	266	777	443
274	1	CaOx+CaP	2300	8.64		6	0.9934	0.5529	0.114	207	118	475	271
275	1	CaP+CaOX	2060	8.26		6	0.9934	0.5529	0.085	154	88	317	181
276	1	Uric acid	350	8.33		3	0.9934	0.5529	0.101	182	104	64	36
277	1	CaOx	870	7.35		3	0.9934	0.5529	0.100	181	103	158	90
278	1	Uric acid	550	7.24		4	0.9934	0.5529	0.196	354	202	195	111
279	1	CaOx	1520	7.76		4	0.9934	0.5529	0.301	544	310	827	472
280	1	CaP+CaOX	880	8.40		5	0.9934	0.5529	0.287	519	296	456	260
281	1	CaOx	1340	8.05		3	0.9934	0.5529	0.055	99	56	133	76
282	1		1720	6.68		5-10-6	0.9934	0.5529	0.505	913	521	1570	896



**Table 31** (supplement S20) Number of cases and percentage of non-stone and stone group.

urine sample	n	%
<b>non-stone cases</b>	122	
<b>stone cases, stone types:</b>	141	100
CaOx	17	12
mixed of CaOx, CaP (CaOx is more than CaP)	17	12
mixed of CaP, CaOx (CaP is more than CaOx)	11	9
CaP	4	3
Uric acid	11	8

**Table 32** (supplement S21) Number of cases and percentage, representing their urinary precipitated CalCit level, corresponding to LoD and LoQ of Mrx IDA.

CalCit level of sample	NS group		ST group	
	n	%	n	%
between LoD to LLoQ (0.08 - 0.4 mM)	2	1.64	21	14.89
between LLoQ to ULoQ (0.4 - 1.4 mM), within linearity	120	98.36	120	85.11
higher than ULoQ (>1.4 mM)	0	0	0	0
<b>total</b>	<b>122</b>	<b>100</b>	<b>141</b>	<b>100</b>

**Table 33** (supplement S22) Frequency distribution of urinary precipitated CalCit level from non-stone and stone group.

range of CalCit (uM)	NS group		ST group	
	n	%	n	%
0-99	0	0.0	4	2.8
100-299	9	7.4	41	29.1
300-499	13	10.7	43	30.5
500-699	29	23.8	31	22.0
700-899	42	34.4	16	11.3
900-1099	24	19.7	5	3.5
1100-1299	5	4.1	1	0.7
1300-1499	0	0.0	0	0.0
total	122	100.0	141	100.0

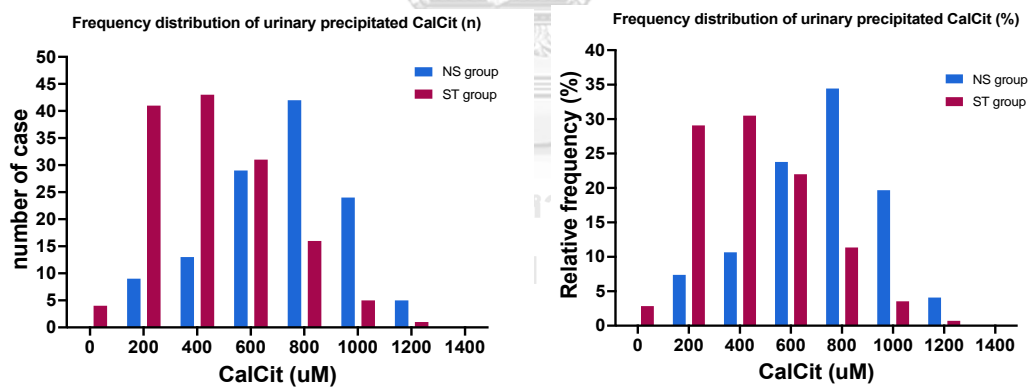


**Figure 27.** (supplement S3) Histogram, demonstrating urinary precipitated CalCit level from non-stone and stone group. left) number of cases, right) percentage.

## REFERENCES

1. Stamatelou K, Goldfarb DS. Epidemiology of Kidney Stones. *Healthcare* [Internet]. 2023; 11(3).
2. Moftakhar L, Jafari F, Ghodduji Johari M, Rezaeianzadeh R, Hosseini SV, Rezaianzadeh A. Prevalence and risk factors of kidney stone disease in population aged 40-70 years old in Kharameh cohort study: a cross-sectional population-based study in southern Iran. *BMC Urol*. 2022;22(1):205.
3. Wang K, Ge J, Han W, Wang D, Zhao Y, Shen Y, et al. Risk factors for kidney stone disease recurrence: a comprehensive meta-analysis. *BMC Urol*. 2022;22(1):62.
4. Lordumrongkiat N, Chotechuang N, Prasanth MI, Jindatip D, Ma-On C, Chuenwisad K, et al. HydroZitLa inhibits calcium oxalate stone formation in nephrolithic rats and promotes longevity in nematode *Caenorhabditis elegans*. *Sci Rep*. 2022;12(1):5102.
5. Liu Y, Chen Y, Liao B, Luo D, Wang K, Li H, et al. Epidemiology of urolithiasis in Asia. *Asian J Urol*. 2018;5(4):205-14.
6. Udomsilp P, Saepoo S, Ittiwut R, Shotelersuk V, Dissayabutra T, Boonla C, et al. rs11567842 SNP in SLC13A2 gene associates with hypocitraturia in Thai patients with nephrolithiasis. *Genes Genomics*. 2018;40(9):965-72.
7. Caudarella R, Vescini F. Urinary citrate and renal stone disease: the preventive role of alkali citrate treatment. *Arch Ital Urol Androl*. 2009;81(3):182-7.
8. Youngjermchan P, Pumpaisanchai S, Ratchanon S, Pansin P, Tosukhowong P, Tungsanga K, et al., editors. Hypocitraturia and hypokaliuria : major metabolic risk factors for kidney stone disease 2006. จุฬาลงกรณ์มหาวิทยาลัย
9. Saepoo SA, D.; Tosukhowong, P.; C., Predanon; Shotelersuk, V.; and Boonla, C. Comparison of urinary citrate between patients with nephrolithiasis and healthy controls. *Chulalongkorn Medical Journal*. 2009;53(1).
10. Ruiz-Agudo E, Burgos-Cara A, Ruiz-Agudo C, Ibanez-Velasco A, Colfen H, Rodriguez-Navarro C. A non-classical view on calcium oxalate precipitation and the role of citrate. *Nat Commun*. 2017;8(1):768.
11. Zhang J, Zhang W, Putnis CV, Wang L. Modulation of the calcium oxalate dihydrate to calcium oxalate monohydrate phase transition with citrate and zinc ions. *CrystEngComm*. 2021;23(48):8588-600.
12. Prochaska M, Taylor E, Ferraro PM, Curhan G. Relative Supersaturation of 24-Hour Urine and Likelihood of Kidney Stones. *J Urol*. 2018;199(5):1262-6.

13. Tavallali H, Karimi MA, Espergham O. Efficient ensemble and IDA system based on the metal binding motif for highly sensitive and selective detection and determination of carbonate and citrate ions. *International Journal of Environmental Analytical Chemistry*. 2019;99(8):776-95.
14. Qin Y, Wang W, Zhang H, Dai Y, Hou H, Dong H. Effects of Citric Acid on Structures and Properties of Thermoplastic Hydroxypropyl Amylomaize Starch Films. *Materials (Basel)*. 2019;12(9).
15. Srikaeo K, Hao PT, Lerdluksamee C. Effects of Heating Temperatures and Acid Concentrations on Physicochemical Properties and Starch Digestibility of Citric Acid Esterified Tapioca Starches. *Starch - Stärke*. 2019;71(1-2):1800065.
16. Suciani NN, Said I, Diah AWM. Citric Acid Extraction in Citrus hystrix Peels as an Alternative Material for Reducing Water Hardness. *Jurnal Akademika Kimia*. 2021;10(1):53-8.
17. Hakim YAH, Mohammed DH, Abdelrahim YM, Abbas A, Kehail MAA, Talaha A, editors. CORRELATION OF THE CHEMICAL COMPOSITION OF KIDNEY STONES WITH THE DIET STYLE, GEZIRA STATE, SUDAN, MARCH 2016, SEPTEMBER 20162017.
18. Kwak E-J, Lim S-I. Inhibition of browning by antibrowning agents and phenolic acids or cinnamic acid in the glucose-lysine model. *Journal of the Science of Food and Agriculture*. 2005;85(8):1337-42.
19. Jayaram U, Gurusamy A. Review on Uro-Lithiasis Pathophysiology and Aesculapian Discussion. *IOSR Journal Of Pharmacy*. 2018;8:30-42.
20. Sigurjonsdottir VK, Runolfsdottir HL, Indridason OS, Palsson R, Edvardsson VO. Impact of nephrolithiasis on kidney function. *BMC Nephrol*. 2015;16:149.
21. Gambaro G, Croppi E, Bushinsky D, Jaeger P, Cupisti A, Ticinesi A, et al. The Risk of Chronic Kidney Disease Associated with Urolithiasis and its Urological Treatments: A Review. *Journal of Urology*. 2017;198(2):268-73.
22. Bargagli M, Mochhala S, Robertson WG, Gambaro G, Lombardi G, Unwin RJ, et al. Urinary metabolic profile and stone composition in kidney stone formers with and without heart disease. *Journal of Nephrology*. 2022;35(3):851-7.
23. Sayer J, Mochhala S, Thomas D. The Medical Management of Urolithiasis. *British Journal of Medical and Surgical Urology*. 2010;3:87-95.
24. Chang CW, Ke HL, Lee JI, Lee YC, Jhan JH, Wang HS, et al. Metabolic Syndrome Increases the Risk of Kidney Stone Disease: A Cross-Sectional and Longitudinal Cohort Study. *J Pers Med*. 2021;11(11).

25. Qian X, Wan J, Xu J, Liu C, Zhong M, Zhang J, et al. Epidemiological Trends of Urolithiasis at the Global, Regional, and National Levels: A Population-Based Study. *Int J Clin Pract*. 2022;2022:6807203.
26. Romero V, Akpınar H, Assimos DG. Kidney stones: a global picture of prevalence, incidence, and associated risk factors. *Rev Urol*. 2010;12(2-3):e86-96.
27. Alatab S, Pourmand G, El Howairis Mel F, Buchholz N, Najafi I, Pourmand MR, et al. National Profiles of Urinary Calculi: a Comparison Between Developing and Developed Worlds. *Iran J Kidney Dis*. 2016;10(2):51-61.
28. Shin S, Srivastava A, Alli NA, Bandyopadhyay BC. Confounding risk factors and preventative measures driving nephrolithiasis global makeup. *World J Nephrol*. 2018;7(7):129-42.
29. Bansal AD, Hui J, Goldfarb DS. Asymptomatic nephrolithiasis detected by ultrasound. *Clin J Am Soc Nephrol*. 2009;4(3):680-4.
30. Uribarri J, Oh MS, Carroll HJ. The first kidney stone. *Ann Intern Med*. 1989;111(12):1006-9.
31. Tzelvels L, Berdempes M, Mourmouris P, Mitsogiannis I, Skolarikos A. Optimal Delivery of Follow-Up Care for the Prevention of Stone Recurrence in Urolithiasis Patients: Improving Outcomes. *Res Rep Urol*. 2022;14:141-8.
32. Zeng J, Wang S, Zhong L, Huang Z, Zeng Y, Zheng D, et al. A Retrospective Study of Kidney Stone Recurrence in Adults. *J Clin Med Res*. 2019;11(3):208-12.
33. Maruyama M, Sawada KP, Tanaka Y, Okada A, Momma K, Nakamura M, et al. Quantitative analysis of calcium oxalate monohydrate and dihydrate for elucidating the formation mechanism of calcium oxalate kidney stones. *PLoS One*. 2023;18(3):e0282743.
34. Jing Z, GuoZeng W, Ning J, JiaWei Y, Yan G, Fang Y. Analysis of urinary calculi composition by infrared spectroscopy: A prospective study of 625 patients in Eastern China. *Urological research*. 2010;38:111-5.
35. Pfau A, Knauf F. Update on Nephrolithiasis: Core Curriculum 2016. *American Journal of Kidney Diseases*. 2016;68(6):973-85.
36. Tosukhowong P, Boonla C, Ratchanon S, Tanthanuch M, Poonpirome K, Supataravanich P, et al. Crystalline composition and etiologic factors of kidney stone in Thailand: Update 2007. *Asian Biomed*. 2007;1.
37. Khan SR, Pearle MS, Robertson WG, Gambaro G, Canales BK, Doizi S, et al. Kidney stones. *Nature Reviews Disease Primers*. 2016;2(1):16008.
38. Mayans L. Nephrolithiasis. *Prim Care*. 2019;46(2):203-12.
39. Curhan GC. Epidemiology of Stone Disease. *Urologic Clinics of North America*. 2007;34(3):287-93.

40. Chanchai B. Oxidative Stress in Urolithiasis. In: Cristiana F, Elena A, editors. *Reactive Oxygen Species (ROS) in Living Cells*. Rijeka: IntechOpen; 2018. p. Ch. 8.
41. Khan SR. Hyperoxaluria-induced oxidative stress and antioxidants for renal protection. *Urol Res*. 2005;33(5):349-57.
42. Izatulina A, Gurzhiy V, Krzhizhanovskaya M, Kuz'mina M, Leoni M, Frank-Kamenetskaya O. Hydrated Calcium Oxalates: Crystal Structures, Thermal Stability, and Phase Evolution. *Crystal Growth & Design*. 2018;18.
43. Sun XY, Gan QZ, Ouyang JM. Calcium oxalate toxicity in renal epithelial cells: the mediation of crystal size on cell death mode. *Cell Death Discov*. 2015;1:15055.
44. Wang T, Thurgood LA, Grover PK, Ryall RL. A comparison of the binding of urinary calcium oxalate monohydrate and dihydrate crystals to human kidney cells in urine. *BJU Int*. 2010;106(11):1768-74.
45. Erdem M, Bedir A. A novel method for the determination of urinary citrate levels: Ion-pair and high performance liquid chromatography with liquid membrane extraction technique. *Journal of Experimental & Clinical Medicine*. 2014;31.
46. Li W, Zheng J, Chen M, Liu B, Liu Z, Gong L. Simultaneous determination of oxalate and citrate in urine and serum of calcium oxalate kidney stone rats by IP-RP LC-MS/MS. *J Chromatogr B Analyt Technol Biomed Life Sci*. 2022;1208:123395.
47. Li Q, Liu G, Cheng Y, Tang W. Three-channel ion chromatograph for improved metabolic evaluation of urolithiasis. *BMC Urology*. 2021;21(1):151.
48. Duan X, Zhang T, Ou L, Kong Z, Wu W, Zeng G. (1)H NMR-based metabolomic study of metabolic profiling for the urine of kidney stone patients. *Urolithiasis*. 2020;48(1):27-35.
49. Thongprayoon C, Vuckovic I, Vaughan LE, Macura S, Larson NB, D'Costa MR, et al. Nuclear Magnetic Resonance Metabolomic Profiling and Urine Chemistries in Incident Kidney Stone Formers Compared with Controls. *J Am Soc Nephrol*. 2022;33(11):2071-86.
50. Matyus SP, Wolak-Dinsmore J, Garcia E, Young RM, Connelly MA. Vantera Mediated Quantification of Urine Citrate and Creatinine: A New Technology to Assess Risk of Nephrolithiasis. *Diagnostics* [Internet]. 2022; 12(11).
51. Shadbolt S, Jackson GE, Rodgers AL. Successful urinary discrimination between calcium oxalate kidney stone patients and healthy subjects using 1H NMR spectroscopy: Suggestion of a possible link to protein content. *NMR in Biomedicine*. 2019;32(12):e4177.
52. Bhushan B, Upadhyay D, Sharma U, Jagannathan N, Singh SB, Ganju L. Urine metabolite profiling of Indian Antarctic Expedition members: NMR spectroscopy-based metabolomic investigation. *Heliyon*. 2021;7(5):e07114.

53. Sharma SS, Vyas N, Priyadarshi S, Ali A. To study the normal values of citrate in urine: A population based study. *European Journal of Molecular and Clinical Medicine*. 2022;9:797+.
54. Rodriguez A, Saez-Torres C, Mir C, Casasayas P, Rodriguez N, Rodrigo D, et al. Effect of sample time on urinary lithogenic risk indexes in healthy and stone-forming adults and children. *BMC Urology*. 2018;18(1):116.
55. Grases F, Costa-Bauza A, Prieto RM, Arrabal M, De Haro T, Lancina JA, et al. Urinary lithogenesis risk tests: comparison of a commercial kit and a laboratory prototype test. *Scand J Urol Nephrol*. 2011;45(5):312-8.
56. Seker R, Fidanci V, Erol D, Yalbuzağ O, Saydam G, Senes M, et al. A Simple Modified Method for Urine Citrate Determination. *Turkish Journal of Biochemistry*. 2009;34:173-7.
57. Elgstoen KBP, Woldseth B, Hoie K, Morkrid L. Liquid chromatography-tandem mass spectrometry determination of oxalate in spot urine. *Scandinavian Journal of Clinical and Laboratory Investigation*. 2010;70(3):145-50.
58. Keevil BG, Thornton S. Quantification of Urinary Oxalate by Liquid Chromatography–Tandem Mass Spectrometry with Online Weak Anion Exchange Chromatography. *Clinical Chemistry*. 2006;52(12):2296-9.
59. Marshall DJ, Adaway JE, Keevil BG. A combined liquid chromatography tandem mass spectrometry assay for the quantification of urinary oxalate and citrate in patients with nephrolithiasis. *Ann Clin Biochem*. 2018;55(4):461-8.
60. Mudunkotuwa IA, Grassian VH. Citric acid adsorption on TiO<sub>2</sub> nanoparticles in aqueous suspensions at acidic and circumneutral pH: surface coverage, surface speciation, and its impact on nanoparticle-nanoparticle interactions. *J Am Chem Soc*. 2010;132(42):14986-94.
61. Inoue K, Zhuang L, Maddox DM, Smith SB, Ganapathy V. Structure, function, and expression pattern of a novel sodium-coupled citrate transporter (NaCT) cloned from mammalian brain. *J Biol Chem*. 2002;277(42):39469-76.
62. Graffmann G, Domels H, Sträter ML. Schnelle Bestimmung von Citrat in Wasch- und Reinigungsmitteln durch Titration mit Cu-Lösung. *Fette, Seifen, Anstrichmittel*. 1974;76(5):218-20.
63. Sun S-K, Tu K-X, Yan X-P. An indicator-displacement assay for naked-eye detection and quantification of histidine in human urine. *Analyst*. 2012;137(9):2124-8.
64. Armstrong MD, Shaw KN, Wall PE. The phenolic acids of human urine; paper chromatography of phenolic acids. *J Biol Chem*. 1956;218(1):293-303.

65. Nirumand MC, Hajialyani M, Rahimi R, Farzaei MH, Zingue S, Nabavi SM, et al. Dietary Plants for the Prevention and Management of Kidney Stones: Preclinical and Clinical Evidence and Molecular Mechanisms. *Int J Mol Sci.* 2018;19(3).
66. Ahmed S, Hasan MM, Khan H, Mahmood ZA, Patel S. The mechanistic insight of polyphenols in calcium oxalate urolithiasis mitigation. *Biomed Pharmacother.* 2018;106:1292-9.
67. Grases F, Prieto RM, Fernandez-Cabot RA, Costa-Bauza A, Tur F, Torres JJ. Effects of polyphenols from grape seeds on renal lithiasis. *Oxid Med Cell Longev.* 2015;2015:813737.
68. Janrod M, Srisa-Art M. Simultaneous colorimetric detection of nephrolithiasis biomarkers using a microfluidic paper-based analytical device. *Analytical Methods.* 2023;15(6):752-61.
69. Ye R, Zhao Z, Gao R, Wan J, Cao X. Conversion of Calcium Citrate to Citric Acid with Compressed CO<sub>2</sub>. *ACS Omega.* 2022;7(1):683-7.
70. Bizek V, Horacek J, Rericha R, Kousova M. Amine extraction of hydroxycarboxylic acids. 1. Extraction of citric acid with 1-octanol/n-heptane solutions of trialkylamine. *Industrial & Engineering Chemistry Research.* 1992;31(6):1554-62.
71. Araújo EMR, Coelho FEB, Balarini JC, Miranda TLS, Salum A. Solvent Extraction of Citric Acid with Different Organic Phases. *Advances in Chemical Engineering and Science.* 2017;07:304-24.
72. Li J, Liu Y, Gao Y, Zhong L, Zou Q, Lai X. Preparation and properties of calcium citrate nanosheets for bone graft substitute. *Bioengineered.* 2016;7(5):376-81.
73. Gao Y, Zhang P, Li J, Cao W, Lai X, Zhong L. Preparation and characterisation of calcium citrate wires. *Micro & Nano Letters.* 2015;10:419-21.
74. Hacherl JM, Paul EL, Buettner HM. Investigation of impinging-jet crystallization with a calcium oxalate model system. *AIChE Journal.* 2003;49(9):2352-62.
75. Paik SY, Nguyen HH, Ryu J, Che JH, Kang TS, Lee JK, et al. Robust size control of bovine serum albumin (BSA) nanoparticles by intermittent addition of a desolvating agent and the particle formation mechanism. *Food Chem.* 2013;141(2):695-701.
76. Yedomon B, Fessi H, Charcosset C. Preparation of Bovine Serum Albumin (BSA) nanoparticles by desolvation using a membrane contactor: a new tool for large scale production. *Eur J Pharm Biopharm.* 2013;85(3 Pt A):398-405.
77. Chalermnon M, Cherdchom S, Sereemasapun A, Rojanathanes R, Khotavivattana T. Biguanide-Based Synthesis of 1,3,5-Triazine Derivatives with Anticancer Activity and 1,3,5-Triazine Incorporated Calcium Citrate Nanoparticles. *Molecules.* 2021;26(4).



78. Shinta Y, Zaman B, Sumiyati S. Citric Acid and EDTA as chelating agents in phytoremediation of heavy metal in polluted soil: a review. *IOP Conference Series: Earth and Environmental Science*. 2021;896:012023.
79. Choi Y, Lee S-Y, Bae J-S, Lee S-J, Kim HK, Jeong ED, et al. Nitrogen and Sulfur Co-Doped Porous Carbon Derived from Thiourea and Calcium Citrate for Lithium-Sulfur Batteries. *Applied Sciences* [Internet]. 2020; 10(4).
80. Martinez-Huitle CA, Souza S, Araújo E, Morais F, Dos santos E, Silva M, et al. Determination of calcium in tablets containing calcium citrate using thermogravimetry (TG). *Brazilian Journal of Thermal Analysis*. 2013;2:17.
81. Reckziegel P, Dias V, Benvegnú D, Boufleur N, Barcelos R, Segat H, et al. Antioxidant protection of gallic acid against toxicity induced by Pb in blood, liver and kidney of rats. *Toxicology Reports*. 2016;3.
82. Alshatwi A. Catechin hydrate suppresses MCF-7 proliferation through TP53/Caspase-mediated apoptosis. *Journal of experimental & clinical cancer research : CR*. 2010;29:167.
83. Yang G-Z, Wang Z-J, Bai F, Qin X, Cao J, Lv J-Y, et al. Epigallocatechin-3-Gallate Protects HUVECs from PM2.5-Induced Oxidative Stress Injury by Activating Critical Antioxidant Pathways. *Molecules (Basel, Switzerland)*. 2015;20:6626-39.
84. Vargas hernandez C. Spectrophotometric Determination of the pKa, Isosbestic Point and Equation of Absorbance vs. pH for a Universal pH Indicator. *American Journal of Analytical Chemistry*. 2014.
85. Goss SL, Lemons KA, Kerstetter JE, Bogner RH. Determination of calcium salt solubility with changes in pH and P(CO(2)), simulating varying gastrointestinal environments. *J Pharm Pharmacol*. 2007;59(11):1485-92.
86. Chutipongtanate S, Thongboonkerd V. Systematic comparisons of artificial urine formulas for in vitro cellular study. *Anal Biochem*. 2010;402(1):110-2.
87. Häring M, Pérez-Madrigal M, Kühbeck D, Pettignano A, Quignard F, Díaz D. DNA-Catalyzed Henry Reaction in Pure Water and the Striking Influence of Organic Buffer Systems. *Molecules (Basel, Switzerland)*. 2015;20:4136-47.
88. Davis JW. Biomarker classification, validation, and what to look for in 2017 and beyond. *BJU Int*. 2017;119(5):812-4.
89. Stoving C, Jensen H, Gammelgaard B, Sturup S. Development and validation of an ICP-OES method for quantitation of elemental impurities in tablets according to coming US pharmacopeia chapters. *J Pharm Biomed Anal*. 2013;84:209-14.
90. Ravisankar P, Sankar R. A Review on Step-by-Step Analytical Method Validation. 2015:7-19.

91. Shabir G. Step-by-step analytical methods validation and protocol in the quality system compliance industry. *Journal of validation technology*. 2004;10:314-24.
92. Armbruster DA, Pry T. Limit of blank, limit of detection and limit of quantitation. *Clin Biochem Rev*. 2008;29 Suppl 1(Suppl 1):S49-52.
93. Tkachenko Y, Niedzielski P. FTIR as a Method for Qualitative Assessment of Solid Samples in Geochemical Research: A Review. *Molecules* [Internet]. 2022; 27(24).
94. Riaz. Summary Urine normal values, their significant [Internet]2020 2020/1/25. Available from: <https://labpedia.net/urine-hemoglobin-hemoglobinuria/>.
95. Yeon J-Y, Sung C. A Study on Dietary Mineral Intakes, Urinary Mineral Excretions, and Bone Mineral Density in Korean Postmenopausal Women. *Korean Journal of Community Nutrition*. 2011;16:569.
96. Huang Y, Zhang YH, Chi ZP, Huang R, Huang H, Liu G, et al. The Handling of Oxalate in the Body and the Origin of Oxalate in Calcium Oxalate Stones. *Urol Int*. 2020;104(3-4):167-76.
97. Fung S-T, Ho CK, Choi S-W, Chung W-Y, Benzie IFF. Comparison of catechin profiles in human plasma and urine after single dosing and regular intake of green tea (*Camellia sinensis*). *British Journal of Nutrition*. 2013;109(12):2199-207.
98. Zambrano CN, Lu W, Johnson C, Beeber M, Panitz A, Ibrahim S, et al. Dietary behavior and urinary gallic acid concentration differences among underserved elder racial and ethnic minorities in New York City. *Cancer Causes & Control*. 2022;33(7):929-37.
99. Shahrzad S, Bitsch I. Determination of gallic acid and its metabolites in human plasma and urine by high-performance liquid chromatography. *J Chromatogr B Biomed Sci Appl*. 1998;705(1):87-95.
100. Hagen T, Korson MS, Wolfsdorf JI. Urinary lactate excretion to monitor the efficacy of treatment of type I glycogen storage disease. *Mol Genet Metab*. 2000;70(3):189-95.
101. Domínguez-López I, Parilli-Moser I, Arancibia-Riveros C, Tresserra-Rimbau A, Martínez-González MA, Ortega-Azorín C, et al. Urinary Tartaric Acid, a Biomarker of Wine Intake, Correlates with Lower Total and LDL Cholesterol. *Nutrients*. 2021;13(8):2883.
102. Regueiro J, Vallverdu-Queralt A, Simal-Gandara J, Estruch R, Lamuela-Raventos RM. Urinary tartaric acid as a potential biomarker for the dietary assessment of moderate wine consumption: a randomised controlled trial. *Br J Nutr*. 2014;111(9):1680-5.
103. Rodgers AL, Webber D, de Charmoy R, Jackson GE, Ravenscroft N. Malic Acid Supplementation Increases Urinary Citrate Excretion and Urinary pH: Implications for the Potential Treatment of Calcium Oxalate Stone Disease. *Journal of Endourology*. 2013;28(2):229-36.

104. Tinti F, Umbro I, D'Alessandro M, Lai S, Merli M, Noce A, et al. Cholemic Nephropathy as Cause of Acute and Chronic Kidney Disease. Update on an Under-Diagnosed Disease. *Life*. 2021;11(11):1200.
105. Tapp DC, Copley JB. Effect of red blood cell lysis on protein quantitation in hematuric states. *Am J Nephrol*. 1988;8(3):190-3.
106. Nahm FS. Receiver operating characteristic curve: overview and practical use for clinicians. *Korean J Anesthesiol*. 2022;75(1):25-36.
107. More-Krong P, Tubsaeng P, Madared N, Srisa-Art M, Insin N, Leeladee P, et al. Clinical validation of urinary indole-reacted calcium oxalate crystallization index (iCOCI) test for diagnosing calcium oxalate urolithiasis. *Sci Rep*. 2020;10(1):8334.
108. Garcia AC, Vavrusova M, Skibsted LH. Supersaturation of calcium citrate as a mechanism behind enhanced availability of calcium phosphates by presence of citrate. *Food Res Int*. 2018;107:195-205.
109. Deeks JJ, Altman DG. Diagnostic tests 4: likelihood ratios. *BMJ*. 2004;329(7458):168-9.
110. Jaeschke R, Guyatt GH, Sackett DL. Users' guides to the medical literature. III. How to use an article about a diagnostic test. B. What are the results and will they help me in caring for my patients? The Evidence-Based Medicine Working Group. *JAMA*. 1994;271(9):703-7.

## REFERENCES



จุฬาลงกรณ์มหาวิทยาลัย  
**CHULALONGKORN UNIVERSITY**



จุฬาลงกรณ์มหาวิทยาลัย  
**CHULALONGKORN UNIVERSITY**

## VITA

NAME ไชยดล ตัณฑสิทธิ์  
DATE OF BIRTH 21 พฤศจิกายน 2528  
PLACE OF BIRTH กรุงเทพมหานคร  
INSTITUTIONS ATTENDED Mahidol University  
HOME ADDRESS 34/279 ม.วังทอง ซ.วิภาวดี47 ถ.วิภาวดีรังสิต สนามบิน ดอนเมือง  
กทม. 10210  
PUBLICATION -  
AWARD RECEIVED -



จุฬาลงกรณ์มหาวิทยาลัย  
CHULALONGKORN UNIVERSITY